Role of FGF signaling in the adipogenic and osteogenic differentiation of human bone marrow stromal cells in a three-dimensional *in vitro* model.

Rolle der FGF-Signalgebung bei der adipogenen und osteogenen Differenzierung von humanen Knochenmarkstromazellen in einem dreidimensionalen *in vitro* Modell.

Doctoral thesis for a doctoral degree
at the Graduate School of Life Sciences,
Julius-Maximilians-Universität Würzburg,
Section Biomedicine

submitted by

Solange Le Blanc Soto

from

Santiago, Chile

Würzburg, 2017

Submitted on:

Members of the thesis committee:

Chairperson: Prof. Dr. Thomas Hünig

Primary Supervisor: Prof. Dr. Norbert Schütze

Supervisor (Second): PD Dr. Knut Ohlsen

Supervisor (Third): Prof. Dr. Albrecht Müller

Date of Public Defence: ……

Date of Receipt of Certificates: ……..

Affidavit

I hereby declare that my thesis entitled “Role of FGF signaling in the adipogenic and osteogenic differentiation of human bone marrow stromal cells in a three-dimensional *in vitro* model” is the result of my own work. I did not receive help or support from commercial consultants. All sources and/or materials applied are listed and specified in the thesis.

Furthermore, I verify that this thesis has not yet been submitted as part of another examination process neither in identical nor in similar form.

_____ _____

Place, date Signature

Table of contents

Acknowledgments

I would like to express my gratitude to all the people that in one way or another contributed to this work or supported me during my doctoral studies.

I would like to thank my primary supervisor Prof. Dr. Norbert Schütze as well as Dr. Tatjana Schilling for allowing me to work in this project under their supervision at the Orthopedic Center for Musculoskeletal Research. I am very grateful to Prof. Dr. Franz Jakob for his permanent expert support and valuable contributions to my thesis.

To the members of my thesis committee, PD. Dr. Knut Ohlsen and Prof. Dr. Albrecht Müller for their support and for the discussions and contributions during the committee meetings.

To the Graduate School of Life Sciences for all the support, workshops, courses and other scientific and social activities.

To CONICYT and the Formation of Advanced Human Capital Program BECAS CHILE for providing the funding during my doctoral studies.

To all the colleagues from the lab of Prof. Schütze and Prof. Jakob, in particular to my PhD fellows Dr. Julia Dotterweich, Dr. Meike Simann, Dr. Bettina Hafen and Dr. Sylvia Hondke. To the technical assistants Viola Zehe, Susanne Wiesner, Beate Geyer and Jutta Schneidereit. My very special gratitude goes to Julia Dotterweich for all her help and great support.

To Prof. Dr. Heike Walles and her lab members at the Institute of Tissue Engineering and Regenerative Medicine for hosting our lab at their premises for some time and for providing the collagen solutions used in this work.

To the wonderful group of friends that I had the chance to meet in Würzburg and the great time that we had together.

To my family in Chile, my parents and sister, for their love and support regardless of the distance.

Finally, to Cinthia, for sharing this journey, for her extraordinary patience, support and encouragement and for being always by my side.

Abstract

Adult human skeletal stem cells are considered to give rise to the bone marrow stromal compartment, including bone-forming osteoblasts and marrow adipocytes. Reduced osteogenesis and enhanced adipogenesis of these skeletal progenitors may contribute to the bone loss and marrow fat accumulation observed during aging and osteoporosis, the main disorder of bone remodeling. Concordantly, *in vitro* evidence indicates that adipogenic and osteogenic differentiation of human bone marrow stromal cells (hBMSCs) display an inverse relationship under numerous conditions. Hence, the identification of factors modulating inversely both differentiation pathways is of great therapeutic interest.

Based on mRNA expression analysis of inversely regulated genes after switching differentiation conditions, our group had previously proposed that fibroblast growth factor 1 (FGF1) might play such a modulator role in hBMSC differentiation. The main aim of this work was, therefore, to investigate the role of FGF1 signaling in the adipogenic and osteogenic differentiation of hBMSCs using a three-dimensional (3D) culture system based on collagen type I hydrogels in order to better mimic the natural microenvironment.

Adipogenic and osteogenic differentiation of hBMSCs embedded in collagen gels was successfully established. Treatment with recombinant human FGF1 (rhFGF1), as well as rhFGF2, throughout differentiation induction was found to exert a dose-dependent inhibitory effect on adipogenesis in hBMSCs. This inhibitory effect was found to be reversible and dependent on FGF receptors (FGFR) signaling, given that simultaneous pharmacological blockage of FGFRs rescued adipogenic differentiation. Additionally, matrix mineralization under osteogenic induction was also inhibited by rhFGF1 and rhFGF2 in a dose-dependent manner. A transient treatment with rhFGF1 and rhFGF2 during an expansion phase, however, enhanced proliferation of hBMSCs without affecting the differentiation capacity, although matrix mineralization under osteogenic conditions was hindered.

Additionally, rhFGF1 and rhFGF2 treatments affected the matrix remodeling ability of hBMSCs, which displayed alterations in the cytoskeletal phenotype and the expression patterns of matrix metalloproteinases (MMPs) and tissue inhibitors of metalloproteinases (TIMPs).

On the other hand, inhibition of FGFR signaling throughout differentiation induction elicited a strong enhancement of matrix mineralization under osteogenic conditions but had no significant effect on adipocyte formation under adipogenic induction.

In conclusion, FGF1 and FGF2 signaling was found to support the expansion of bone marrow stromal precursors with adipogenic and osteogenic capacities, to hinder adipogenic and osteogenic differentiation if continuously present during differentiation induction and to alter the matrix remodeling ability of hBMSCs within a 3D collagenous microenvironment.

Zusammenfassung

Es wird angenommen, dass humane adulte skelettale Stammzellen das Knochenmarkstroma, einschliesslich der knochenbildenden Osteoblasten und den Knochenmark-Adipozyten bilden. Eine verringerte Osteogenese und eine erhöhte Adipogenese dieser skelettalen Vorläufer kann zu einem Knochenverlust und zu einer Verfettung des Knochenmarks beitragen, was während der Alterung und der Osteoporose, der Hauptstörung des Knochenumbaus, beobachtet wird. Übereinstimmend dazu konnte in einem *in vitro* Nachweis gezeigt werden, dass sich die adipogene und osteogene Differenzierung von humanen Knochenmarkstromazellen (hBMSCs) unter einer Vielzahl von Bedingungen invers verhält. Somit ist die Identifikation von Faktoren, welche beide Differenzierungssignalwege invers regulieren, von großem therapeutischem Interesse.

Basierend auf mRNA Expressionsanalysen von Genen, die nach Änderung der Differenzierungsbedingungen invers reguliert wurden, hat unsere Gruppe bereits seit längerem angenommen, dass der Fibroblasten-Wachstumsfaktor 1 (FGF1) eine solche Regulatorfunktion in der hBMSC Differenzierung einnehmen könnte. Das Hauptziel dieser Arbeit war deshalb die Rolle der FGF1 Signalgebung in der adipogenen und osteogenen Differenzierung von hBMSCs zu untersuchen. Dies erfolgte unter Einsatz von einem dreidimensionalen (3D) Kultursystem basierend auf Kollagen-Typ I-Hydrogelen um die natürliche Mikroumgebung besser imitieren zu können.

Die adipogene und osteogene Differenzierung von in Kollagengelen eingebetteten hBMSCs konnte erfolgreich etabliert werden. Die Behandlung mit rekombinantem humanen FGF1 (rhFGF1), sowie mit rhFGF2, während der Differenzierungsinduktion führte zu einem dosisabhängigen hemmenden Effekt auf die Adipogenese in den hBMSCs. Dieser inhibierende Effekt ist reversibel und abhängig von Signalgebung der FGF Rezeptoren (FGFRs), da die gleichzeitige pharmakologische Blockierung von FGFRs die adipogene Differenzierung wiederhergestellt hatte. Zusätzlich wurde auch die Matrixmineralisierung durch rhFGF1 und rhFGF2 Gabe während der osteogenen Induktion in dosisabhängiger Weise inhibiert. Eine vorrübergehende Behandlung mit rhFGF1 und rhFGF2 während der Expansionsphase jedoch erhöhte die Proliferation von hBMSCs ohne die Differenzierungskapazität zu beeinflussen, obwohl die Matrixmineralisierung unter osteogenen Bedingungen verhindert wurde.

Zudem beeinflussten die Behandlungen mit rhFGF1 und rhFGF2 die Fähigkeit von hBMSCs die Matrix umzubauen, was sich durch phänotypische Veränderungen des Zytoskeletts und in einem veränderten Expressionsmuster von Metalloproteinasen (MMPs) und Gewebeinhibitoren von Metalloproteinasen (TIMPs) zeigte.

Andererseits löste die Inhibition der FGFR Signalgebung während der Differenzierungsinduktion eine deutliche Zunahme der Matrixmineralisierung unter osteogenen Bedingungen aus, zeigte aber keinen signifikanten Effekt auf die Bildung von Adipozyten bei adipogener Induktion.

Zusammenfassend lässt sich sagen, dass die FGF1 und FGF2 Signalgebung die Expansion von Vorläufern des Knochenmarkstroma mit adipogenen und osteogenen Kapazitäten unterstützt, deren Differenzierung hemmt bei kontinuierlicher Gabe während der Differenzierungsinduktion gegeben wird und die Fähigkeit des Matrixumbaus von hBMSCs innerhalb einer kollagenen 3D Mikroumgebung verändert.

1. Introduction

1.1. Human bone marrow stromal cells

1.1.1. Bone and bone marrow adipose tissue

Adult bone is far from being a static tissue as it is constantly being remodeled throughout life by cycles of sequential bone resorption and bone formation (Figure 1). During bone resorption, old bone is removed by osteoclasts, specialized cells that digest the mineralized bone matrix by acidification and releasing of lysosomal enzymes, creating a resorption lacuna. After a brief transition phase in which the created pit is prepared for the formation phase, another specialized cell type, the osteoblasts, synthesize a scaffold of bone matrix composed of collagen and non-collagenous proteins that is later mineralized, forming the new bone (Bilezikian et al., 2002).

The most common disorder of bone remodeling is osteoporosis, a pathology in which the equilibrium between bone resorption and bone formation is disrupted, resulting in bone mass loss, structural deterioration of the bone and therefore, increased risk to fractures. Higher levels of bone resorption and a diminished osteoblastic function are the main factors responsible for this outcome (Duque & Troen, 2008; Kassem & Marie, 2011). Osteoporosis can be triggered by estrogen deficiency in menopausal women or by aging in both women and men. Additionally, osteoporosis can arise as a secondary consequence of other conditions or therapies such as immobilization and glucocorticoid treatment (Feng & McDonald, 2011). Besides bone loss, osteoporosis is characterized by a parallel increment in bone marrow adiposity (Justesen et al., 2001; Meunieret al., 1971; Verma et al., 2002). Remarkably, a reciprocal relation between bone mass and marrow fat is not only observed in osteoporotic subjects but also in healthy young and aged adults (Di Iorgi et al., 2010; 2008; Justesen et al., 2001; Wren et al., 2011).

Despite being virtually inexistent at birth, marrow adipose tissue accounts for approximately 70% of the marrow volume in healthy adults (Rosen et al.). It continuously accumulates over time replacing the hematopoietic tissue and, although it was originally considered a “filler” tissue, currently it is thought to play a role in skeletal and systemic metabolism (Cawthorn et al., 2014; Scheller & Rosen, 2014).

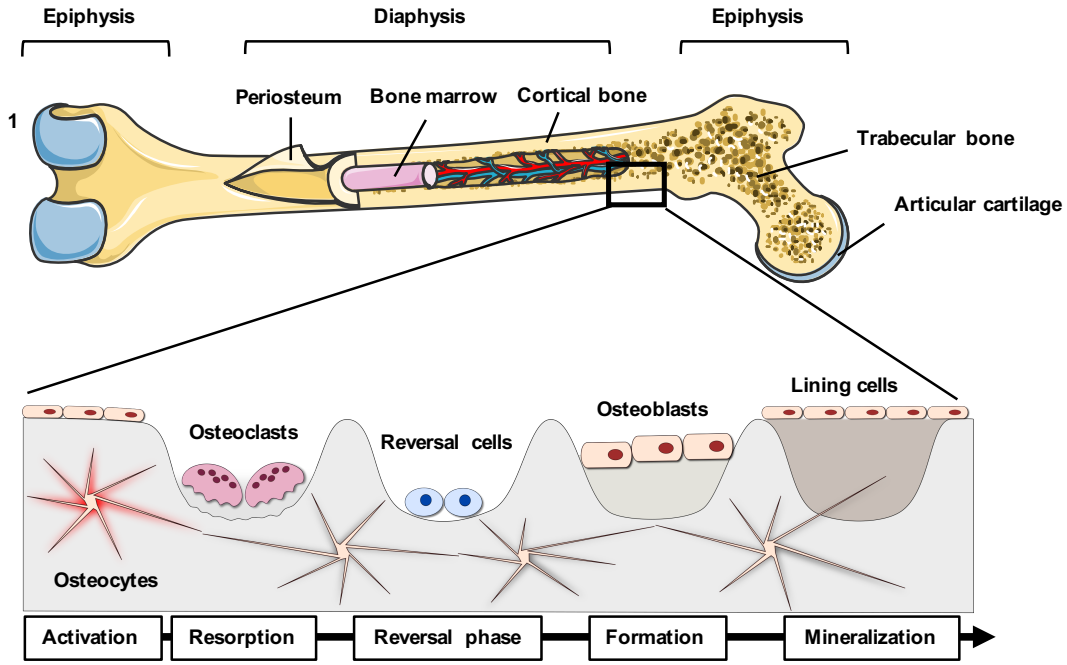

Figure 1. Bone structure and remodeling.
The bone remodeling cycle begins with an activation phase in which signals coming from bone cells and bone matrix lead to the recruitment of osteoclasts progenitors from the hematopoietic lineage, their differentiation and attachment to the bone surface. The mineralized bone matrix is dissolved by osteoclastic activity through acidification and the release of lysosomal enzymes. Resorption is tightly couple to the recruitment of osteoblast and the control of osteoblastic activity by factors secreted by osteoclasts as well as by factors released from the bone matrix. After resorption is complete, reversal cells complete the cleaning and preparation of the remodeling pit for the formation phase, in which osteoblasts deposit osteoid, the collagenous organic matrix of the bone. After osteoid formation, osteoblasts can differentiate into lining cells, covering the bone surface, into osteocytes that remained embedded within the bone matrix or undergo apoptosis. The final step of remodeling is the mineralization of the newly formed osteoid by deposition of hydroxyapatite crystals (Sims & Gooi, 2008). [1]Adapted from Servier Medical Art.

Several hypotheses aiming to explain the inverse relation between bone and marrow adipocytes have been suggested. Some of the existing evidence points to causative roles of marrow adipocytes in bone loss due to negative effects of adipokines on osteoblast differentiation and function (Liu et al., 2010; Taipaleenmäki et al., 2011), adipose tissue-induced lipotoxicity affecting osteoblasts (Elbaz et al., 2010; Gunaratnam et al. , 2014; Maurin et al., 2002) and increased osteoclast activity induced by adipocyte-secreted factors (Goto et al., 2011; Holt et al., 2014). Another possible explanation for this inverse relationship is based on the current "common stromal progenitor" hypothesis. Osteoblasts differentiate from a population of postnatal non-hematopoietic stem cells (Sacchetti et al., 2007), known as skeletal, stromal or mesenchymal stem cells, which also sustain the other stromal components of the bone marrow, including the marrow adipocytes (Bianco & Robey, 2015; Bianco et al., 2006) (Figure 2). Hence, a skewed differentiation of the common precursor towards the adipogenic lineage in detriment of the osteogenic pathway

is thought to play a role in bone loss and the concomitant marrow adiposity observed in osteoporosis and aging (Sadie-Van Gijsen et al., 2013).

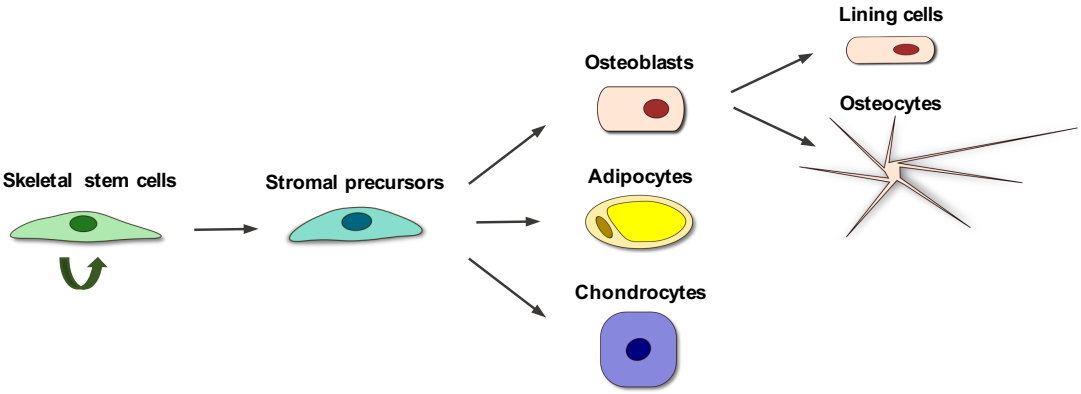

Figure 2. Postnatal skeletal stem cell and derived stromal components.
Postnatal skeletal stem cells residing in the bone marrow, probably located in the surface of blood vessel and sinusoids, are capable of self-renewal and are considered to be the common progenitor of osteoblasts, chondrocytes and marrow adipocytes. Osteoblasts can terminally differentiate into lining cells that cover the bone surface or bone-embedded osteocytes, which form a network within the bone matrix through long cell processes and represent up to 95% of all bone cells.

1.1.2. *In vitro* culture and differentiation of hBMSCs

Bone marrow stromal cells (BMSCs) were first isolated by Friedenstein and colleagues as plastic-adherent fibroblastic cells with the ability to form colonies when cultured *in vitro* (Friedenstein et al., 1974). Later, *in vitro* expanded BMSCs isolated from adult human bone marrow (hBMSCs) were shown to have bone forming capacity when implanted into immunodeficient mice (Haynesworth et al., 1992; Kuznetsov et al., 1997).

When exposed to inductive chemical cocktails in culture, bulk hBMSC cultures showed the capacity to differentiate into osteoblasts, chondrocytes and adipocytes. A clonal analysis revealed that cells expanded from some individual hBMSCs were able to differentiate into the three cell types, suggesting that those tripotent colony forming units corresponded to multipotent skeletal stem cells (Pittenger et al., 1999).

Bulk heterogeneous hBMSCs cultures, which include those multipotent skeletal progenitors as well as partially and fully committed progenies (Bianco, 2014), have been extensively used as a cellular model for osteogenic and adipogenic differentiation of the stromal common precursor of osteoblasts and marrow adipocytes. In addition, their relatively easy isolation and their *in vitro* expansion and differentiation capacity has turned them into an attractive candidate for clinical use in regenerative medicine, although some studies linked their therapeutic benefit to immune

and microenvironmental modulatory properties due to secreted factors rather than engraftment (Galderisi & Giordano, 2014; Mezey, 2011).

The major determinants of BMSC differentiation are the transcription factors runt-related transcription factor 2 (Runx2; formerly known as Cbfa1) and the peroxisome proliferator-activated receptor γ 2 (PPARγ2). Pro-osteogenic signals eventually trigger the activation of Runx2, whereas pro-adipogenic signaling activates PPARγ2, the "master" regulator of adipogenesis (James, 2013).

1.1.2.1. Osteogenic differentiation

Throughout the course of osteogenesis, BMSCs progress through the stages of pre-osteoblasts, immature osteoblasts and mature osteoblasts, each one characterized by the induction of a particular set of genes which allow for proliferation, matrix production and matrix mineralization, respectively (Rosen, 2009).

Early events in the commitment of BMSCs into pre-osteoblasts include the essential upregulation and activation of Runx2 (Ducy et al., 1999; Komori et al., 1997). This early transcriptional regulator, in conjunction with interacting factors such as its co-activators CBFβ1 (Kanatani et al., 2006; Kundu et al., 2002) and TAZ (Hong et al., 2005), trigger the expression of early osteoblastic genes such as the osteogenic transcription factor Osterix (Nakashima et al., 2002; Nishio et al., 2006), alkaline phosphatase and collagen type I. Later, the progression into mature osteoblasts is characterized by the upregulation of bone sialoprotein, osteopontin and osteocalcin, among others (Rosen, 2009).

Differentiated osteoblasts deposit an organic extracellular matrix compose mainly of collagen type I, proteoglycans and other non-collagenous matrix proteins. Subsequently, the organic matrix is mineralized by the deposition of hydroxyapatite crystals, build from calcium and phosphate ions. Alkaline phosphatase as well as the non-collagenous matrix proteins bone sialoprotein, osteopontin and osteocalcin are considered to play important roles in matrix mineralization (Clarke, 2008; Florencio-Silva et al., 2015).

Osteoblasts can further transition into matrix-embedded osteocytes, a process characterized by the downregulation of osteoblastic markers and the expression of specific osteocytic proteins such as dentin matrix acidic phosphoprotein 1 (DMP1), which participate in phosphate homeostasis, and the negative regulator of bone formation sclerostin (SOST) (Dallas & Bonewald, 2010).

Conventional *in vitro* induction of hBMSC osteogenesis is achieved by culturing the cells as a plastic-adherent monolayer with ascorbic acid, β-glycerophosphate and the glucocorticoid

dexamethasone in the presence of fetal calf serum (FCS) (Jaiswal et al., 1997). Under these osteogenic conditions, differentiating cells recapitulate the step-wise upregulation of Runx2, early- and late-osteogenic markers which finally result in the deposition of a mineralized extracellular matrix. Specifically, dexamethasone induces the expression and activation of Runx2, ascorbic acid induces the production of type I collagen and β-glycerophosphate acts as a source of phosphate required for mineralization (Langenbach & Handschel, 2013).

1.1.2.2. Adipogenic differentiation

Although marrow and peripheral adipose tissue have been shown to be metabolically and phenotypically distinct (Hardouin et al., 2016), the current model assumes that the molecular mechanisms controlling adipocyte differentiation from bone marrow and peripheral progenitors are shared (Rosen et al., 2009).

Adipogenesis is generally described as a two-phase process that begins with the commitment and progression of progenitors into pre-adipocytes and ends with the terminal differentiation into mature adipocytes (Tang & Lane, 2012).

While adipogenic commitment involves several signaling cascades including Wnt, bone morphogenetic protein (Bmp), insulin-like growth factor (IGF) and fibroblast growth factor (FGF) signaling (Lowe et al., 2011), differentiation is controlled by PPARγ2 and C/EBPα, a member of the CCAAT-enhancer-binding protein (C/EBP) family (Lefterova et al., 2008; Z. Wu et al., 1999). Additionally, other members of the C/EBP family, C/EBPβ and C/EBPδ, play an important role as early regulators of PPARγ2 and C/EBPα expression (Hamm et al., 2001; Yeh et al., 1995). Mature marrow adipocytes are characterized by a unilocular lipid droplet, as white adipocytes, and the expression of adipocytic genes such glycerol-3-phosphate dehydrogenase (GPDH), fatty acid binding protein 4 (FABP4; formerly knowns as adipocyte protein 2 or aP2), lipoprotein lipase (LPL) and adiponectin (Poloni et al., 2013).

For the modeling of hBMSC adipogenic differentiation *in vitro*, FCS-containing culture medium is supplemented with a cocktail consisting of insulin, 3-isobutyl-1-methylxanthine (IBMX), indomethacin and dexamethasone (Pittenger et al., 1999). Adipocytic induction results in the progressive accumulation of intracellular lipid droplets that eventually fuse into a unique one and the expression of typical adipocytic markers.

1.1.2.3. hBMSC differentiation balance

Several extracellular signals are candidate regulators of the lineage commitment of bone marrow stromal progenitors. Although the *in vivo* evidence is frequently unclear and controversial, several

physiological factors such as hormones, growth factors, cytokines and adipokines as well as therapeutic drugs have been found to modulate *in vitro* the hBMSC differentiation into the adipogenic or the osteogenic fate in an inverse manner.

For instance, estrogens (Heim et al., 2004), leptin (Thomas et al., 1999), melatonin (Zhang et al., 2010), lovastatin (Li et al., 2003), oxytocin (Elabd et al., 2008) and the bisphosphonate alendronate (Duque & Rivas, 2007) have all shown a positive effect on osteogenic differentiation and a parallel inhibition of adipogenic differentiation in hBMSC *in vitro*. On the other hand, the PPARγ ligand rosiglitazone (Benvenuti et al., 2007) and the prostaglandin E_2 (Noack et al., 2016) have a suppressive effect on osteogenic differentiation while enhancing adipocyte formation.

Additionally, several signaling pathways involved in differentiation of skeletal progenitors have been reported to exert opposite effects on adipogenesis and osteogenesis *in vitro*. For example, activation of the canonical Wnt signaling by Wnt6, Wnt10a and Wnt10b increases osteogenic but hampers adipogenic differentiation, while suppression of the signaling results in the opposite outcome (Cawthorn et al., 2012). Similarly, Sonic hedgehog (Spinella-Jaegle et al., 2001) and Notch (Ugarte et al., 2009) signaling have been shown to favor the osteogenic lineage while negatively affecting the adipogenic one.

Of particular interest for this work is the role of fibroblast growth factor (FGF) signaling in hBMSC differentiation balance. More precisely, the ligand FGF1 was identified by our group as a potential modulator of hBMSC differentiation balance using an *in vitro* model of differentiation induction switching (Schilling et al., 2008; 2007). By microarray analysis, FGF1 was found to be reciprocally regulated at the mRNA level when the differentiation inductive conditions changed from osteogenic to adipogenic and vice versa. Specifically, FGF1 was downregulated during osteogenic to adipogenic and upregulated during adipogenic to osteogenic switching, suggesting that FGF1 could play a pro-osteogenic and anti-adipogenic role.

1.2. Fibroblast growth factor signaling

1.2.1. FGFs and FGF receptors

The human FGF family currently consist of 22 members; 18 of them are secreted proteins, namely FGF1 to FGF10 and FGF16 to FGF23, capable of activating surface tyrosine kinase FGF receptors (FGFRs) (Beenken & Mohammadi, 2009). Four FGFs, FGF11 to FGF14, also known as FGF homologous factors, although displaying sequence homology to the other FGFs, act intracellularly and cannot activate FGFRs (Olsen et al., 2003), therefore some authors do not consider them as members of the family. Additionally, FGF15, which is not present in human, is an orthologue of

human FGF19 (Beenken & Mohammadi, 2009). While FGF sizes vary between approximately 150 to 300 amino acids, they share a 120-amino-acid conserved core with an identity of approximately 30-60% (Itoh & Ornitz, 2004).

Secreted FGFs are classified into six subfamilies based on their amino acid sequence, function and phylogenetic analysis. The FGF1 (including FGF1 and FGF2), FGF4 (including FGF4, FGF5 and FGF6), FGF7 (including FGF3, FGF7, FGF10 and FGF22), FGF8 (including FGF8, FGF17 and FGF18) and FGF9 (including FGF9, FGF16 and FGF20) subfamilies act in a paracrine manner while the FGF19 (including FGF19, FGF21 and FGF23) subfamily does it in an endocrine fashion (Ornitz & Itoh, 2015).

Secreted FGFs participate in multiple biological processes including development, metabolism and tissue homeostasis, playing major roles in cellular proliferation, migration and differentiation (Belov & Mohammadi, 2013; Teven et al., 2014). They bind and activate FGFRs, which consist of an extracellular ligand-binding domain with three extracellular immunoglobulin-like domains (D1, D2 and D3), a transmembrane domain and a cytoplasmic tyrosine kinase domain (Itoh & Ornitz, 2011). There are four highly conserved FGFRs, FGFR1 to FGFR4, encoded by four different genes. Alternative splicing occurring for FGFR1, FGFR2 and FGFR3 in the immunoglobulin-like domain D3 generates isoforms b and c for these receptors, which influences ligand specificity. These isoforms display tissue-preferential expression, being the isoforms b mostly expressed in epithelial tissues and the isoforms c in mesenchymal tissues (Ornitz et al., 1996; Zhang et al., 2006). In hBMSCs, for instance, FGFR1b, FGFR1c, and FGFR2c are the only FGFRs consistently expressed (Coutu et al., 2011).

Paracrine FGFs require heparan sulfate (HS) as a mandatory co-factor (Rapraeger et al., 1991; Yayon et al., 1991). HSs are linear chains of disaccharide units composed of glucuronic acid and N-acetylglucosamine with variable N-sulphated domains, which are covalently bound to membrane or ECM proteins. Given that HSs are structurally highly diverse, the interaction of FGFs and HSs also impacts the affinity and specificity for FGFRs (Ornitz & Itoh, 2015).

Signaling through FGFRs occurs after receptor dimerization induced by ligand binding. The resulted complex consists of two FGFs, two heparin sulfate chains, and two FGFRs (Schlessinger et al., 2000). Dimerization leads to a series of sequential trans-autophosphorylations by the cytoplasmic tyrosine kinase domains (Bae et al., 2010; Chen et al., 2008; Furdui et al., 2006).

The main intracellular substrate of activated FGFRs is the scaffold protein FGFR substrate 2α (FRS2α) (Gotoh, 2008), which initiates downstream signaling through the RAS/MAPK and PI3K/AKT pathways. Another prominent substrate targeted by activated FGFRs is phospholipase Cγ1, which then triggers the activation of protein kinase C (Goetz & Mohammadi, 2013).

1.2.2. FGF1 subfamily

FGF1 and FGF2, also known as acidic and basic FGF, respectively, are the two members of the FGF1 subfamily. They are paracrine-acting FGFs that lack secretory signal peptides and, therefore, are released in a non-canonical manner by direct translocation across the plasma membrane (Nickel, 2011). Regarding receptor specificity, whereas FGF2 is not able to activate the b isoforms of FGFR2 and FGFR3, FGF1 activates all FGFR isoforms, a unique characteristic among FGFs (Ornitz et al., 1996).

In addition to its paracrine activity, FGF1 and FGF2 are capable of acting independently of FGFRs, in an intracrine fashion (Bouleau et al., 2005). In humans, five FGF2 isoforms derived from alternative translation initiation of a single gene have been identified (Arnaud et al., 1999; Florkiewicz & Sommer, 1989; Prats et al., 1989). Four of them are referred as high molecular weight (HMW) isoforms of 22, 22.5, 24 and 34 kDa, while the 18 kDa isoform is known as the low molecular weight (LMW) isoform (Chlebova et al., 2009). In contrast to the secreted LMW isoform, the HMW isoforms present a nuclear localization and therefore, they act in an intracrine FGFR-independent manner (Bugler et al., 1991). FGF1, on the other hand, is translated as a 17.5 kDa protein that also contains a nuclear localization signal (Imamura et al., 1990). Moreover, the internalization and nuclear translocation of exogenous FGF1 and FGF2 have been documented as well (Zakrzewska et al., 2008).

Knockout murine models for FGF1 and FGF2 are both viable and fertile but display different phenotypes (Miller et al., 2000). Animals lacking FGF1 do not show any particular phenotype unless challenged with a high-fat diet, when they develop an aberrant visceral fat expansion and a profound diabetic phenotype with severe insulin resistance, indicating that FGF1 plays a critical role in the remodeling of endocrine fat and metabolic homeostasis (Jonker et al., 2012). Animals lacking FGF2, on the other hand, display neuronal (Ortega et al., 1998) and vascular defects (Zhou et al., 1998), impaired blood pressure regulation (Dono et al., 1998), decreased wound healing capacity (Ortega et al., 1998) and skeletal anomalies (Montero et al., 2000).

1.2.3. Paracrine FGF signaling and bone

As learned mainly from animal models and human pathologies, FGF signaling participates in skeletal development as well as in postnatal skeletal homeostasis. Several human skeletal deformities are the result of mutations in FGFRs. For instance, craniosynostosis syndromes, characterized by premature fusion of the cranial sutures, are associated with gain-of-function mutations in FGFR1 (Bellus et al., 1996), FGFR2 (Bellus et al., 1996; Jabs et al., 1994; Reardon et al., 1994; Wilkie et al., 1995) and FGFR3 (Bellus et al., 1996; Muenke et al., 1997). Loss-of-function

mutations in FGFR3, on the other hand, are responsible for several types of short-limbed dwarfism (Bonaventure et al., 1996).

Knockout mice for FGF2 (Homer-Bouthiette et al., 2014; Montero et al., 2000; Xiao et al., 2009), FGF9 (Hung et al., 2007) and FGF18 (Liu et al., 2002; Ohbayashi et al., 2002) display skeletal anomalies. Particularly for FGF2, the skeletal phenotype is isoform-dependent. Homozygous knockout mice for all isoforms of FGF2 show comparable bone mineral density to wild type while young but display increased bone loss together with accumulation of marrow adipose tissue with age (Montero et al., 2000; Xiao et al., 2010b). Additionally, marrow stromal cells isolated from these mice show augmented adipogenic and diminished osteogenic differentiation *in vitro* (Xiao et al., 2010b), indicating the FGF2 signaling participates in controlling the balance between bone and marrow fat in aging. Similarly, LMW-specific knockout mice have reduced bone mass and decreased osteogenic capacity of BMSCs (Xiao et al., 2009). However, knockout mice for HMW isoforms display an opposite skeletal phenotype, with increased bone mineral density and volume and BMSCs isolated from these mice show enhanced osteogenic differentiation and mineralization (Homer-Bouthiette et al., 2014), indicating a divergent role for paracrine and intracrine FGF2 in bone metabolism.

FGF2 transgenic mice also present isoform-dependent anomalies in bone formation. All-isoforms overexpressing animals are dwarf with shortening of the bone length and display impaired mineralization and osteopenia (Coffin et al., 1995; Sobue et al., 2005). The osteoblast-lineage-specific overexpression of the LMW FGF2, however, results in increased bone mass and thickness mediated by the modulation of the Wnt pathway (Xiao et al., 2009), indicating that LMW FGF2 acts as a positive regulator of osteogenesis in osteoblastic cells. On the contrary, mice overexpressing the HMW isoforms display dwarfism, decreased bone mineral density and osteomalacia, in part as the result of increased levels of FGF23, an endocrine FGF family member that triggers hypophosphatemia via signaling through FGFRs and the co-receptor KLOTHO in the kidneys (Xiao et al., 2010a).

1.3. Three-dimensional culture models for hBMSC

In multicellular organisms, basically all cells reside in contact with neighbor cells within the complex three-dimensional (3D) environment provided by the ECM. This interwoven assembly of fibrous proteins and polysaccharides acts as a structural support as well as a source of biochemical and mechanical cues that are able to influence cellular behavior (Frantz et al., 2010). At the same time, cells are able to degrade and rebuild the surrounding fibrous meshwork, resulting in the constant remodeling of the ECM (Daley et al., 2008).

Given the significant role of the ECM in diverse cellular processes such as proliferation (Winer et al. , 2009), morphology, migration, adhesion (Hakkinen et al., 2011) and differentiation (Santiago et al., 2009), it is acknowledged that conventional two-dimensional (2D) culture models lacking the ECM component are very far from representing *in vivo* conditions, which may lead to physiologically irrelevant findings. For instance, mesenchymal cells cultured as 2D monolayers in plastic are forced to be in contact with a very stiff planar substrate by only a segment of the cell, generating an artificial polarity that is not representative of their natural phenotype (Cukierman et al., 2001). Hence, 3D *in vitro* models are considered to be much more representative of the conditions found *in vivo* (Pampaloni et al., 2007).

Several 3D culture platforms, such as multicellular spheroids (Baraniak & McDevitt, 2012; W. Wang et al., 2009), silk-based hydrogels (Calabrese & Kaplan, 2012) and collagen sponges (Neuss et al., 2008) have been shown to support both hBMSC osteogenic and adipogenic differentiation.

1.3.1. Collagen hydrogels

Compared to 2D culture systems and other non-physiological scaffolds, 3D models based on cells embedded in physiologically relevant matrices are considered to represent more closely the *in vivo* situation (Higuchi et al., 2012).

Collagens are the main components of extracellular matrices. The vertebrate collagen family comprises 28 members (I to XXVIII) encoded by 45 different genes (Kadler et al., 2007). A common feature of all collagens is a trimeric structure, i.e. they are formed by three polypeptide chains named α chains, which present at least one triple helix domain. The triple helix conformation contains the sequence motif Gly-X-Y, where X and Y are frequently proline residues, often post-translationally modified to hydroxyproline when in position Y (Ricard-Blum, 2011).

The collagen family is subclassified based on the supramolecular arrangement into fibril-forming collagens (types I, II, III, V, XI, XXIV and XXVII), fibril-associated collagens (IX, XII, XIV, XVI, XIX, XX, XXI, XXII and XXVI), beaded-filament forming collagen (VI), anchoring fibrils forming collagen (VII), transmembrane collagen (XIII, XVII, XXIII and XXV), network forming collagens (IV, VIII and X) and multiplexins (XV and XVIII) (Heino, 2007).

The bone marrow ECM contains several types of collagens, including the fibrillar type I, which is also the main organic component of bone (Chen, 2010). Collagen I is an heterotrimer formed by two α1 chains (encoded by the COL1A1 gene) and one α2 chain (encoded by the COL2A1 gene) (Young, 2003). It contains one major triple helix domain with no imperfections that comprises 96% of the protein structure (Ricard-Blum, 2011) and has a rod-like shape with a diameter of 1.5 nm and a length of 300 nm, approximately (Exposito et al., 2010).

Collagen I is first synthesized as a soluble procollagen heterotrimer containing N- and C-propeptides, which are cleaved in order to generate the mature collagen molecule (Greenspan, 2005). Mature collagen I associates into fibrils held together by hydrogen bonds and covalent cross-linking through lysine aldehyde and hydroxylysine aldehyde pathways (Eyre & Wu, 2005). Beside collagen I molecules, other participants are required for fibril assembling *in vivo,* such as collagens V and XI acting as fibril nucleators, fibronectin and integrins (Kadler et al., 2008).

Purified collagen I is able to assemble spontaneously into fibrils *in vitro*. In acidic solutions, collagen I remains soluble but adjusting the pH and the temperature to physiological values induces the formation of a highly hydrated gel (Higuchi et al., 2012).

1.3.1.1. hBMSCs and collagen matrix interaction

hBMSCs interact with collagen type I via integrins and discoidin domain receptors. Integrins are dimeric adhesion receptors composed by one α and one β subunit. The integrin family comprises 24 members formed by combinations of 18 α and 8 β subunits (Hynes, 2002). The integrins α1β1, α2β1, α10β1, and α11β1 are all collagen receptors with α2β1 acting as a high-affinity receptor for collagen I fibrils (Leitinger, 2011). hBMSCs have been shown to express α1β1 and α2β1 integrins *in vitro* (Gronthos et al., 2001) and that their interaction with collagen I hydrogels is dependent on β1-integrin engagement (Heckmann et al., 2006).

Discoidin domain receptors 1 and 2 (DDR1 and DDR2) are receptor tyrosine kinases that act as collagen sensors (Shrivastava et al., 1997; Vogel et al., 1997). Activation of DDRs by collagens occurs independently of integrins and is a comparatively slow process that requires a sustained binding (Vogel et al., 2000). Both DDR1 and DDR2 can be activated by collagen I fibrils (Shrivastava et al., 1997; Vogel et al., 1997). DDR1 is upregulated in hBMSCs when cultured inside 3D collagen hydrogels and hindering the sensing of the collagenous 3D matrix via DDR1 affects cell morphology and matrix organization (Lund et al., 2009a).

Beside binding and sensing, cells are also able to remodel and exert proteolytic activity on the 3D collagenous ECM (Chevallay & Herbage, 2000). Collagen I proteolysis is mediated by a subgroup of matrix metalloproteinases (MMPs) with collagenolytic activity. The human MMP family comprises at least 23 Ca- and Zn-dependent endopeptidases that present different localization and substrate specificities and are classified accordingly as collagenases (MMP1, MMP8 and MMP13), gelatinases (MMP2 and MMP9), stromelysins (MMP3 and MMP10), matrilysins (MMP7, MMP11 and MMP26), membrane-type (MT1-MMP to MT6-MMP, also known as MMP14, MMP15, MMP16, MMP17, MMP24 and MMP25, respectively) and others (Nagase et al., 2006). Beside collagenases, other MMPs such as MMP2 (Aimes & Quigley, 1995) and MT1-MMP (Ohuchi et al., 1997) also display collagenolytic activity. MMPs are synthesized as zymogens that require the

proteolytic removal of a propeptide to become active. Extracellular activation of soluble MMPs is carried out by other MMPs or serine proteases. MT-MMPs, MMP11 and MMP28, on the other hand, are activated intracellularly by furin-like serine proteases present in the secretory pathway (Stamenkovic, 2003). In addition to regulation at transcriptional (Yan & Boyd, 2007) and activation levels (Ra & Parks, 2007), MMP activity is regulated by endogenous inhibitors. Tissue inhibitors of metalloproteinases (TIMPs) are negative regulators of MMPs that bind with a 1:1 stoichiometry, inhibiting MMP activity (Visse & Nagase, 2003). The four TIMPs, TIMP1 to TIMP4, are able to inhibit virtually all MMPs, although TIMP1 displays poor inhibitory capacity over MT1-MMP, MT3-MMP, MT5-MMP and MMP19 (Murphy, 2011).

1.4. Hypothesis and aims

Bone loss and the parallel accumulation of adipose tissue in the bone marrow during aging and, more extensively, in osteoporosis have been in part related to a shift in the differentiation program of the common stromal progenitor of osteoblasts and marrow adipocytes. Indeed, when compared with healthy donors, hBMSC isolated from osteoporotic patients show an inverse relationship between osteogenic and adipogenic differentiation, in favor of the latter (Astudillo et al., 2008; Rodríguez et al., 1999; Rodríguez et al., 2000). Hence, precluding the adipogenic fate of stromal marrow progenitors arises as a possibility for the treatment of conditions characterized by this increased bone marrow adiposity and reduction of bone tissue, such as aging and osteoporosis (Justesen et al., 2001; Verma et al., 2002).

Our group became interested in FGF1 signaling as a potential modulator of hBMSC differentiation balance after identifying a reciprocally regulated expression under osteogenic/adipogenic inductive condition switching, which suggested a pro-osteogenic/anti-adipogenic role (Schilling et al., 2008). Additionally, *in vivo* evidence supports the potential of FGF1 as a pro-osteogenic factor. A systemic administration of FGF1 in adult rats is able to rescue the bone loss induced by ovariectomization (Dunstan et al., 1999), suggesting that it may be able to modulate the differentiation of osteogenic precursors *in vivo*. Additionally, the role of FGF2, the other member of the FGF1 subfamily, was also investigated for comparison purposes. Given that FGF2 was only found to be downregulated after osteogenic-to-adipogenic condition switching (Schilling et al., 2008), a difference in the potential regulation of adipogenesis and osteogenesis by FGF1 and FGF2 was hypothesized.

Although most of the research investigating hBMSC differentiation balance has been performed in traditional 2D culture on plastic surfaces, this completely fails to re-capitulate the physiological

3D environment, and therefore, an *in vitro* model of hBMSC differentiation in a 3D collagen-based matrix would better mimic the *in vivo* microenvironment.

Based on the hypothesis that autocrine/paracrine FGF1 signaling would play an anti-adipogenic and pro-osteogenic role in hBMSC differentiation, the aims of this thesis were:

I) to establish a 3D hBMSC osteogenic and adipogenic differentiation model based on collagen type I gels,

II) to evaluate the role of FGF1 on adipogenic and osteogenic differentiation of hBMSCs in the 3D model and,

III) to evaluate the role of FGF1 in the adipogenic and osteogenic differentiation potential of hBMSCs.

2. Materials and Methods

2.1. Materials

2.1.1. Reagents and stock solutions

Acetic acid 100%, Carl Roth.

Agarose, LE, Biozym Scientific.

Agarose, Plaque, Biozym Scientific.

Alizarin Red S, Sigma-Aldrich.

1% Alizarin Red S, pH 4.2: dissolved in dH2O, pH adjusted with 0.5% ammonium hydroxide. Filtered and stored protected from light at room temperature.

Anti-TIMP1 antibody; mouse monoclonal anti-human TIMP1, 0.1 mg/ml, ab1827, Abcam.

Ammonium hydroxide, Merck Millipore.

Antibiotic/Antimycotic; 100 U/mL penicillin, 100 mg/mL streptomycin, 0.025 mg/mL fungizone, Life Technologies.

L-Ascorbic acid 2-phosphate, Sigma-Aldrich.

Stock solution: 50 mg/ml L-ascorbic acid 2-phosphate in dH_2O. Sterilized by filtration. Stored in aliquots at -20°C.

Aquatex®, Merck Millipore.

Bovine Serum Albumin (BSA), fatty acid free, low endotoxin, Sigma-Aldrich.

Chloroform, Carl Roth.

Collagen type I, isolated from rat tail, Prof. Heike Walles, University of Wuerzburg.

Collagenase NB4, Serva Electrophoresis.

Stock solution: 10 mg/ml collagenase in PBS^+. Sterilized by filtration. Stored in aliquots at -20°C.

Dexamethasone, Sigma-Aldrich.

Stock solution: 10 mM dexamethasone (392.5 g/mol) in ethanol. Stored in aliquots at -80°C.

Dimethylsulfoxide (DMSO), Carl Roth.

DMEM, high glucose, Life Technologies.

DMEM, powder, high glucose, Life Technologies.

DMEM/F-12, GlutaMAX™ supplement, Life Technologies.

DNA ladder, peqGOLD 100 bp DNA Ladder Plus, PeqLab Biotechnologie.

DNA loading dye, 6x, PeqLab Biotechnologie.

dNTP mix, Bioline.

Dulbecco's phosphate buffered saline, without Ca^{2+}/Mg^{2+} (PBS), Sigma-Aldrich.

Dulbecco's phosphate buffered saline, with Ca^{2+}/Mg^{2+} (PBS^+), Sigma-Aldrich.

Entellan, Merck Millipore.

Eosin, Sigma-Aldrich.

Ethanol, 96%, Carl Roth.

Ethanol, absolute, AppliChem.

Ethylenediaminetetraacetic acid (EDTA), AppliChem.

Fetal Calf Serum (FCS), Biochrom.

FGF1, recombinant human (rhFGF1), *E. coli*-derived Phe16-Asp155, 15.5 kDa, R&D Systems.

Stock solution: 25 µg/ml rhFGF1 in 1 mg/ml BSA. Stored in aliquots at -20°C.

FGF2, recombinant human (rhFGF2), *E. coli*-derived Pro143-Ser288, 16.5 kDa, R&D Systems.

Stock solution: 25 µg/ml rhFGF2 in 1 mg/ml BSA. Stored in aliquots at -20°C.

GelRed®, Genaxxon BioScience.

β-Glycerophosphate, Sigma-Aldrich.

Stock solution: 1 M β-glycerophosphate (216.0 g/mol) in dH_2O. Sterilized by filtration. Stored in aliquots at -20°C.

Hematoxylin Solution, Mayer's, Sigma-Aldrich.

Heparin sodium salt from porcine intestinal mucosa, grade I-A, Sigma-Aldrich.

Stock solution: 26 mg/ml heparin in sterile dH_2O. Stored in aliquots at 4°C.

HEPES, Applichem.

Hydrochloride acid, 1 N, Applichem.

Hydrogen peroxide, Fluka.

Indomethacin, Sigma-Aldrich.

Stock solution: 100 mM indomethacin (357.8 g/mol) in DMSO. Stored in aliquots at -20°C.

Insulin from bovine pancreas, Sigma-Aldrich.

Stock solution: 2 mg/ml insulin in sterile 5% acetic acid. Stored in aliquots at -20°C.

3-Isobutyl-1-methylxanthine (IBMX), Applichem.

Stock solution: 500 mM IBMX (222.2 g/mol) in DMSO. Stored in aliquots at -20°C.

KAPA SYBR® FAST qPCR Kit Universal, KAPA Biosystems.

Leukocyte Alkaline Phosphatase Kit, based on Naphthol AS-BI and Fast Blue BB salt, Sigma-Aldrich.

M-MLV Reverse Transcriptase, Promega.

M-MLV Reverse Transcriptase Buffer, Promega.

Mouse IgG1 Isotype Control; 0.5 mg/ml, MAB002, R&D Systems.

Nonfat dry milk powder, Applichem.

Normal horse serum, PAA Laboratories.

Oil Red O, Sigma-Aldrich.

0.3% Oil Red O: dissolved at 0.5% in 60% triethyl phosphate, diluted to 0.3% with dH_2O. Filtered and stored protected from light at room temperature.

Paraformaldehyde, Merck Millipore.

PD166866, Sigma-Aldrich.

Stock solution: 1 mM PD166866 in DMSO. Stored in aliquots at -20°C.

Phalloidin-CF™488A, Biotium.

Stock solution: 200 units/ml phalloidin-CF™488A in ddH_2O. Stored in aliquots at -20°C protected from light.

2-Propanol, Applichem.

2-Propanol (for molecular biology), Applichem.

Propidium iodide, Calbiochem.

Quant-iT™ PicoGreen® dsDNA Reagent, Life Technologies.

Random hexamer primers, Life Technologies.

Roti®-Histofix 4%, Carl Roth.

Roti®-histol, Carl Roth.

Salmon Sperm DNA, Sigma-Aldrich.

Saponin, Sigma-Aldrich.

Sodium hydrogen carbonate, Applichem.

Sodium hydroxide pellets, Merck Millipore.

Sodium hydroxide, 1 N, Applichem.

SU5402, Calbiochem.

Stock solution: 10 mM SU5402 in DMSO. Stored in aliquots at -20°C.

Tissue-Tek® O.C.T Compound, Sakura.

Triethyl phosphate, Merck Millipore.

Tris, Applichem.

Triton X-100, Sigma-Aldrich.

TRIzol® Reagent, Life Technologies.

Trypan Blue, 0.4%, Sigma-Aldrich.

Trypsin-EDTA, 0.25%, phenol red, Life Technologies.

Tween® 20, Merck Millipore.

VECTASHIELD® mounting medium, Vector Laboratories.

VECTASTAIN® Universal Elite ABC Kit, Vector Laboratories.

Vector® NovaRED™ Substrate Kit, Vector Laboratories.

Water, HPLC grade (HPLC-H_2O), Carl Roth.

2.1.2. Consumables

Cell culture flasks, Greiner Bio-One.

Cell strainer, 100 µm, BD Falcon.

Conical tubes, Greiner Bio-One.

Coverslips, 24 x 50mm, A. Hartenstein.

Filter pipette tips, STARLAB.

Low Profile 8er Strips, Biozym Scientific.

Micro spoon, A. Hartenstein.
Optical Flat Cap Strips, Biozym Scientific.
Pasteur pipettes, A. Hartenstein.
Pestles, A. Hartenstein.
Pipette tips, Brandt.
Plates, 96-wells, black, flat bottom, Greiner Bio-One.
Reaction tubes, Greiner Bio-One.
Serological pipettes, Greiner Bio-One.
Strips, Biozym Scientific.
Superfrost Plus slides, Thermo Scientific.
Syringe filters, 0.2 µm, Carl Roth.

2.1.3. Equipment

Axiocam MRc, Carl Zeiss.
Axioskop 2 MOT, Carl Zeiss.
Balance, analytical, ABS 220-4, KERN.
Balance, precision, PCB 1000-2, KERN.
Biofuge Fresco, Heraeus.
Block heater, VWR.
Camera Canon EOS 1000D, Canon.
CFX Manager™ Software, version 3.0, Bio-Rad.
CFX96™ Real-Time PCR Detection System, Bio-Rad.
Cryostat CM1850, Leica.
Fluorescent Microscope BZ-9000, Keyence.
HERAcell™ 240i CO_2 Incubator, Thermo Scientific.
Heraeus™ Multifuge™ X1R, Thermo Scientific.
Infinite® M200, Tecan.
Magneticstirrer, A. Hartenstein.
NanoQuant Plate™, Tecan.
pH Meter inoLab®, WTW.
Safe 2020 Biological Safety Cabinet, Thermo Scientific.
Vortex-Genie 2, Scientific Industries.
Waterbath WNB 14, Memmert.

2.1.4. Software

AmplifX 1.7.0, by Nicolas Jullien; CNRS, Aix-Marseille Université - http://crn2m.univ-mrs.fr/pub/amplifx-dist
Axiovision Software, version 4.8, Carl Zeiss.
Fiji (Schindelin et al., 2012).
LinRegPCR software, version 2012 (Ramakers et al., 2003).
Papers 2, Mekentosj.
Prism 5 for Mac OS X, GraphPad Software.

2.2. Methods

2.2.1. Cell culture

2.2.1.1. Isolation of hBMSCs from trabecular bone

hBMSCs were isolated from femoral heads of patients undergoing total hip arthroplasty but otherwise healthy. The patient group comprised 10 females and 15 males with an age range of 41-83 years, 63 years in average. The isolation procedure was performed under informed consent of the patients and the approval of the Local Ethics Committee of the University of Wuerzburg.

hBMSCs were harvested from the trabecular bone of the femoral heads as previously described (Noth et al., 2007). Cells were extracted from trabecular bone plugs by sequential washing steps with culture medium and collected by centrifugation at 270 x g for 5 min. Cells were seeded at a density of 4.6 to 5.7 x 10^6 cell/cm^2 into 150 or 175 cm^2 cell culture flasks and cultured in a humidified atmosphere at 37°C with 5% CO_2. The hBMSC growth medium consisted of DMEM/F-12 supplemented with 10% FCS, antibiotic/antimycotic, and 50 mg/ml L-ascorbic acid 2-phosphate. Every 3 or 4 days, adherent hBMSCs were washed with PBS and fresh growth medium was added. Expanded cells were considered to be at passage 0.

2.2.1.2. Subculturing of hBMSCs

hBMSCs were subcultured at 70% confluence by washing the cell monolayer with PBS and incubating with 0.25% trypsin-EDTA for 5 to 10 min at 37°C. Trypsin activity was stopped by addition of growth medium and cells were collected by centrifugation at 280 x g for 5 min. Cell pellets were resuspended in growth medium and strained through a 100 µm cell strainer and

reseeded at a subculturing ratio of 1:3 into 150 or 175 cm^2 cell culture flasks. All the experiments were performed using hBMSCs at passage 2 or 3.

2.2.1.3. hBMSC-laden 3D collagen gels

Rat tail collagen type I at 6 mg/ml in 0.1% acetic acid, kindly provided by Prof. Heike Walles, University of Wuerzburg, was used as a stock solution for preparing cell-laden collagen gels of different final collagen concentration. Two-fold concentrated working solutions of 1.0, 1.5 and 2.0 mg/ml collagen were prepared by diluting the stock solution with 0.1% acetic acid.

Working collagen solutions were mixed 1:1 (v/v) with hBMSCs resuspended in a neutralization solution containing 21.44 µg/ml DMEM High Glucose buffered with 14.24 µg/ml HEPES and 5.92 µg/ml sodium hydrogen carbonate and further supplemented with 20% FCS.

The cell-collagen mixtures were pipetted into 96-well plates (200 µl/well) and placed at 37°C, 5% CO_2 for 30 min to induce gelation. Each gel was transferred with a micro spoon into a well of a 24-well plate pre-coated with 1% agarose to prevent cell attachment to the plastic. These free-floating collagen gels were maintained in 1 ml of growth medium at 37°C, 5% CO_2 for 24 h before induction of differentiation.

Digital images of the collagen gels were taken at different time points during the culture period and gel diameters were measured using Fiji (ImageJ) assuming a circular cross-section.

2.2.1.4. Induction of adipogenic differentiation

Adipogenic differentiation of hBMSCs was chemically induced by culturing the cells in DMEM High Glucose, 10% FCS, antibiotic/antimycotic and further supplemented with an adipogenic cocktail consisting of 100 mM indomethacine, 500 mM IBMX, 0.2 mg/ml insulin and 1 mM dexamethasone.

For hBMSCs embedded in collagen gels, adipogenic differentiation was induced 24 h after gel preparation. For adipogenic differentiation of hBMSCs cultured as 2D monolayers, cells were seeded at 0.08 x 10^6 cells/cm^2 in 12-well plates and maintained in growth medium for 24 h before differentiation induction. The first day the cells received induction medium is referred as day 0. In both cases, cells were maintained at 37°C, 5% CO_2 and adipogenic medium was refreshed every 3–4 days.

2.2.1.5. Induction of osteogenic differentiation

Osteogenic differentiation of hBMSCs was induced with an osteogenic inductive medium consisting of DMEM High Glucose, 10% FCS, antibiotic/antimycotic, plus 10 mM β-glycerophosphate, 50 mg/ml L-ascorbic acid 2-phosphate and 100 nM dexamethasone.

Osteogenic differentiation in collagen gels was induced 24 h after hBMSC embedding. In the case of monolayers, cells were seeded at 0.08 x 10^6 cells/cm^2 in 12-well plates and after 24 h in growth medium differentiation was induced. The first day the cells received induction medium is referred as day 0. Cells were maintained at 37°C, 5% CO_2 and osteogenic medium was replaced every 3–4 days.

2.2.1.6. Treatment with rhFGFs and FGFR inhibitors

Treatment of hBMSCs with rhFGF1 or rhFGF2 during differentiation induction was performed by adding the growth factors directly to the differentiation medium. Treatment was conducted from day 0 using final concentrations of 0, 1, 5 or 25 ng/ml rhFGF1 or rhFGF2. Heparin was always added together at 25 mg/ml as a stabilizing co-factor. Control conditions included the treatment with the carrier BSA alone or in combination with heparin.

Inhibition of FGFR signaling was achieved by addition of the specific small molecule inhibitors PD166866 (Panek et al., 1998) or SU5402 (Mohammadi et al., 1997) to the induction media. Final concentrations of 50, 100 and 250 nM PD166866 and of 10 and 20 µM SU5402 were employed. Addition of the vehicle DMSO was used as a control condition.

For experiments involving expansion of hBMSCs in the presence of rhFGF1 or rhFGF2, final concentrations of 5 and 25 ng/ml were tested. The growth factors were directly added to the growth medium together with 25 mg/ml heparin and maintained throughout one expansion passage.

2.2.1.7. Dead cell staining in collagen gels

Dead cells inside collagen gel were identified by propidium iodide staining. Propidium iodide is excluded from living cells and therefore only dead cells are permeable to the dye. hBMSCs-laden collagen gels were incubated with 2.5 mg/ml propidium iodide in PBS for 30 min at 37°C, washed twice with PBS, embedded in Tissue-Tek O.C.T Compound and snap-frozen in liquid N_2. Sections of 8 µm were cut in a cryostat, washed with PBS and mounted with Vectashield mounting medium containing DAPI.

As a positive control of dead cells, collagen gels were incubated with 0.1% saponin for 30 min before proceeding with the propidium iodide staining.

2.2.1.8. DNA quantification

For quantification of the DNA content inside collagen gels, these were first washed with PBS and completely digested with 0.2% collagenase, 0.025% trypsin in PBS^+ at 37°C. The resulting digestion solutions were diluted with one volume of 0.2% Triton X-100 in PBS and exposed to three freeze-thaw cycles. Lysates were diluted 5 times with TE buffer (10 mM Tris-HCl, 1 mM EDTA, pH 8.0) and stored at -80°C.

For DNA quantification in monolayer cultures, cells were washed with PBS^+, lysed with 0.1% Triton X-100 in PBS and exposed to three freeze-thaw cycles. Lysates were diluted 5 times with TE buffer and stored at -80°C.

DNA was quantified using the Quant-it PicoGreen assay according to the manufacturer's instructions. DNA standard curves were prepared using Salmon Sperm DNA. 50 µl of the DNA standards and samples were pipetted in duplicate into black 96-well plates. 50 µl of a 200-fold dilution of PicoGreen was added to each well, mixed and incubated for 5 min at room temperature, protected from light. Fluorescence emission at 520 nm after excitation at 480 nm was measured in an Infinite M200 plate reader.

2.2.2. Histo- and cytochemistry

For histochemical procedures, at indicated time points collagen gels were washed with PBS, embedded in Tissue-Tek O.C.T Compound and snap-frozen in liquid N_2. Cryosections of 10 µm thickness were cut in a cryostat and stored at -20°C until stained.

2.2.2.1. Hematoxylin and eosin staining

To visualize the distribution of hBMSCs embedded in collagen gels, cryosections were stained with hematoxylin and eosin. For this, cryosections were fixed with Roti-Histofix 4% for 10 min before stained with hematoxylin and 1% eosin. Stained sections were then dehydrated through a series of alcohols, cleared with Roti-histol and mounted with Entellan.

2.2.2.2. Oil Red O staining

Adipogenic differentiation was assessed by staining accumulated intracellular lipid droplets with Oil Red O. Based in a previously described method (Koopman et al., 2001), after adipogenic differentiation in 3D, collagen gel cryosections were rinsed once with PBS, fixed with Roti-Histofix 4% for 10 min and rinsed three times with distillate water. Samples were stained for 10 min with a 0.3% Oil Red O solution prepared from a 0.5% solution in 60% triethyl phosphate and diluted with distillate water. After rinsing three times with distillate water, cryosections were counterstained with hematoxylin for 10 min, rinsed three times with distillate water and three times with tap water, and mounted with Aquatex and a coverslip. Monolayer cultures were stained following the same protocol.

2.2.2.3. Alkaline phosphatase activity

Alkaline phosphatase activity was evaluated as an indicator of osteogenic differentiation. Histochemical demonstration of alkaline phosphatase activity was performed by staining using the Leukocyte Alkaline Phosphatase Kit, according to the manufacturer's instructions. Collagen gel cryosections or monolayer cultures were rinsed once with PBS, fixed with citrate-acetone-formaldehyde fixative solution for 30 s, rinsed three times with distillate water, stained with a staining solution containing nitrite, Naphthol AS-BI phosphate and Fast Blue BB base for 15 min, rinsed three times with distillate water, and mounted with Aquatex and a coverslip.

2.2.2.4. Alizarin Red S staining

After osteogenic differentiation induction in hBMSCs, deposition of mineralized matrix by differentiated osteoblasts was assessed by staining of calcium deposits with Alizarin Red S. Collagen gel cryosections were rinsed with PBS and fixed with Roti-Histofix 4% for 10 min. Samples were rinsed with distilled water and stained with 1% Alizarin Red S staining solution, pH 4.2 for 2 min, rinsed with distilled water, dehydrated with an alcohol series, cleared with Roti-histol and mounted with Entellan. The same staining protocol was followed for monolayer cultures directly in the culture plates, however, after rinsing of the staining solution, the samples were allowed to dry.

2.2.2.5. TIMP1 immunocytochemical staining

The expression levels of the extracellular matrix protein TIMP1 in collagen gels were evaluated by immunohistochemical staining. For this, cryosections were fixed with ice-cold methanol for 5 min, endogenous peroxidase activity was quenched by incubation with 0.3% hydrogen peroxide

in PBS for 30 min and blocking was performed using 1% normal horse serum in PBS. Cryosections were then incubated overnight with a mouse monoclonal anti-human TIMP1 antibody (2 mg/ml) or with an IgG1 isotype control at 4°C. After three washes with 0.1% Tween 20 in PBS, cryosections were incubated with a biotinylated anti-mouse IgG antibody for 1 h at room temperature, washed three times with PBS and incubated for 1 h with avidin and biotinylated horseradish peroxidase. Peroxidase activity was detected using the Vector NovaRED Substrate Kit. Cryosections were counterstained with hematoxylin, dehydrated through an alcohols series, cleared with Roti-histol and mounted with Entellan.

2.2.2.6. Phalloidin staining of actin cytoskeleton

Visualization of actin filaments was achieved by staining with a fluorescent phalloidin conjugate (Phalloidin-CF™488A). For this, hBMSCs were embedded in collagen gels at a density of 1 x 10^4 cells/ml and plated as 20 µl drops on 12 mm coverslips inside a well of a 12-well plate. Gels were maintained in 1 ml growth medium for 24 h before performing the staining. After rinsing once with PBS, cells were fixed with 4% paraformaldehyde for 10 min, washed 3 times with PBS and permeabilized with 0.5% Triton X-100 in PBS for 5 min. After three washes with PBS, gels were blocked with 3% non-fat dry milk in PBS for 30 min and washed once with PBS. Incubation with phalloidin staining solution (5 units/ml) was performed for 20 min in a covered container protected from light. After three washes with PBS, samples were mounted with VECTASHIELD-mounting medium containing DAPI and fixed with nail polish. Mounted samples were store at 4°C protected from light until imaged.

2.2.2.7. Image acquisition

Bright field images were captured using an Axioskop 2 MOT microscope equipped with an Axiocam MRc and the Axiovision 4.8 software. Fluorescence images were acquired using a BZ-9000 fluorescent microscope.

2.2.3. Molecular biology

2.2.3.1. RNA isolation

Total RNA was isolated using TRIzol Reagent according to the manufacturer's instructions. Six collagen gels per condition were collected together, snap-frozen in liquid N_2, ground with a pestle and homogenized with TRIzol Reagent. Samples were centrifuged at 12,000 x g for 10 min at 4°C to discard insoluble material. Supernatants were transferred into new tubes and 200 µl

chloroform per ml of TRIzol were added. Tubes were shaken vigorously by hand for 15 s, incubated for 2 min at room temperature and centrifuged at 12,000 x g for 15 min at 4°C. The aqueous phases were transferred into new tubes. 500 µl 2-propanol per ml of TRIzol were added. Samples were incubated for 10 min at room temperature and centrifuged at 12,000 x g for 10 min at 4°C. Pellets were washed with 1000 µl 75% ethanol and centrifuged at 7,500 x g for 5 min at 4°C. Pellets were resuspended in HPLC-H_2O and stored at -80°C. RNA quantity and purity were assessed using the NanoQuant Plate and the Infinite M200 plate reader.

2.2.3.2. cDNA synthesis

Reverse-transcription reactions were performed using 0.5–1.0 mg total RNA, random primers and the M-MLV reverse transcriptase (RT). Each sample of total RNA was diluted to 13 µl with HPLC-H_2O and 1 µl random hexamer primers were added. Samples were heated for 5 min at 70°C and then cooled 5 min on ice. 6 µl of a master mix containing M-MLV RT buffer, dNTPs and the M-MLV RT were added to each sample. The final reagent concentrations were: 1x M-MLV RT buffer, 0.5 mM dNTPs, 0.5 µg random primers per µg RNA and 200 units M-MLV RT. Reactions were incubated for 50 min at 37°C and for 15 min at 70°C. cDNAs were diluted with HPLC-H_2O to 50-100 µl.

2.2.3.3. Quantitative PCR

Real-time quantitative PCR (qPCR) was performed using technical duplicates of cDNA samples, specific intron-spanning primer pairs (Table 1) and the KAPA SYBRs FAST Master Mix (2X) Universal in a CFX96 reader. qPCR primers were design using the software AmplifX. The primer pairs were located in different exons to avoid amplification of genomic DNA. A temperature gradient qPCR was used to identify the optimal annealing temperature and the products were run in 2% agarose gels to verified correct product size. The efficiency of each primer pair was determined with the LinRegPCR software (Ramakers et al., 2003), based on the mean of individual reaction efficiencies for serial dilutions of a reference cDNA. The qPCR reaction setting and running protocol are described in Table 2. Relative mRNA levels of target genes were determined using the Pfaffl method (Pfaffl, 2001), using the geometrical average of the reference genes RPS27A (ribosomal protein S27a) and RPLP0 (ribosomal protein, large, P0) for normalization (Vandesompele et al., 2002). Relative mRNA levels were expressed as fold changes relative to the corresponding control sample. Data were logarithmically transformed prior to statistical analyses.

Table 1. Primers for qPCR.
Primers were synthesized by Eurofins Genomics.

Target	Primers (5'-3')	Reverse primer (5'-3')	Tm	Size	Efficiency
RPS27A	TCGTGGTGGTGCTAAGAAAA	TCTCGACGAAGGCGACTAAT	62ºC	141 bp	2.05
RPLP0	TGCATCAGTACCCCATTCTATCAT	AGGCAGATGGATCAGCCAAGA	62ºC	122 bp	2.03
PPARγ2	CCAGAAAGCGATTCCTTCAC	ACGGAGCTGATCCCAAAG	62ºC	110 bp	2.03
FABP4	TACTGGGCCAGGAATTTGAC	GACACCCCCATCTAAGGTTATG	62ºC	77 bp	2.05
LPL	CCGGTTTATCAACTGGATGG	TGGTCAGACTTCCTGCAATG	62ºC	110 bp	2.07
Runx2	CTTCACAAATCCTCCCCAAG	ATGCGCCCTAAATCACTGAG	62ºC	147 bp	2.03
OPN	TATGATGGCCGAGGTGATAG	CATTCAACTCCTCGCTTTCC	62ºC	133 bp	2.02
OCN	TCACACTCCTCGCCCTATTG	TCCCAGCCATTGATACAGGTAG	62ºC	164 bp	2.02
DMP1	CCCAACTATGAAGATCAGCATCC	GACCCTTCCATTCTTCAGAATCC	62ºC	113 bp	2.01
Col1A1	CCCTGGAAAGAATGGAGATG	CCATCCAAACCACTGAAACC	62ºC	150 bp	2.03
MMP2	CCAAGTGGGACAAGAACCAGATCA	AGACTTGGAAGGCACGAGCAAA	62ºC	102 bp	2.09
MMP13	GACGATGTACAAGGGATCCAGTCT	TGGCATCAAGGGATAAGGAAGGGT	62ºC	109 bp	1.91
MT1-MMP	ACAGGCAAAGCTGATGCAGACA	CGTAGCGCTTCCTTCGAACATT	62ºC	109 bp	2.07
TIMP1	TTCTGCAATTCCGACCTCGTCATC	ATCCCCTAAGGCTTGGAACCCTTT	62ºC	129 bp	1.99
TIMP2	AAAGCGGTCAGTGAGAAGGAAGTG	TCCTTCTCAGGCCCTTTGAACATC	62ºC	113 bp	2.08
FGF1	ACCGACGGGCTTTTATACGG	AATGGTTCTCCTCCAGCCTTTC	62ºC	76 bp	2.02
FGFR1	CTGGGTAGCAACGTGGAGTT	ACCATGCAGGAGATGAGGAA	62ºC	121 bp	2.13

Table 2. qPCR reaction setting and running protocol.

Reagent	Volume	Final concentration
KAPA SYBR Fast qPCR MasterMix (2x) Universal	10.0 µl	1x
HPLC-H_2O	7.5 µl	-
10 µM primer pair mix	0.5 µl	250 nM
Template	2.0 µl	-
	20.0 µl	

Running protocol

Temperature	Time	
95ºC	3 min	
95ºC	10 s	40 cycles
Tm	20 s	
60ºC to 95ºC	6 s	

2.2.4. Statistical analyses

All experiments were done at least in triplicate, using hBMSCs from different donors. Statistical analyses were carried out using GraphPad Prism software. In order to compare differences between two or more experimental groups, two-tailed Student's t-test or one-way ANOVA followed by a Tukey's post hoc test were respectively used. When comparing mRNA levels of adipogenic markers in 2D and 3D culture, two-way ANOVA followed by a Bonferroni's post hoc test was used. Differences were considered statistically significant for p-values ≤ 0.05.

3. Results

3.1. Establishment and characterization of a 3D culture model for adipogenic and osteogenic differentiation of hBMSCs based on collagen gels

3.1.1. Optimization of collagen gel setting conditions for hBMSCs differentiation

In order to find the optimal setup conditions for both adipogenic and osteogenic differentiation of hBMSCs embedded in collagen gels, different combinations of cell and collagen concentrations were used to set up the 3D gels for evaluation of the differentiation outcome after culture under adipogenic or osteogenic conditions. Six cell-collagen mixtures with final concentrations of 0.5 x 10^6 and 1.0 x 10^6 cells/ml and 0.5, 0.75 and 1.0 mg/ml of collagen were evaluated.

Since the hBMSCs-laden collagen gels were allowed to float freely in culture medium after preparation, a cell-mediated contraction of the gels was observed from the first day of culture in growth medium. This resulted in the formation of collagen gel spheroids whose sizes continued decreasing over the 21 days under adipogenic and osteogenic induction (Figure 3).

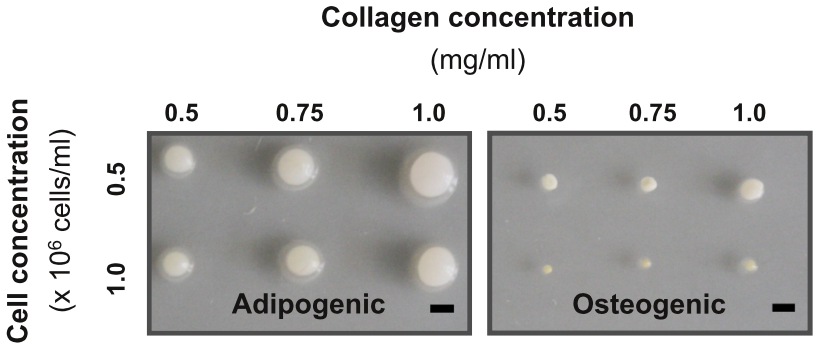

Figure 3. Collagen gels after hBMSC differentiation.
hBMSC-laden collagen gels of initial collagen concentrations of 0.5, 0.75 and 1.0 mg/ml and cell concentrations of 0.5 and 1.0 x 10^6 cells/ml after 21 days under adipogenic or osteogenic culture conditions. Scale bars represent 1 mm.

The extent of this size reduction was dependent on the initial collagen and cell concentration, the hBMSC batch as well as on the induced differentiation pathway. As a rule, the final diameter of the gels under osteogenic induction was smaller than the gels under adipogenic induction. In both cases, gel size increased with higher collagen concentration and with lower cell number (Figure 3, Table 3).

Table 3. Collagen gel sizes after differentiation induction.
Final size of hBMSC-laden collagen gels of different initial collagen and cell concentration after 21 days under adipogenic or osteogenic culture conditions.

Collagen (mg/ml)	Adipogenesis		Osteogenesis	
	0.5 x 10^6 cells/ml	1.0 x 10^6 cells/ml	0.5 x 10^6 cells/ml	1.0 x 10^6 cells/ml
0.5	1.18 ± 0.37	1.13 ± 0.31	0.51 ± 0.01	0.48 ± 0.09
0.75	1.50 ± 0.45	1.36 ± 0.40	0.64 ± 0.24	0.56 ± 0.18
1.0	1.87 ± 0.40	1.59 ± 0.36	0.88 ± 0.41	0.67 ± 0.33

The differentiation outcome of hBMSCs after three weeks under adipogenic or osteogenic induction in the collagen gels was assessed by histochemical staining of gel cryosections. Adipogenic differentiation was evaluated regarding the accumulation of intracellular lipid droplets, which were stained with Oil Red O (Figure 4).

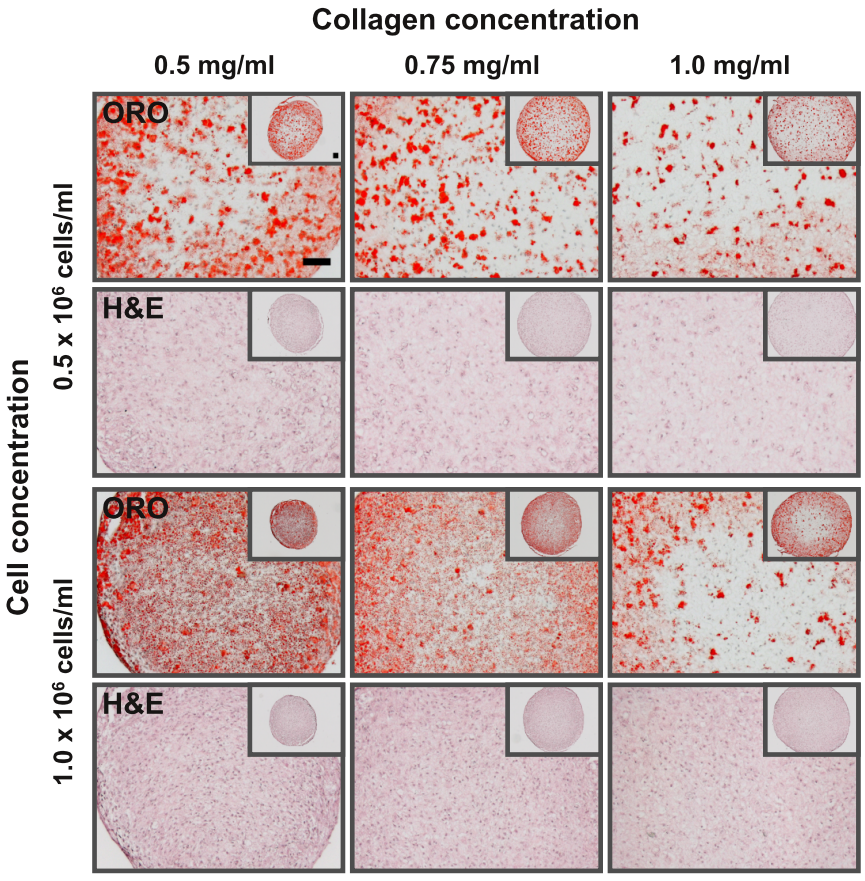

Figure 4. Adipogenic differentiation in collagen gels.
Cryosections of hBMSC-laden collagen gels of initial collagen concentrations of 0.5, 0.75 and 1.0 mg/ml and cell concentrations of 0.5 and 1.0 x 10^6 cells/ml stained with Oil Red O (ORO) for lipid droplet visualization or hematoxylin and eosin (H&E) for cell distribution evaluation after 21 days of culture under adipogenic induction. Insets show lower magnification images. Scale bars represent 100 µm.

Lipid droplets were observed in all six combinations of collagen and cell concentrations, indicating that these conditions allowed for adipogenesis of hBMSCs. Frequently, a lower accumulation of lipid droplets was observed at the center of the gels beside a lower cellularity according to the hematoxylin and eosin staining. Gels with lower collagen and cell concentrations presented larger lipid droplets, typical of mature adipocytes.

Osteogenic differentiation of hBMSCs in collagen gels maintained for three weeks under osteogenic induction was assessed by staining gel cryosections for alkaline phosphatase activity as well as for mineralized extracellular matrix with Alizarin Red S (Figure 5). The staining pattern for alkaline phosphatase activity was very variable among different hBMSC batches but often a higher activity was detected at the rim of the collagen gels and a lower or null activity was detected at sites of mineralization. Generally, mineralized matrix deposition was favored by lower cell and collagen concentration although it was not always observed after 21 days of osteogenic induction.

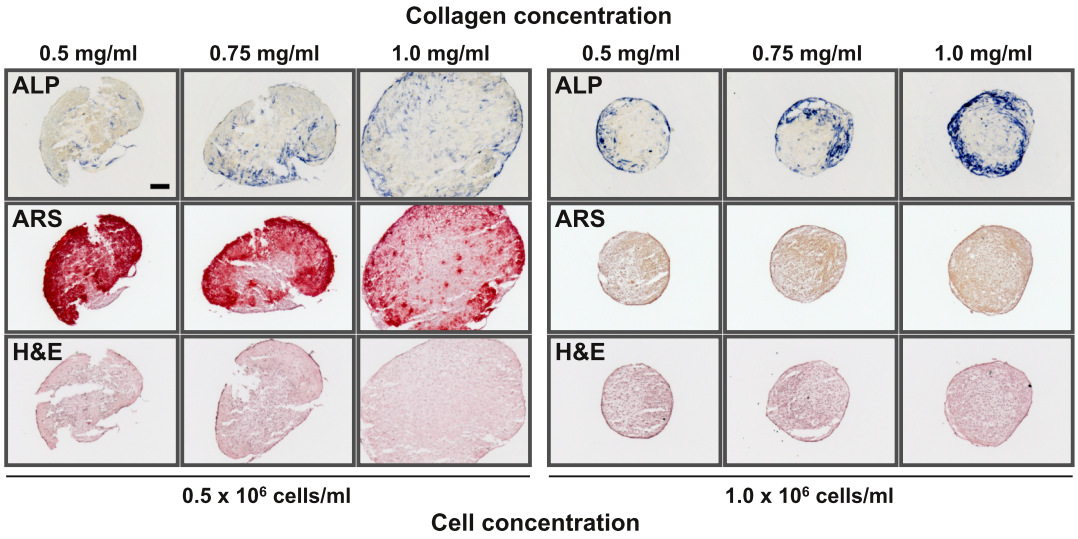

Figure 5. Osteogenic differentiation in collagen gels.
Cryosections of hBMSC-laden collagen gels of initial collagen concentrations of 0.5, 0.75 and 1.0 mg/ml and cell concentrations of 0.5 and 1.0 x 10^6 cells/ml stained for alkaline phosphatase activity (ALP), with Alizarin Red S (ARS) for visualization of mineralized extracellular matrix or hematoxylin and eosin (H&E) for cell distribution assessment after 21 days of culture under osteogenic conditions. Scale bar represents 100 µm.

Given that gels of 0.5 x 10^6 cells/ml and 0.5 mg/ml were frequently very small and fragile if mineralized, the combination of 0.5 x 10^6 cells/ml and 0.75 mg/ml collagen was chosen to be used in the following experiments because mineralized matrix deposition was similarly enhanced in

the case of osteogenic induction and the accumulation of lipid droplets after adipogenic induction appeared to be more efficient than in gels of 1.0 mg/ml initial collagen concentration.

3.1.2. hBMSCs differentiation in 3D collagen gels

3.1.2.1. Adipogenic and osteogenic differentiation

Using the chosen conditions for the setting of the gels, the next aim was to study the time course of adipogenic and osteogenic differentiation of hBMSCs embedded in collagen gels using the aforementioned histochemical stainings. Additionally, the differentiation outcome was evaluated by measuring the mRNA levels of specific differentiation markers using quantitative PCR (qPCR).

When hBMSCs-laden collagen gels were subjected to adipogenic conditions, a progressive accumulation of lipid droplets over time was observed (Figure 6). At the same time, the mRNA levels of the adipogenic markers PPARγ2, FABP4 and LPL were highly induced after adipogenic stimulation (Figure 7).

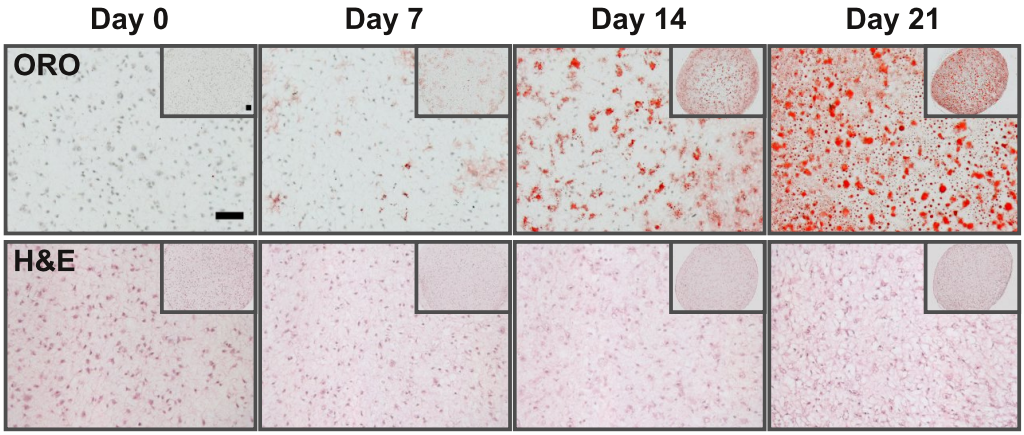

Figure 6. Time-course of adipogenic differentiation in collagen gels.
Collagen gel cryosections stained for lipid droplets (ORO) or with hematoxylin and eosin (H&E) at day 0 and after 7, 14 and 21 days under adipogenic differentiation induction. Insets show lower magnification images. Scale bars represent 100 μm.

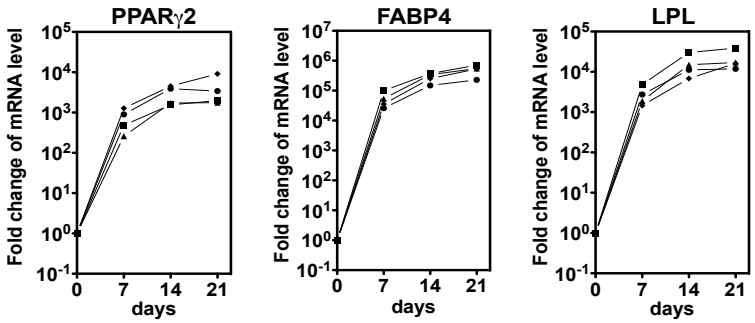

Figure 7. mRNA levels of adipogenic markers throughout differentiation in collagen gels.
Relative mRNA levels of the adipogenic markers PPARγ2, FABP4 and LPL throughout adipogenic differentiation of hBMSCs embedded in collagen gels. Data are presented as fold change relative to day 0. Individual results for four different hBMSC batches are shown.

In the case of gels under osteogenic induction, the differentiation outcome was highly variable among different hBMSC batches. Generally, alkaline phosphatase activity was detected from day 0 and increased initially but then decreased when mineralization of the extracellular matrix took place (Figure 8). However, not every hBMSC batch showed positive matrix mineralization but when it occurred, it was first observed at day 21. Despite the variability among different hBMSC batches, the mRNA levels of the early osteogenic marker Runx2 and the later osteogenic markers osteopontin and osteocalcin showed a tendency to increase over time (Figure 9).

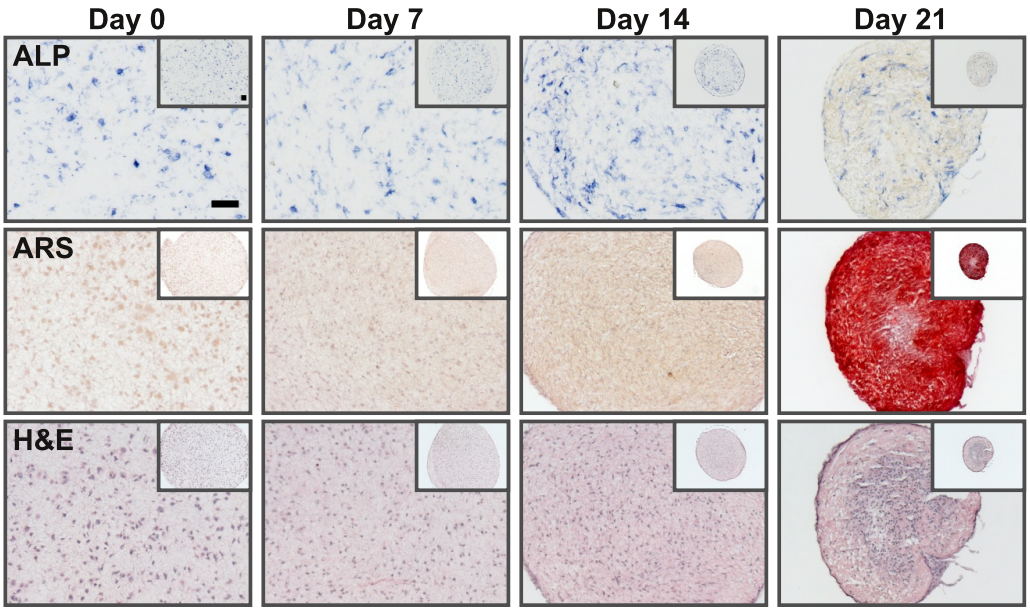

Figure 8. Time-course of osteogenic differentiation in collagen gels.
Collagen gel cryosections stained for alkaline phosphatase activity (ALP), for mineralized extracellular matrix (ARS) or with hematoxylin and eosin (H&E) at day 0 and after 7, 14 and 21 days under osteogenic culture conditions. Insets show lower magnification images. Scale bars represent 100 μm.

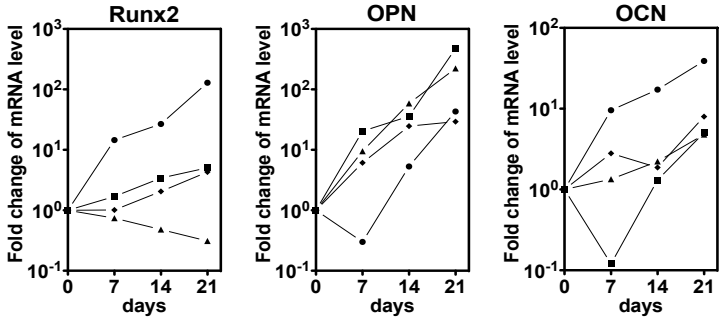

Figure 9. mRNA levels of osteogenic markers throughout differentiation in collagen gels.
Relative mRNA levels of the osteogenic markers Runx2, osteopontin (OPN) and osteocalcin (OCN) in the course of osteogenic differentiation of hBMSCs embedded in collagen gels. Data are presented as fold change relative to day 0. Individual results for four different hBMSC batches are shown.

In order to test the viability of the cells inside collagen gels under differentiation induction, a propidium iodide exclusion test was used to identify dead cells (Figure 10). After 7 days of culture under adipogenic or osteogenic conditions, the vast majority of the embedded cells did not incorporate propidium iodide, indicating that they remained viable, whereas all cells of the saponin-treated control incorporated the dye.

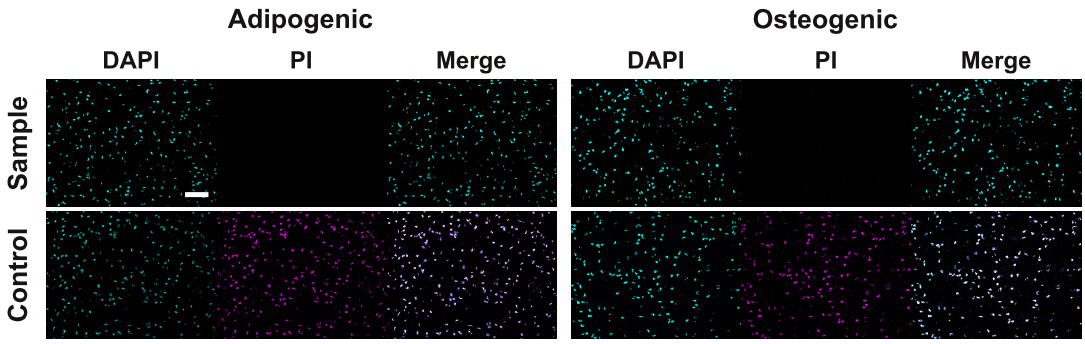

Figure 10. Cell viability in collagen gels.
Propidium iodide staining (PI) of dead cells in collagen gels at day 7 of adipogenic or osteogenic differentiation induction. Cell nuclei were counterstain with DAPI. Gels treated with 0.1% saponin prior to propidium iodide staining were used as positive controls. Scale bar represents 100 µm.

In addition to cell viability, changes in the number of cells in the collagen gels from day 0 and throughout the differentiation period was estimated by measuring the DNA content inside the gels (Figure 11).

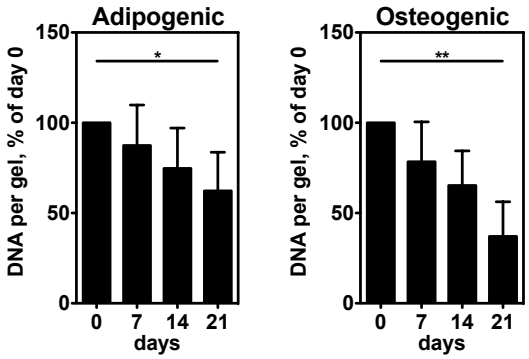

Figure 11. DNA content in collagen gels.
DNA content in collagen gels at day 0 and after 7, 14 and 21 days of culture under adipogenic and osteogenic conditions, expressed as percentage (mean ± SD) of DNA content at day 0. * $p < 0.05$; ** $p < 0.01$.

In spite of the high viability at day 7, a continuous decrease in DNA content was observed for gels under adipogenic as well as osteogenic conditions, being more marked for the latter, reaching day 21 with approximately 60 and 40 percent of the initial DNA content, respectively.

3.1.2.2. Expression of matrix remodeling markers

As mentioned before, a drastic contraction of the collagen gels was observed during the first 24 hours in culture, resulting in an average gel diameter reduction of approximately 70 percent (Figure 12). From day 0 and throughout the differentiation induction, the gels displayed a continuous size reduction, which was much sharper for collagen gels under osteogenic conditions than for gels under adipogenic stimulation. The average gel diameter reduction from day 0 to day 21 under adipogenic and osteogenic culture conditions was of approximately 30 and 60 percent, respectively.

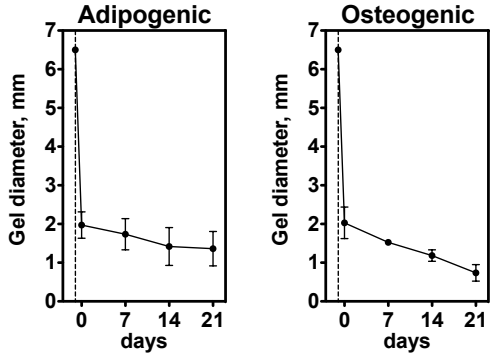

Figure 12. Collagen gel size change throughout differentiation.
Diameter of collagen gels with embedded hBMSCs after setting (day −1, dotted line), at day 0 and after 7, 14 and 21 days under adipogenic or osteogenic culture conditions.

Since differences in gel size reduction extent suggest differences in matrix remodeling capacities, the expression of matrix remodeling markers belonging to the collagen, MMP and TIMP families was investigated. First, the mRNA levels of Col1A1, MMP2, MMP13, MT1-MMP, TIMP1 and TIMP2 after adipogenic differentiation in collagen gels were assessed. Compared to day 0, adipogenic induction for 14 days resulted in a significant decrease of Col1A1, TIMP1 and TIMP2 mRNA levels, while MMP13 was strongly upregulated (Figure 13).

Osteogenic differentiation of hBMSCs in collagen gels, on the other hand, was characterized by the upregulation of MMP2, MMP13, MT1-MMP and TIMP2 and the downregulation of Col1A1 and TIMP1 (Figure 13).

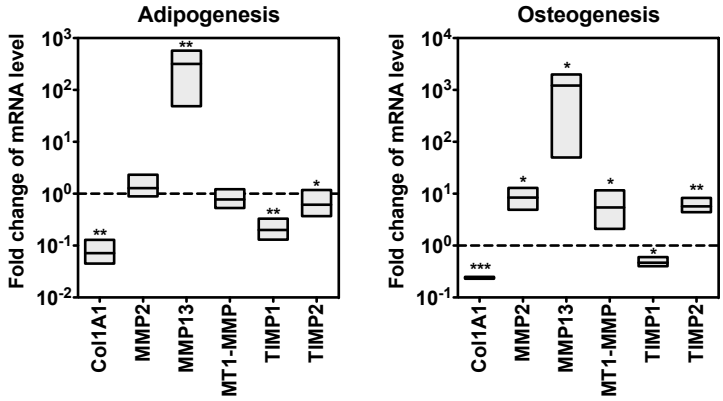

Figure 13. mRNA levels of matrix remodeling markers during differentiation in collagen gels. Relative mRNA levels of the matrix remodeling markers Col1A1, MMP2, MMP13, MT1-MMP, TIMP1 and TIMP2 after 14 days of adipogenic or osteogenic induction in collagen gels. Data are presented as fold change relative to day 0 (dotted line). The floating bars denote the minimum-to-maximum values with the line representing the mean. * $p < 0.05$; ** $p < 0.01$; *** $p < 0.001$.

Together, these results show that the expression pattern of matrix remodeling markers differed in hBMSCs undergoing adipogenesis and osteogenesis in collagen gels. Whereas the mRNA levels of MMP2 and MT1-MMP did not change after adipogenic induction, they were upregulated after osteogenic differentiation. In addition, the mRNA levels of TIMP2 were slightly lower after adipogenic differentiation while upregulated after osteogenic differentiation.

3.1.2.3. 3D collagen gels vs monolayer culture

Next, differentiation of hBMSCs in collagen gels was compared with differentiation in the conventional 2D monolayer culture. After 21 days under adipogenic stimulation, both setups displayed a substantial accumulation of lipid droplets (Figure 14A). At day 0, the mRNA levels of PPARγ2 were slightly higher in collagen gels compared to monolayers although the difference

was not statistically significant (Figure 14B). At day 21 of adipogenic differentiation, the strong induction of PPARγ2, FABP4 and LPL mRNA levels was similar in both systems. Hence, adipogenic differentiation of hBMSCs in collagen gels is comparable with the conventional differentiation in monolayers.

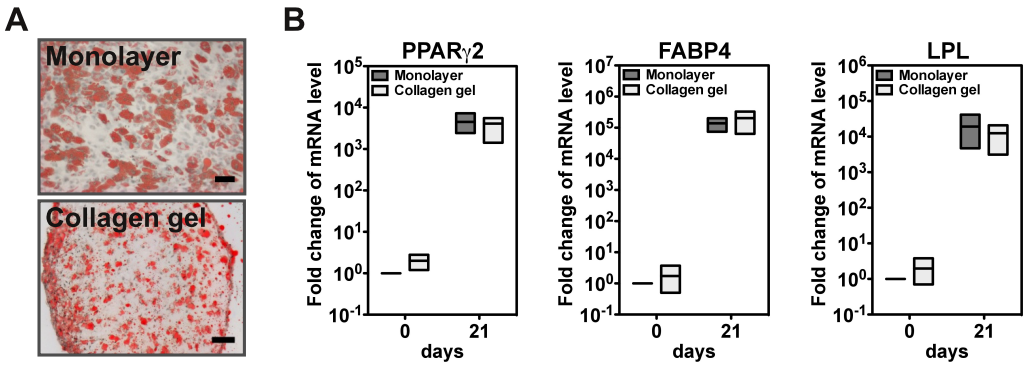

Figure 14. Adipogenic differentiation in collagen gels and monolayers.
A) Staining of lipid droplets with Oil Red O after 21 days of adipogenic differentiation induction of hBMSCs in 2D monolayer culture or embedded in collagen gel. Scale bars represent 100 µm. **B)** Relative mRNA levels of the adipogenic differentiation markers PPARγ2, FABP4 and LPL in monolayers and collagen gels after 14 days of adipogenic induction. Data are presented as fold change relative to monolayers at day 0. The floating bars denote the minimum-to-maximum values with the line representing the mean.

As mentioned before, the outcome under osteogenic conditions in terms of mineralized matrix deposition was highly donor-dependent. Differences in the extent of matrix mineralization between monolayers and collagen gels were observed although no consistent relation was found (Figure 15A). When the mRNA levels of Runx2, osteopontin and osteocalcin were compared, no significant difference was found at day 0 between monolayers and collagen gels, however, at day 21, whereas the cells in monolayers did not show a significant induction of these osteogenic markers, their levels were upregulated in collagen gels (Figure 15B). Hence, compared to monolayers, osteogenesis of hBMSCs in collagen gels was characterized by a higher expression of osteogenic markers.

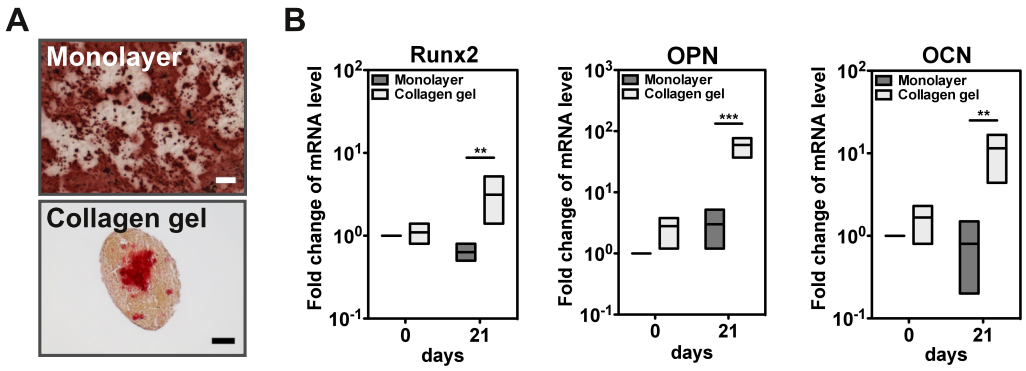

Figure 15. Osteogenic differentiation in collagen gels and monolayers.
A) Staining of mineralized matrix deposition with Alizarin Red S after 21 days of hBMSC osteogenic differentiation induction in 2D monolayer culture or in collagen gel. Scale bars represent 100 µm. **B)** Relative mRNA levels of the osteogenic differentiation markers Runx2, osteopontin (OPN) and osteocalcin (OCN) in monolayers and collagen gels after 14 days of osteogenic induction. Data are presented as fold change relative to monolayers at day 0. The floating bars denote the minimum-to-maximum values with the line representing the mean. ** $p < 0.01$; *** $p < 0.001$.

3.2. Inhibitory effect of FGF1 signaling on hBMSC differentiation in 3D collagen gels

After establishing and characterizing adipogenic and osteogenic differentiation of hBMSCs embedded in collagen gels, the next aim of this work was to use this 3D culture system to study the role of FGF1 in adipogenesis and osteogenesis of hBMSCs. Firstly, changes in the expression of FGF1 after adipogenic and osteogenic differentiation of hBMSCs in collagen gels were evaluated. After 21 days of adipogenic induction, the mRNA levels of FGF1 significantly decreased compared to day 0 (Figure 16). In contrast, after 21 days of osteogenic differentiation, the mRNA levels of FGF1 did not change with respect to day 0. Additionally, changes in the expression of FGFR1 after adipogenic and osteogenic differentiation of hBMSCs in collagen gels were assessed. While the mRNA levels of FGFR1 did not display any change after 21 days of adipogenic differentiation, a tendency to increased levels was observed after 21 days of osteogenic induction, although the difference was not significant (Figure 16). Similar to previous findings (Schilling et al., 2008), these results suggest that a reduction in FGF1 signaling occurred along with adipogenic but not with osteogenic differentiation of hBMSCs.

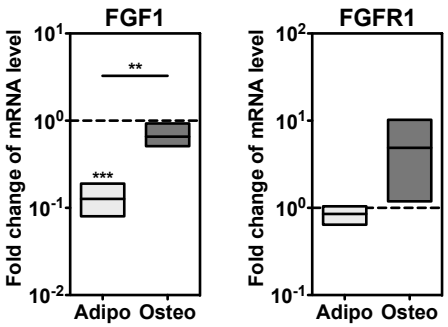

Figure 16. mRNA levels of FGF1 and FGFR1 following differentiation.
Relative mRNA levels of FGF1 and FGFR1 after 21 days of adipogenic or osteogenic differentiation of hBMSCs embedded in collagen gels. Data are presented as fold change relative to day 0 (dotted line). The floating bars denote the minimum-to-maximum values with the line representing the mean. ** $p < 0.01$.

3.2.1. rhFGF1 treatment inhibits hBMSC adipogenesis and osteogenesis in 3D collagen gels

In order to evaluate the effect of extracellular FGF1 signaling during adipogenic and osteogenic differentiation of hBMSCs embedded in 3D collagen gels, cells were induced to differentiate in the presence of rhFGF1. Heparin was added simultaneously as a stabilizer and cofactor. Differentiation in the presence of BSA alone and heparin (plus BSA) alone were included as control conditions. Additionally, the effect of rhFGF2, the other member of the FGF1 subfamily, was investigated in parallel for comparison.

3.2.1.1. Inhibition of adipogenic differentiation by rhFGF1 in 3D collagen gels

After 21 days of adipogenic induction in the presence of 25 µg/ml heparin in combination with increasing concentrations of 1, 5 and 25 ng/ml rhFGF1, lipid droplet accumulation was inhibited in a dose-dependent manner (Figure 17). The same effect was observed for rhFGF2. Heparin alone had no significant effect on lipid droplet formation compared to the BSA control. Noteworthy, heparin alone, rhFGF1 and rhFGF2 had an effect on the size reduction of the collagen gels, which was attenuated by heparin and further mitigated by rhFGF1 and rhFGF2 in a dose-dependent manner (Figure 17, insets). Supporting the histological observations, the mRNA levels of the adipogenic markers PPARγ2, FABP4, and LPL were significantly lower after 14 days of treatment with 25 ng/ml rhFGF1 or rhFGF2 compared to the heparin alone control (Figure 18). Although heparin alone did not enhance the formation of lipid droplets as mentioned above, it tended to increase the expression of these adipogenic markers with respect to the BSA control, but only significantly for LPL.

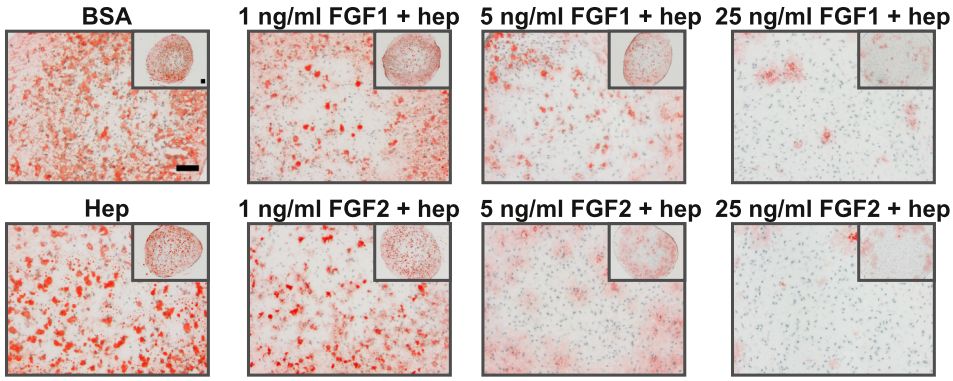

Figure 17. Adipogenic differentiation in the presence of rhFGF1 or rhFGF2 in collagen gels. Oil Red O staining of lipid droplets in cryosections of hBMSCs-laden collagen gels after 21 days of adipogenic differentiation induction in the presence of BSA, heparin alone (Hep) or heparin combined with 1, 5 or 25 ng/ml of rhFGF1 (FGF1 + hep) or rhFGF2 (FGF2 + hep). Insets show lower magnification images. Scale bars represent 100 µm.

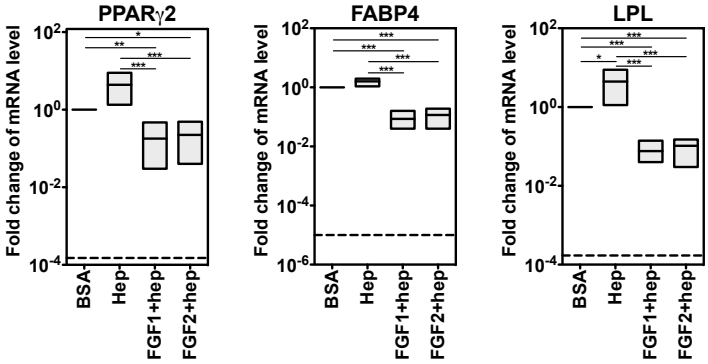

Figure 18. mRNA levels of adipogenic markers in the presence of rhFGF1 or rhFGF2. Relative mRNA levels of the adipogenic differentiation markers PPARγ2, FABP4 and LPL after 14 days of adipogenic induction in collagen gels in the presence of BSA, heparin alone (Hep) or heparin combined with 25 ng/ml rhFGF1 (FGF1+hep) or rhFGF2 (FGF2+hep). Data are presented as fold change relative to the BSA control. The dotted lines represent the relative mRNA levels at day 0. The floating bars denote the minimum-to-maximum values with the line representing the mean. * $p < 0.05$; ** $p < 0.01$; *** $p < 0.001$.

Therefore, these results show that a continuous rhFGF1 treatment during adipogenic induction had an inhibitory role in the differentiation of hBMSCs into the adipogenic lineage. Additionally, this effect was not particular for rhFGF1 since the subfamily co-member rhFGF2 also exerted equivalent inhibitory effects.

In order to verify that the inhibitory effect of rhFGF1 and rhFGF2 was specific and mediated by signaling through FGFRs, hBMSCs were induced to differentiate in collagen gels in the presence of rhFGF1 or rhFGF2 together with the specific FGFR small molecule inhibitor PD166866. The inhibitory effect of 25 ng/ml rhFGF1 and rhFGF2 on lipid droplet accumulation was completely

abrogated when 250 nM PD166866 was added simultaneously throughout the adipogenic induction (Figure 19A). The same result was obtained using 20 µM SU5402, another specific FGFR small molecule inhibitor (Figure 19B). These results indicate that hBMSC adipogenic differentiation inhibition by rhFGF1 and rhFGF2 treatments was specific and fully dependent on FGFR signaling activation.

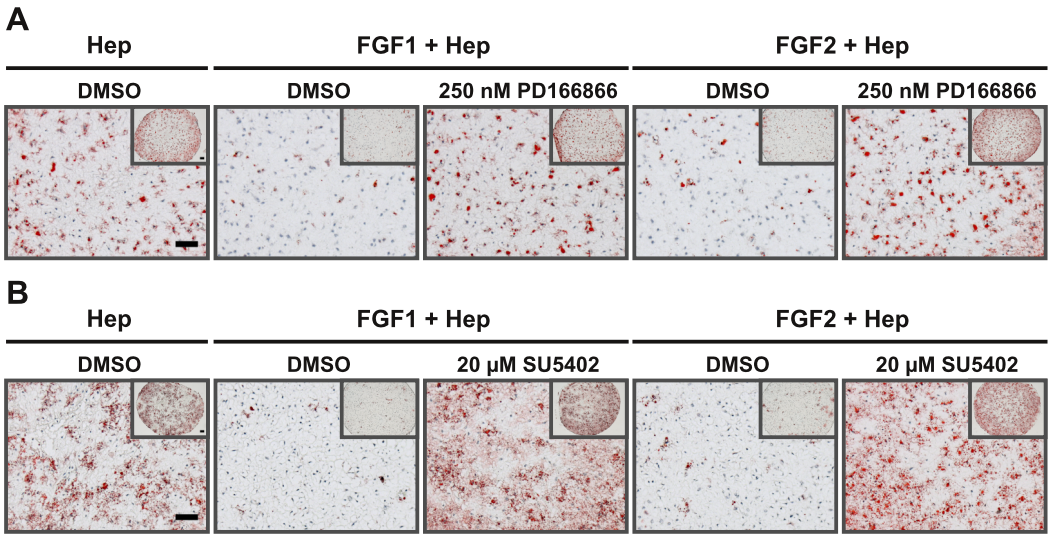

Figure 19. Adipogenic differentiation in the presence of rhFGF1 or rhFGF2 and FGFR inhibitors.
Cryosections of collagen gels stained for lipid droplets with Oil Red O after 21 days of adipogenic differentiation induction of hBMSCs in the presence of 25 µg/ml heparin (Hep) alone and in combination with 25 ng/ml rhFGF1 (FGF1+hep) or rhFGF2 (FGF2+hep). The FGFR inhibitors PD166866 at 250 nM **(A)** or SU5402 at 20 µM **(B)** were added from day 0 when indicated. The vehicle DMSO was added to the control conditions.

To assess if the observed differentiation inhibition required a persistent FGF signaling activation, adipogenic induction of hBMSCs in collagen gels was combined with rhFGF1 or rhFGF2 treatments, which were either maintained during the whole differentiation induction period of 21 days or withdrawn after the first 24 or 72 hours. In contrast with the extensive reduction of lipid droplet accumulation when rhFGF1 or rhFGF2 treatments were maintained throughout the differentiation period, short stimulations of 24 or 72 hours resulted in a differentiation extent comparable to the heparin alone condition (Figure 20). This result indicates that a sustained FGFR signaling activation by either rhFGF1 or rhFGF2 is necessary for the observed inhibitory effects on adipogenesis and therefore, it points out the reversibility of the inhibitory process.

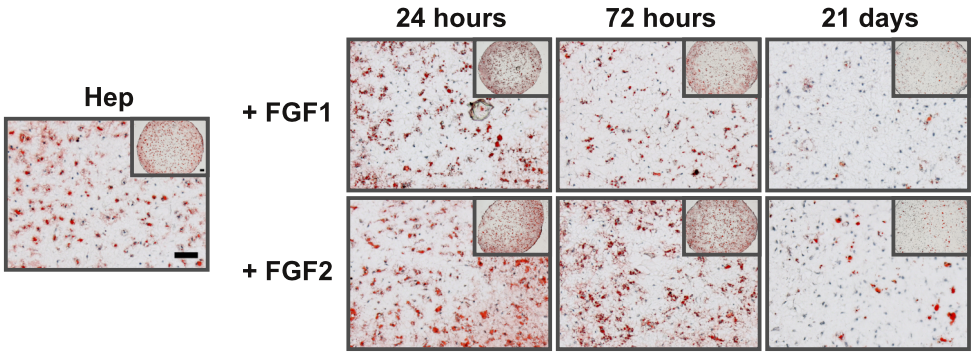

Figure 20. Effect of rhFGF1 or rhFGF2 treatment duration on adipogenic differentiation in collagen gels.
Cryosections of collagen gels stained with Oil Red O to assess adipogenic differentiation of hBMSCs in the presence of 25 µg/ml heparin (Hep) alone or in combination with 25 ng/ml rhFGF1 (FGF1) or rhFGF2 (FGF2) during the complete differentiation period (21 days) or only for the first 24 or 72 hours. Insets show lower magnification images.

3.2.1.2. Inhibition of osteogenic differentiation by rhFGF1 in 3D collagen gels

Osteogenic induction for 21 days in the presence of 1, 5 and 25 ng/ml rhFGF1, as well as rhFGF2, resulted in the inhibition of matrix mineralization in a dose-dependent manner (Figure 21).

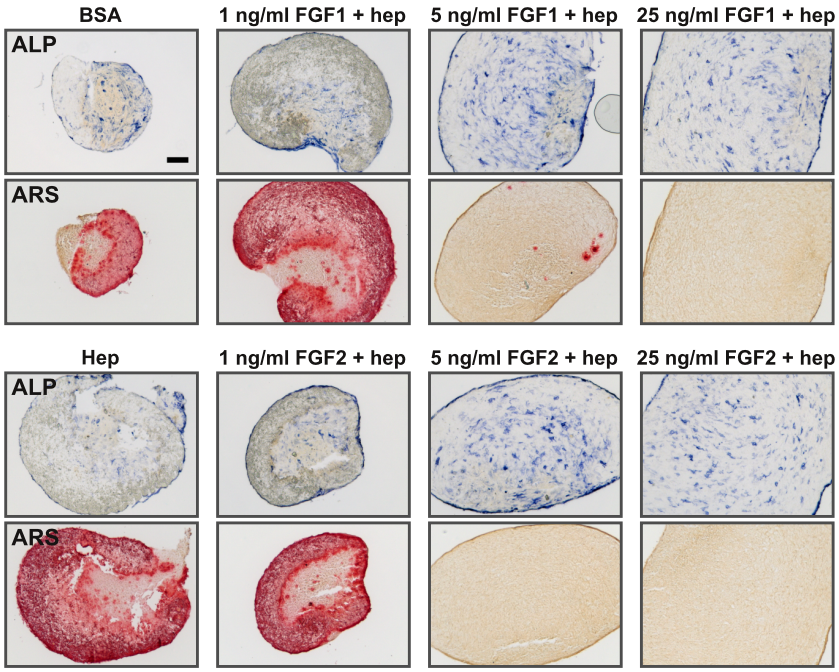

Figure 21. Osteogenic differentiation in the presence of rhFGF1 and rhFGF2 in collagen gels.
Cryosections of hBMSCs-laden collagen gels stained for alkaline phosphatase activity (ALP) and for mineralized matrix with Alizarin Red S (ARS) after 21 days of osteogenic differentiation induction in the presence of BSA, heparin alone (Hep) or heparin combined with 1, 5 or 25 ng/ml of rhFGF1 (FGF1 + hep) or rhFGF2 (FGF2 + hep). Scale bar represents 100 µm.

Despite the lack of mineralization, alkaline phosphatase activity was still detected under rhFGF1 or rhFGF2 conditions. As observed in the case of adipogenic induction, heparin, rhFGF1 and rhFGF2 had an attenuating effect on the size reduction of the collagen gels. Regarding the expression of osteogenic differentiation markers, the mRNA levels of Runx2, osteopontin and osteocalcin showed, however, no significant variation after 14 days of osteogenic induction in the presence of 25 ng/ml rhFGF1 or rhFGF2 compared to the heparin or the BSA controls, despite a tendency in the mRNA levels of Runx2 to diminish (Figure 22).

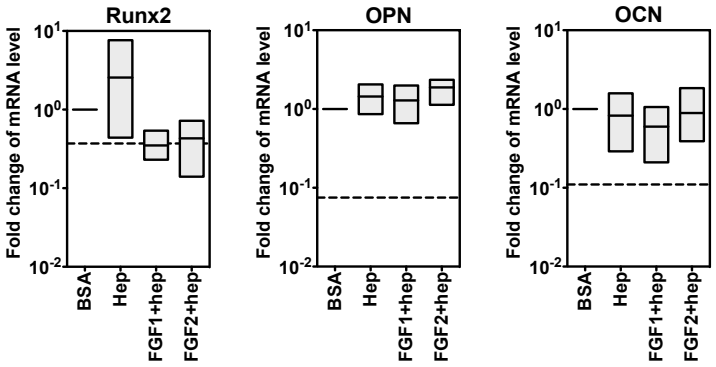

Figure 22. mRNA levels of osteogenic markers in the presence of rhFGF1 or rhFGF2 in collagen gels.
Relative mRNA levels of the osteogenic differentiation markers Runx2, osteopontin (OPN), osteocalcin (OCN) after 14 days of osteogenic induction in collagen gels in the presence of BSA, heparin alone (Hep) or heparin combined with 25 ng/ml rhFGF1 (FGF1+hep) or rhFGF2 (FGF2+hep). Data are presented as fold change relative to the BSA control. The dotted lines represent the relative mRNA levels at day 0. The floating bars denote the minimum-to-maximum values with the line representing the mean.

Hence, these results suggest that, during osteogenic induction, the continuous presence of rhFGF1 did not affect significantly the osteogenic commitment of hBMSCs in collagen gels but it inhibited the differentiation into mature mineralized matrix-producing osteoblasts. This effect, however, was also observed in the presence of rhFGF2, indicating that both growth factors have a comparable inhibitory impact on the maturation of osteogenically differentiating hBMSCs.

3.2.1.3. DNA content after hBMSC differentiation inhibition by rhFGF1 in 3D collagen gels

In order to estimate whether cell proliferation of hBMSCs in the collagen gels was altered by the inhibition of adipogenic and osteogenic differentiation resulted by rhFGF1 or rhFGF2 treatments, total DNA content was determined. After 21 days under adipogenic induction, the DNA content in the collagen gels did not change significantly for BSA or heparin control conditions relative to day 0 (Figure 23). With the addition of rhFGF1 or rhFGF2, however, the DNA content tended to increase, although there were no statistically significant differences among treatments. Similar

results were observed after osteogenic induction. In this case, compared to day 0, the DNA content tended to strongly decrease for the BSA control as well as for the heparin control but less pronouncedly (Figure 23). On the contrary, after osteogenic induction in the presence of rhFGF1 or rhFGF2, the collagen gels displayed a strong tendency towards increased DNA content.

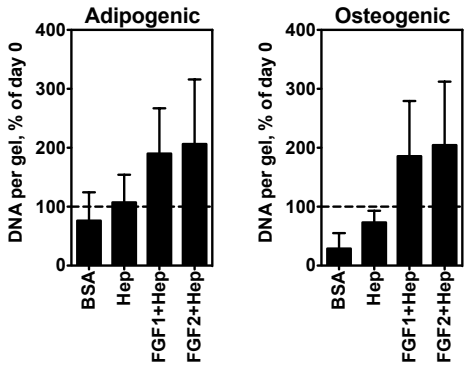

Figure 23. DNA content in the presence of rhFGF1 or rhFGF2 in collagen gels.
DNA content in collagen gels after 21 days under adipogenic and osteogenic induction in the presence of BSA, heparin alone (Hep) or heparin combined 25 ng/ml rhFGF1 (FGF1+Hep) or rhFGF2 (FGF2+Hep), expressed as percentage (mean ± SD) of DNA content at day 0 (dotted line).

Taken together, these results indicate that FGF1 as well as FGF2 signaling inhibits adipogenesis, as well as osteogenesis, in collagen gels via FGFR signaling by reversibly entrapping hBMSCs in a pre-differentiated state while inducing sustained proliferation.

3.2.2. Impact of FGFR signaling inhibition during hBMSC differentiation induction in 3D collagen gels

In order to study the effect of inhibiting the basal FGF signaling on adipogenic and osteogenic differentiation of hBMSCs in collagen gels, differentiation induction was performed in the presence of increasing concentrations of the specific FGFR inhibitor PD166866 or SU5452.

3.2.2.1. hBMSC adipogenic differentiation in 3D collagen gels under FGFR signaling inhibition

After 21 days of adipogenic induction, a slight increase in lipid droplet accumulation was observed only for the higher concentration of PD166866 tested, 250 nM, compared to the DMSO control (Figure 24A). However, with the other FGFR inhibitor, SU5452, no significant alterations in lipid droplet accumulation were observed, neither at 10 or 20 µM SU5452 (Figure 24B).

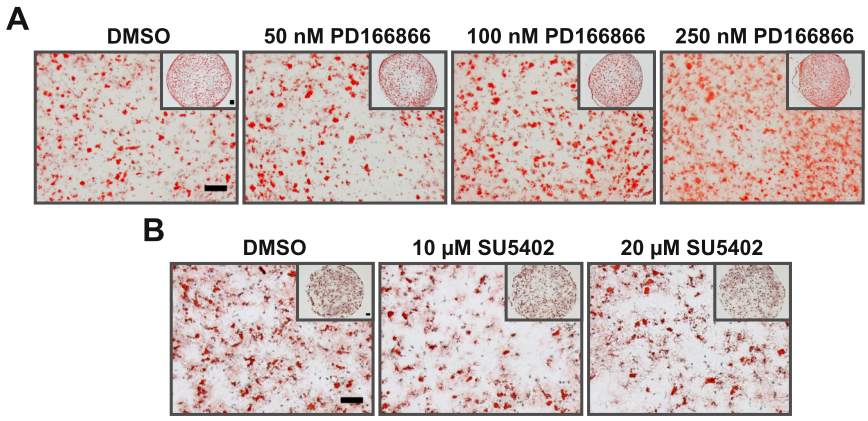

Figure 24. Effect of FGFR inhibition on adipogenic differentiation in collagen gels.
Oil Red O staining of lipid droplets in cryosections of hBMSCs-laden collagen gels after 21 days of adipogenic differentiation induction in the presence of increasing concentrations of the FGFR inhibitor PD166866 **(A)** or SU5402 **(B)**. The vehicle DMSO was used as control. Insets show lower magnification images. Scale bars represent 100 µm.

Likewise, the mRNA levels of the adipogenic markers PPARγ2, FABP4 and LPL did not significantly change after 14 days of adipogenic differentiation in the presence of 250 nM PD166866 (Figure 25).

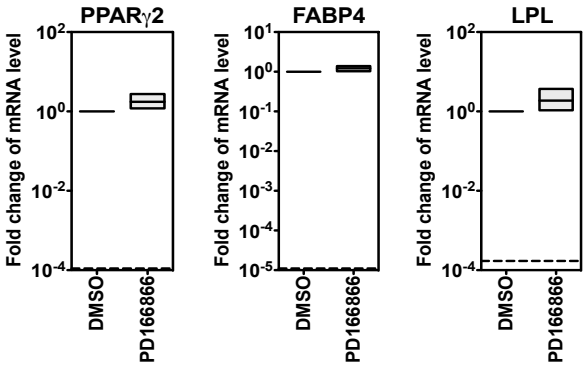

Figure 25. mRNA levels of adipogenic markers under FGFR inhibition.
Relative mRNA levels of the adipogenic differentiation markers PPARγ2, FABP4 and LPL after 14 days under adipogenic induction of hBMSCs in collagen gels in the presence of DMSO or 250 nM of the FGFR inhibitor PD166866. Data are presented as fold change relative to the DMSO control. The dotted lines represent the relative mRNA levels at day 0. The floating bars denote the minimum-to-maximum values with the line representing the mean.

3.2.2.2. hBMSC osteogenic differentiation in 3D collagen gels under FGFR signaling inhibition

The inhibition of FGFR signaling with increasing concentrations of PD166866 resulted in a striking dose-dependent enhancement of matrix mineralization after 21 days of osteogenic induction (Figure 26). Curiously, the mRNA levels of Runx2, osteopontin and osteocalcin did not change significantly after 14 days of osteogenic induction in the presence of 250 nM PD166866, although a tendency towards downregulation was observed (Figure 27). The mRNA levels of the osteocyte marker DMP1 were also determined but were not found to be different from the control.

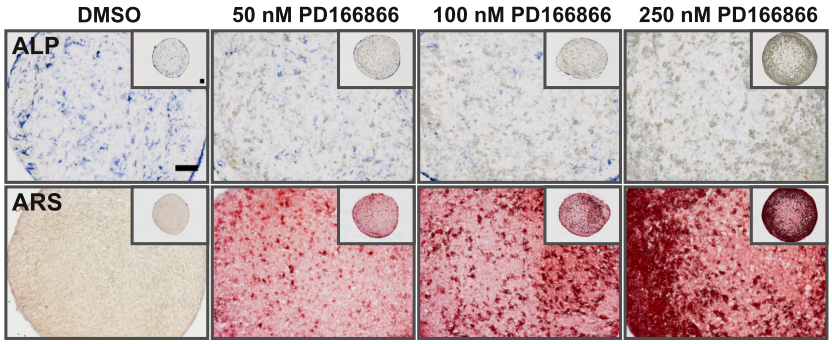

Figure 26. Effect of FGFR inhibition on osteogenic differentiation in collagen gels.
Staining for alkaline phosphatase activity (ALP) and mineralized matrix deposition (ARS) in cryosections of hBMSC-laden collagen gels after 21 days under osteogenic induction in the presence of DMSO or increasing concentrations of the FGFR inhibitor PD166866. Insets show lower magnification images. Scale bars represent 100 µm.

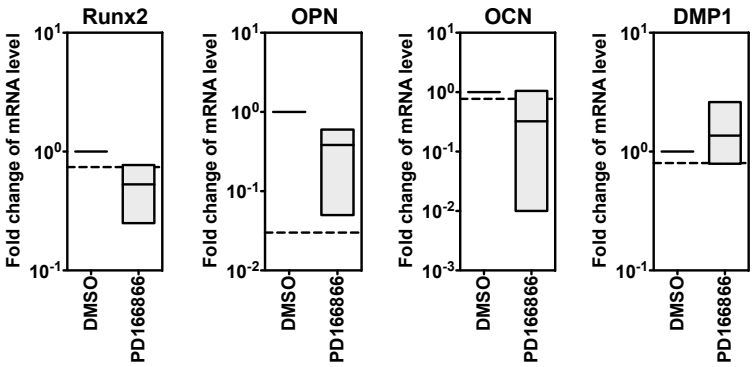

Figure 27. Effect of FGFR inhibition on the mRNA levels of osteogenic markers.
Relative mRNA levels of the osteogenic differentiation markers Runx2, osteopontin (OPN), osteocalcin (OCN) and DMP1 after 14 days under osteogenic conditions in collagen gels in the presence of DMSO or 250 nM of the FGFR inhibitor PD166866. Data are presented as fold change relative to the DMSO control. The dotted lines represent the relative mRNA levels at day 0. The floating bars denote the minimum-to-maximum values with the line representing the mean.

These results show that the basal FGFR signaling does not seem to participate significantly in the adipogenic differentiation of hBMSCs in collagen gels. Conversely, in the case of osteogenic differentiation, FGFR inhibition greatly augmented matrix mineralization without affecting significantly the expression of osteogenic or osteocytic markers, indicating that signaling through FGFRs plays an inhibiting role in the deposition of mineralized matrix by differentiating osteoblasts *in vitro*.

3.2.3. Matrix remodeling is affected by rhFGF1 treatment during hBMSC differentiation induction in 3D collagen gels

As mentioned before, besides the inhibition of adipogenic and osteogenic differentiation of hBMSCs, rhFGF1 and rhFGF2 treatments affected the size of the collagen gels as well as did heparin alone, although to a much lower extent (Figure 28). Gels under adipogenic induction and treated with heparin alone were in average 1.3-times larger than BSA-control gels at day 21. Likewise, gels treated with 25 ng/ml rhFGF1 or rhFGF2 during adipogenic induction were 1.5-times larger than gels of the heparin control. In the same way, gels of the heparin control under osteogenic conditions were in average 1.5-times larger than gels of the BSA control, while gels under rhFGF1 or rhFGF2 treatments were approximately 2-times larger than gels of the heparin control.

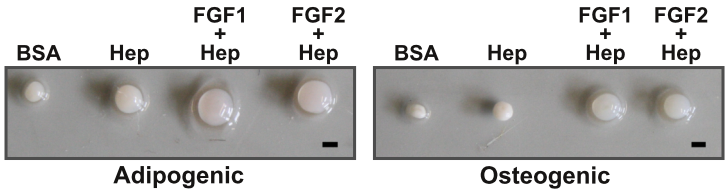

Figure 28. Collagen gels after adipogenic and osteogenic induction in the presence of rhFGF1 or rhFGF2.
Collagen gels after 21 days under adipogenic and osteogenic induction in the presence of BSA, heparin alone (Hep) or heparin combined with 25 ng/ml rhFGF1 (FGF1 + Hep) or rhFGF2 (FGF2 + Hep). Scale bars represent 1 mm.

Since the attenuation in the gel size reduction may be caused by changes in the ability of the cells to remodel the collagen matrix, the effect of heparin alone, rhFGF1 and rhFGF2 on the mRNA levels of Col1A1, MMPs and TIMPs was assessed.

When comparing the mRNA levels after 14 days of adipogenic induction in the presence of heparin alone, none of the analyzed remodeling markers, Col1A1, MMP2, MMP13, MT1-MMP, TIMP1 and TIMP2, showed significant differences in the mRNA levels with respect to the BSA

control (Figure 29). However, the mRNA levels of MMP13 and TIMP1 showed significant differences between the heparin control and rhFGF1 or rhFGF2 treatments. The mRNA levels of MMP13 increased by 5.8-fold and 5.2-fold in the presence of FGF1+heparin and FGF2+heparin, respectively, while TIMP1 mRNA levels increased by 30-fold and 29-fold, respectively, reaching even higher levels than at day 0. The elevated levels of TIMP1 mRNA were also correlated with increased protein levels as determined by immunohistochemical staining of collagen gel cryosections (Figure 30). Noteworthy, the mRNA levels of MT1-MMP were upregulated under the rhFGF1 and rhFGF2 conditions when compared with the BSA control, but not when compared with the heparin control. These results suggest that, concomitant with the inhibition of adipogenesis, rhFGF1 and rhFGF2 treatments during adipogenic induction affected the MMP/TIMP balance in collagen gels in favor of higher TIMP1 expression.

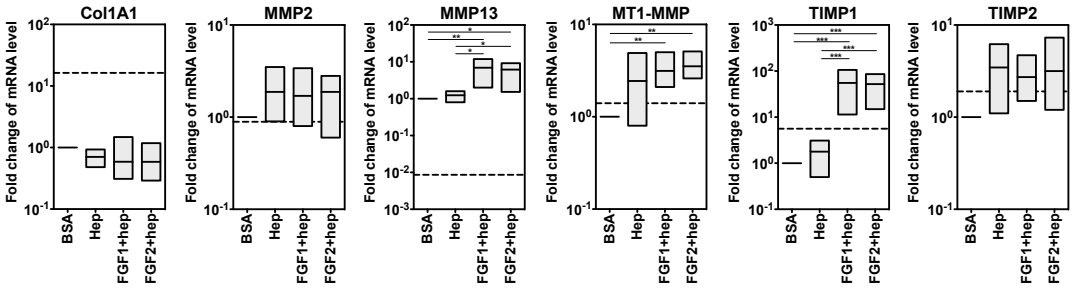

Figure 29. mRNA levels of matrix remodeling markers during adipogenic induction under rhFGF1 or rhFGF2 treatment.
Relative mRNA levels of the matrix remodeling markers Col1A1, MMP2, MMP13, MT1-MMP, TIMP1 and TIMP2 after 14 days of adipogenic induction in collagen gels in the presence of BSA, heparin alone (Hep) or heparin combined with 25 ng/ml rhFGF1 (FGF1+hep) or rhFGF2 (FGF2+hep). Data are presented as fold change relative to the BSA control. The dotted lines represent the relative mRNA levels at day 0. The floating bars denote the minimum-to-maximum values with the line representing the mean. * $p < 0.05$; ** $p < 0.01$; *** $p < 0.001$.

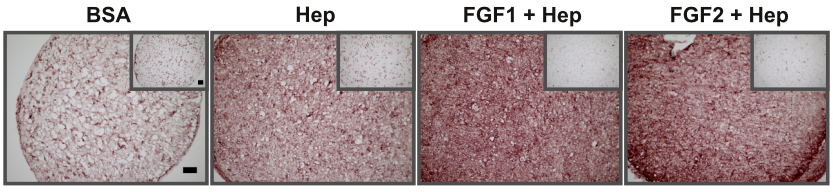

Figure 30. TIMP1 expression in the presence of rhFGF1 or rhFGF2 during adipogenic induction in collagen gels.
Immunohistochemical staining of TIMP1 in cryosections of collagen gels after 21 days under adipogenic differentiation in the presence of BSA, heparin alone (Hep) or heparin combined with 25 ng/ml rhFGF1 (FGF1 + Hep) or rhFGF2 (FGF2 + Hep). Insets show the corresponding isotype controls. Scale bars represent 100 µm.

When osteogenic differentiation was induced in the presence of heparin alone, there were no significant differences in the mRNA levels of the remodeling markers compared to the BSA control (Figure 31). Now, when the osteogenic induction was performed in the presence of rhFGF1 or rhFGF2, the mRNA levels of Col1A1, MMP2, and TIMP2 were significantly different from the heparin control. Col1A1 mRNA levels were downregulated approximately 4.4 and 4.0 times under rhFGF1 and rhFGF2 treatments, respectively. The same pattern was observed for the mRNA levels of MMP2, which were 4.8-fold lower under osteogenic induction in the presence of rhFGF1 and rhFGF2 than for the heparin control. Similarly, TIMP2 mRNA levels were downregulated under rhFGF1 and rhFGF2 stimulation by 4.4-fold and 4.2-fold, respectively, regarding heparin alone. In contrast to the previous observation for adipogenic inhibition, the mRNA levels of TIMP1 were not significantly different under the rhFGF1 or rhFGF2 conditions when compared to the heparin control, but only when compared with the BSA control.

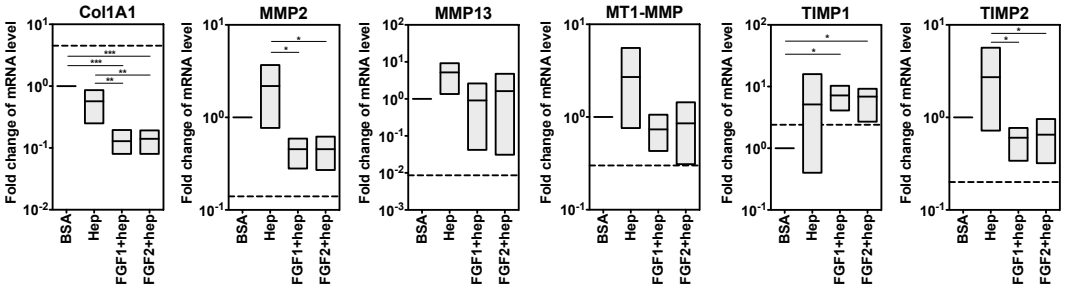

Figure 31. mRNA levels of matrix remodeling markers during osteogenic induction under rhFGF1 or rhFGF2 treatment.
Relative mRNA levels of the matrix remodeling markers Col1A1, MMP2, MMP13, MT1-MMP, TIMP1 and TIMP2 after 14 days under osteogenic induction in collagen gels in the presence of BSA, heparin alone (Hep) or heparin combined with 25 ng/ml rhFGF1 (FGF1+hep) or rhFGF2 (FGF2+hep). Data are presented as fold change relative to the BSA control. The dotted lines represent the relative mRNA levels at day 0. The floating bars denote the minimum-to-maximum values with the line representing the mean. * $p < 0.05$; ** $p < 0.01$; *** $p < 0.001$.

In summary, these results show that the presence of rhFGF1, as well as of rhFGF2, during adipogenic and osteogenic induction affects differently the expression of matrix remodeling markers with the net result in both cases of decreased collagen remodeling.

3.3. Expansion of hBMSCs in the presence of rhFGF1

In addition to the effect of a continuous stimulation with rhFGF1 throughout adipogenic and osteogenic induction, the effect of a pre-stimulation with rhFGF1 on the differentiation potential of hBMSCs in collagen gels was evaluated. For this, hBMSCs were expanded in conventional 2D culture for one passage in the presence of recombinant rhFGF1 (or rhFGF2) together with heparin

before embedding in collagen gels for subsequent adipogenic and osteogenic differentiation induction.

3.3.1. Effect of rhFGF1 on expanding hBMSCs

3.3.1.1. hBMSC proliferation

When hBMSCs were expanded in monolayers for one passage in the presence of 25 µg/ml heparin in combination with 5 or 25 ng/ml rhFGF1 or rhFGF2, both growth factors exerted a strong mitogenic effect, increasing in approximately 120% the DNA content at the end of the expansion period compared to the heparin alone condition, which in turn resulted in 30% less DNA content compared with the BSA control (Figure 32).

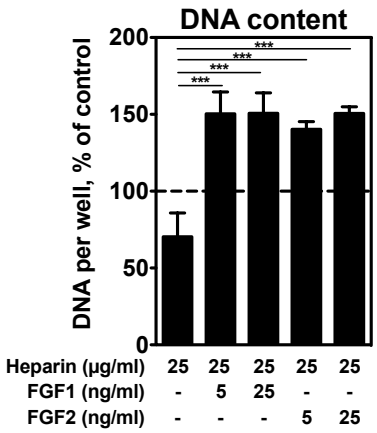

Figure 32. DNA content after hBMSC expansion in the presence of rhFGF1 or rhFGF2.
DNA content after one expansion round of hBMSCs in the presence of heparin alone or in combination with 5 or 25 ng/ml rhFGF1 or rhFGF2, expressed as percentage (mean ± SD) of DNA content after expansion in the presence of BSA (dotted line). *** $p < 0.001$.

Both concentrations used, 5 and 25 ng/ml rhFGF, showed comparable effects. In addition to this mitogenic effect, rhFGF1 and rhFGF2 induced morphological changes in expanding hBMSCs, which adopted a more spindle-shaped morphology, while cells expanded with heparin alone displayed a more flattened cuboidal shape (Figure 33).

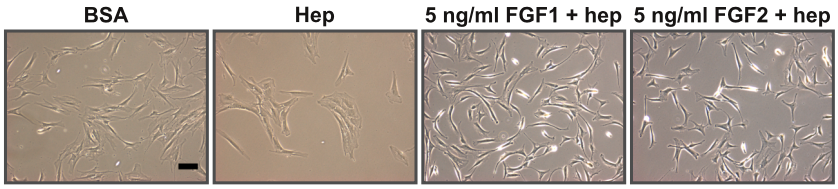

Figure 33. hBMSC expanded in the presence of rhFGF1 or rhFGF2.
hBMSCs expanded for one passage in the presence of BSA, heparin (Hep) alone or heparin plus 5 ng/ml rhFGF1 (FGF1 + hep) or rhFGF2 (FGF2 + hep). Scale bar represents 100 µm.

3.3.1.2. Collagen matrix contraction

At the end of the expansion phase with rhFGF1 or rhFGF2, hBMSCs were embedded in collagen gels for adipogenic and osteogenic differentiation induction. The first remarkable observation was that cell-mediated contraction of the collagen gels was substantially impaired for cells that were expanded in the presence of 5 or 25 ng/ml rhFGF1 or rhFGF2, with a similar outcome for both concentrations (Figure 34).

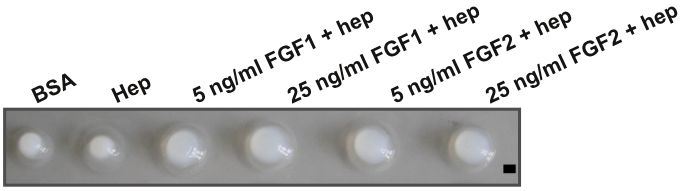

Figure 34. Collagen gels loaded with hBMSCs expanded in the presence of rhFGF1 or rhFGF2.
Collagen gels at day 0 after embedding of hBMSCs expanded in the presence of BSA, heparin alone (Hep) or heparin in combination with 5 or 25 ng/ml rhFGF1 (FGF1 + hep) or rhFGF2 (FGF2 + hep). Scale bar represents 1 mm.

Since contraction of collagen fibers is mediated by the actin cytoskeleton, phalloidin staining was used to visualize actin filaments in expanded hBMSCs 24 hours after seeding in collagen gels (Figure 35). Expansion in the presence of heparin alone induced the formation of dense actin stress fibers, yet it did not result in enhanced contraction compared to the BSA control. Expansion in the presence of rhFGF1 or rhFGF2, on the other hand, resulted in the absence of actin filament bundles and only cortical actin fibers were observed. Therefore, the diminished contraction of collagen gels by hBMSCs expanded in the presence of rhFGF1 or rhFGF2 appears to be, at least in part, due to the disruption of an organized actin cytoskeleton.

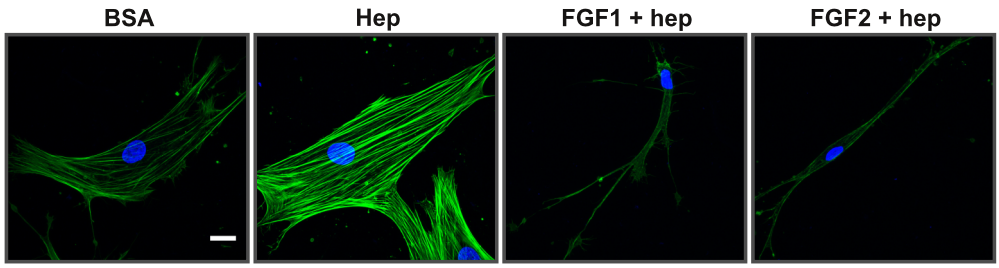

Figure 35. hBMSC actin cytoskeleton after expansion in the presence of rhFGF1 or rhFGF2.
Phalloidin staining of hBMSC actin cytoskeleton in collagen gels at day 0 after hBMSC expansion for one passage in the presence of BSA, heparin alone (Hep) or heparin plus 25 ng/ml rhFGF1 (FGF1 + hep) or rhFGF2 (FGF2 + hep). Scale bar represents 20 µm.

3.3.2. Differentiation potential of hBMSCs in 3D collagen gels after expansion with rhFGF1

3.3.2.1. Adipogenic potential

hBMSCs expanded for one passage in the presence of 5 and 25 ng/ml rhFGF1 or rhFGF2 that were then induced to differentiate into adipocytes for 21 days in collagen gels showed no differences in lipid droplet accumulation when compared to BSA and heparin controls (Figure 36).

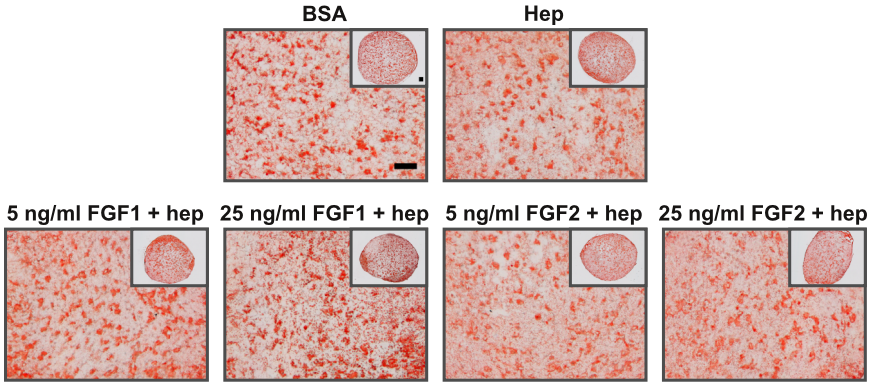

Figure 36. Adipogenic differentiation in collagen gels after expansion in the presence of rhFGF1 or rhFGF2.
Oil Red O staining of lipid droplets in collagen gels cryosections after 21 days of adipogenic induction of hBMSCs expanded in the presence of BSA, heparin alone (Hep) or heparin in combination with 5 or 25 ng/ml of rhFGF1 (FGF1 + hep) or rhFGF2 (FGF2 + hep). Insets show lower magnification images. Scale bars represent 100 µm.

Likewise, the mRNA levels of the adipogenic markers PPARγ2, FABP4 and LPL after 14 days of adipogenic induction of expanded hBMSCs were similar, irrespective of the condition during the expansion phase (Figure 37). Hence, these results indicate that the adipogenic potential of hBMSCs is not affected by a pre-stimulation of rhFGF1 or rhFGF2 signaling before the differentiation induction.

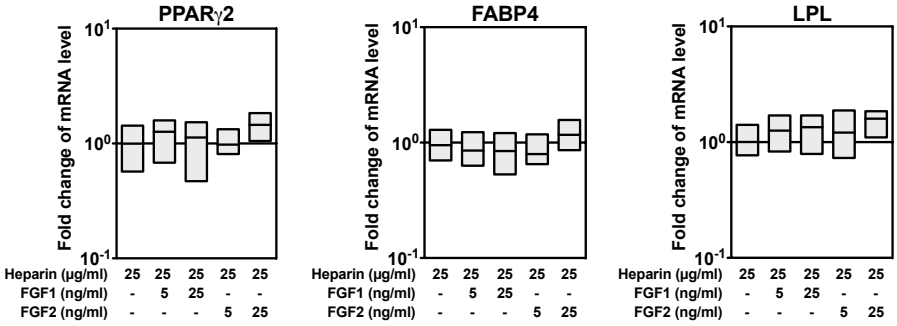

Figure 37. Expression of adipogenic markers after adipogenic induction on hBMSCs expanded with rhFGF1 or rhFGF2.
Relative mRNA levels of the adipogenic differentiation markers PPARγ2, FABP4 and LPL after 14 days of adipogenic induction of hBMSCs in collagen gels after expansion in the presence of heparin alone or heparin combined with 5 or 25 ng/ml rhFGF1 (FGF1 + hep) or rhFGF2 (FGF2 + hep). Data are presented as fold change relative to hBMSCs expanded in the presence of BSA (continuous line). The floating bars denote the minimum-to-maximum values with the line representing the mean.

3.3.2.2. Osteogenic potential

Osteogenic differentiation in collagen gels after expansion of hBMSCs for one passage with 5 and 25 ng/ml rhFGF1 or rhFGF2 resulted in the inhibition of mineralized matrix deposition for both FGF concentrations tested, whereas alkaline phosphatase activity was nevertheless detected (Figure 38). Regarding mRNA levels of osteogenic markers, Runx2 and osteopontin mRNA levels did not show differences among the different expansion conditions, however, osteocalcin mRNA levels were upregulated after osteogenic induction in hBMSCs that were expanded in the presence of rhFGF1 or rhFGF2 (Figure 39). Although similar levels of upregulation were observed, statistical significance was only achieved for the 5 ng/ml rhFGF1 and 25 ng/ml rhFGF2 conditions. These results suggest that the transient stimulation of rhFGF1 and rhFGF2 signaling during the expansion phase of hBMSCs does not affect their osteogenic potential but enhances osteocalcin expression with the parallel inhibition, or at least delay, of their maturation into mineralizing osteoblasts.

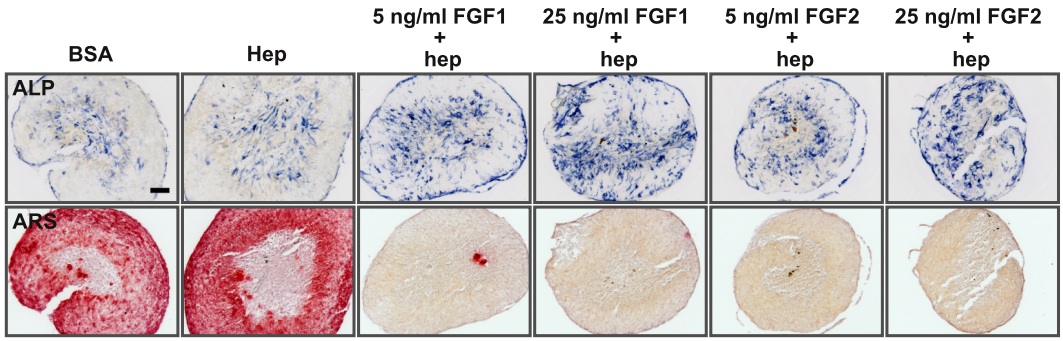

Figure 38. Osteogenic differentiation in collagen gels after expansion in the presence of rhFGF1 or rhFGF2.
Collagen gel cryosections stained for alkaline phosphatase activity (ALP) and for mineralized matrix with Alizarin Red S (ARS) after 21 days of osteogenic induction of hBMSCs expanded for one passage in the presence of BSA, heparin alone (Hep) or heparin in combination with 5 or 25 ng/ml of rhFGF1 (FGF1 + hep) or rhFGF2 (FGF2 + hep). Scale bar represents 100 µm.

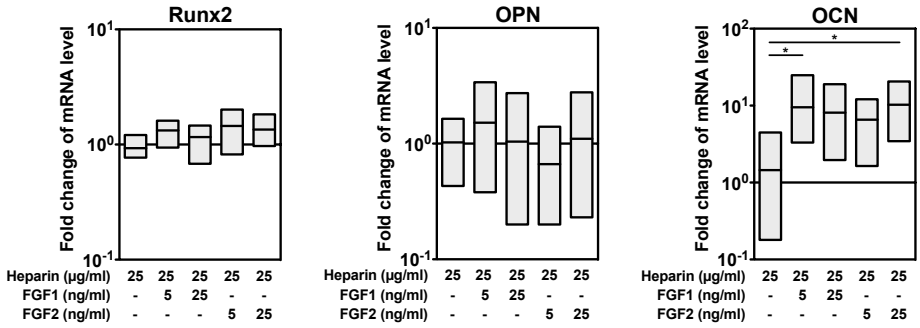

Figure 39. Expression of osteogenic markers after osteogenic induction on hBMSCs expanded with rhFGF1 or rhFGF2.
Relative mRNA levels of the osteogenic differentiation markers Runx2, osteopontin (OPN) and osteocalcin (OCN) after 14 days of osteogenic induction of hBMSCs in collagen gels after expansion in the presence of heparin alone or heparin in combination with 5 or 25 ng/ml rhFGF1 (FGF1) or rhFGF2 (FGF2). Data are presented as fold change relative to hBMSCs expanded in the presence of BSA (continuous line). The floating bars denote the minimum-to-maximum values with the line representing the mean. * $p < 0.05$.

In order to analyze early events that could lead to the increased expression of the osteoblastic marker osteocalcin, the mRNA levels of a member of the early commitment signaling WNT pathway (WNT5A) as well as the osteogenic factors Runx2 and osteocalcin itself were measured in monolayers right after the expansion phase (Figure 40). The mRNA levels of osteocalcin were already highly upregulated after expansion of hBMSCs with 5 and 25 ng/ml rhFGF1 or rhFGF2, before the beginning of osteogenic induction in collagen gels. The mRNA levels of Runx2, however, were found to be similar among all conditions after the expansion phase. Interestingly, hBMSCs expanded with rhFGF1 or rhFGF2 displayed elevated levels of WNT5A mRNA, although the

difference was not statistically significant with respect to the heparin control but only to the BSA control.

In summary, these results indicate that the enhanced expansion of hBMSCs by rhFGF1 or rFGF2 treatments did not affected the adipogenic potential of these cells when cultured in collagen gels. During the expansion, however, the expression of the osteogenic marker osteocalcin was upregulated by rhFGF1 and rhFGF2, the upregulation was maintained after osteogenic differentiation induction in collagen gels but matrix mineralization was negatively affected.

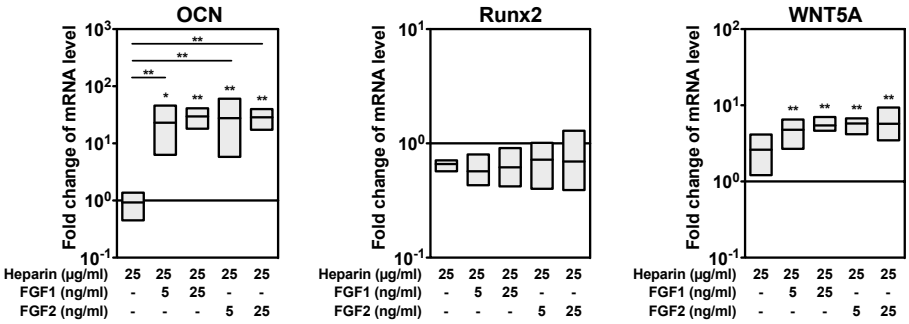

Figure 40. mRNA levels of osteogenic markers in hBMSCs after expansion in the presence of rhFGF1 or rhFGF2.
Relative mRNA levels of osteocalcin (OCN), Runx2 and WNT5A in hBMSCs at the end of the expansion round in the presence of heparin alone or heparin in combination with 5 or 25 ng/ml rhFGF1 (FGF1 + hep) or rhFGF2 (FGF2 + hep). Data are presented as fold change relative to hBMSCs expanded in the presence of BSA (continuous line). The floating bars denote the minimum-to-maximum values with the line representing the mean. * $p < 0.05$; ** $p < 0.01$.

4. Discussion

4.1. Differentiation of hBMSCs in 3D collagen gels

A robust body of evidence indicates that *in vitro* cellular behavior can be tremendously affected by dimensionality as well as the characteristics of the environment in which cells are cultured (Cukierman et al., 2001; Lee et al., 1984; Roskelley et al., 1994; Théry et al., 2006; van Susante et al., 1995).

Particularly in the case of hBMSCs, several studies clearly highlight the importance of the chemical, physical and mechanical properties of the microenvironment, such as composition (Santiago et al., 2009), adhesion ligands (Frith et al., 2012), geometry (Kilian et al., 2010; McBeath et al., 2004) and stiffness (Engler et al., 2006; Park et al., 2011) in hBMSC fate determination.

Therefore, the incorporation of three-dimensionality to the relevant ECM microenvironment allows for the development of *in vitro* model systems that relate much closer to the complex *in vivo* conditions found in stem cell niches, providing an improved way to study the influence of soluble and mechanical cues on lineage specification (Lund et al., 2009b).

4.1.1. 3D collagen gels and hBMSC differentiation

Most of the existing studies employing 3D culture systems for hBMSC differentiation have a tissue engineering orientation, mostly for bone or cartilage regeneration, and therefore, they aim at the enhancement of a particular differentiation pathway, frequently using natural or synthetic biomaterials as 3D scaffolds but which are not representative of the physiological ECM. The first aim of this work was to establish a 3D culture model for adipogenic and osteogenic differentiation of hBMSCs in conditions similar to those found in their physiological niche. Since collagen type I is the main component of bone and marrow ECM (Hamilton & Campbell, 1991; Young, 2003), the chosen 3D system was based on collagen gels for hBMSC embedding.

Collagen type I hydrogels consist of a highly hydrated network of interconnected collagen fibers that provides physiologically relevant cell adhesion via integrin engagement. Additionally, collagen gels are susceptible to matrix remodeling by cell-mediated contraction and proteolysis by the activity of collagenases (Chevallay & Herbage, 2000). Due to the high abundance of collagen in native ECM, collagen gels offer an attractive option for mimicking the natural cellular microenvironment and hence, they have been extensively used for 3D cell encapsulation (Burdick & Vunjak-Novakovic, 2009), including hBMSCs, which have been shown to preserve their

immunophenotype and differentiation capacity after embedding and subsequent migration from collagen gel microspheres to culture plates (Chan et al., 2007). Yoneno and colleagues were the first to demonstrate that hBMSCs were able to differentiate embedded in collagen gels into chondrogenic and osteogenic lineages when chemically induced with the corresponding differentiation cocktails (Yoneno et al., 2005).

Using an encapsulation method similar as the one described by Chan and colleagues (Chan et al., 2010), both adipogenic and osteogenic differentiation of hBMSCs were achieved in the collagen gels (Figures 4-9). Differences in initial cell and collagen concentrations had a greater effect on osteogenesis, for which matrix mineralization was more efficient at lower initial cell and collagen concentrations (Figure 5), although not every hBMSC batch displayed matrix mineralization after osteogenic induction. A much less pronounced effect was observed in the case of adipogenesis, although lower initial collagen and higher initial cell concentration seemed to favor lipid droplet accumulation (Figure 4).

The observed variation in the differentiation outcome may be influenced by the distinct conditions encountered by the cells in the gels, such as local cell density and collagen concentration as well as different mechanical cues, all depending on the initial conditions and the extent of cell-mediated contraction of the 3D collagenous matrix.

The study of differentiation balance in an environment mechanically closer to the physiological takes particular relevance given that the mechanical properties of the ECM have been shown to have a strong impact on BMSC fate determination. For example, using collagen-coated polyacrylamide gels of tunable elasticity, Engler and colleagues (Engler et al., 2006) reported that BMSCs seeded on top of these gels respond to matrix stiffness by adopting the morphology and upregulating the expression of markers corresponding to tissues of matching stiffness, all in the absence of chemical differentiation cues. Similarly, matrices mimicking the stiffness of osteoid have been reported to enhanced chemically-induced osteogenic differentiation of hBMSCs when compared to softer matrices (Shih et al., 2011), whereas softer gels have been found to favor adipogenic differentiation of hBMSCs (Park et al., 2011). The interaction between matrix elasticity and cell density has also been shown to influence osteogenic differentiation of hBMSCs on collagen-coated polyacrylamide gels (Xue et al., 2013). While harder matrices favor osteogenesis at low cell density, this effect is abolished at high cell density possibly due to restricted cell spreading.

Although less information is available, similar effects of matrix elasticity on BMSC differentiation in 3D systems have been reported. For instance, using alginate gels of different stiffness, Huebsch and colleagues observed that osteogenic differentiation was favored over adipogenic differentiation in hydrogels of higher stiffness (Huebsch et al., 2010). Another important

consequence of the physical properties of the ECM is its influence on cell shape and spreading, which in turn have been shown to influence hBMSC differentiation (Kilian et al., 2010; McBeath et al., 2004). In 2D, cell spreading favors osteogenic differentiation while adipogenesis is the preferred differentiation pathway for cells that are forced into a rounded morphology (McBeath et al., 2004), although Huebsch and colleagues found that matrix elasticity does not influence cell morphology in 3D alginate gels (Huebsch et al., 2010). Nevertheless, it has been suggested that the observed effects on cell differentiation are due to differences in matrix porosity and anchoring density rather than matrix elasticity per se (Trappmann et al., 2012). A higher local collagen concentration is concomitant with a higher density of adhesion ligands. In 3D, higher density of the cell adhesion sequence Arg-Gly-Asp (RGD) has been associated with enhanced osteogenesis whereas blocking of RGD binding enhances adipogenesis (Huebsch et al., 2010).

Comparing adipogenesis in 2D monolayers and in collagen gels, a similar outcome in terms of marker expression levels was observed (Figure 14B), whereas for osteogenesis, the mRNA levels of the osteogenic markers were significantly higher in collagen gels (Figure 15B). An enhancement in the expression of osteogenic markers after hBMSC differentiation induction in 3D cultures compared with 2D has also been observed by others. For instance, higher mRNA levels of osteogenic markers have been observed for hBMSC differentiated in 3D spheroids (Wang et al., 2009) and microaggregates (Kabiri et al., 2012).

4.1.2. hBMSC differentiation and collagen matrix remodeling

A remarkable difference between adipogenic and osteogenic differentiation of hBMSCs in 3D was the final size of the collagen gels (Figure 3, 12 and Table 3). For both adipogenic and osteogenic differentiation, the final gel size correlated positively with the collagen concentration and negatively with the initial cell number, similarly as described for undifferentiated hBMSCs (Chan et al., 2007), but the size of gels under osteogenic conditions was notably smaller than the size of gels under adipogenic induction.

4.1.2.1. Collagen matrix contraction by differentiating hBMSCs

Cells inside the gels can remodel the collagen matrix by contraction, synthesis and degradation. Matrix contraction in free-floating collagen gels occurs as a consequence of the tractional forces generated by migrating cells, which through pseudopodial protrusion and retraction pull together the surrounding collagen fibrils resulting in gel size reduction (Bell et al., 1979; Dahlmann-Noor et al., 2007; Meshel et al., 2005; Stopak & Harris, 1982). Hence, one possible explanation for the dissimilar gel sizes is a difference in the protrusion activity and the tractional forces that osteoblasts and adipocytes are able to exert on the collagen fibrils, resulting in distinct matrix

contractile capacities. A reduced contraction capacity under adipogenic conditions compared with osteogenic conditions is in agreement with a previous report showing differences in the extent of matrix contraction exerted by differentiating hBMSC seeded on top of collagen gels (Schneider et al., 2010). Since actin cytoskeleton is indispensable for the generation of contractile forces (Kolodney & Wysolmerski, 1992), differences in its organization in hBMSCs undergoing osteogenesis and adipogenesis might be responsible for the disparity in collagen gel sizes. Although a comparison between changes in the actin cytoskeleton organization throughout hBMSC adipogenesis and osteogenesis has, to the best of our knowledge, not been reported, cytoskeletal rearrangements have been described for hBMSCs differentiating into osteoblasts in 2D cultures, with thick actin bundles in undifferentiated hBMSCs converting into a meshwork of thin actin filaments after osteogenic induction (Titushkin & Cho, 2007). In the case of hBMSC adipogenesis, the chemical disruption of the actin cytoskeleton has been shown to enhance adipogenic differentiation (McBeath et al., 2004), suggesting that disassembly occurs in hBMSCs undergoing adipogenesis. Supporting this, it has been reported that murine 3T3L1 pre-adipocytes reduce the expression of actin (Rodríguez Fernández & Ben-Ze'ev, 1989) and lose the actin stress fibers during differentiation, displaying a punctuated cytoplasmic pattern of actin with fibers restricted to the cortical region (Kanzaki & Pessin, 2001). However, extrapolation from observations made in 2D culture systems might not be valid in 3D. For instance, even between 3D free floating collagen gels and gels that remained attached to the culture dishes differences have been observed concerning the organization of the actin cytoskeleton in fibroblasts; cells in floating gels develop much less actin stress fibers than cells in attached gels (Grinnell, 2000). The ability to contract collagen gels seems also be related to cell shape. Contraction extent appears to be positively correlated to cell spreading whereas a rounded morphology, is associated with low contraction capacity (Martin-Martin et al., 2011), which correlates with osteoblastic and adipocytic cell morphology, respectively.

In addition to cytoskeletal differences, differential expression profile of integrins may contribute as well to the uneven matrix remodeling capabilities. Cells communicate with collagen fibrils mainly through integrin receptors, which have also a fundamental role in collagen matrix remodeling, in particular the α2β1 integrin (Jokinen et al., 2004; Schiro et al., 1991). In the case of bone-marrow mesenchymal progenitors, contraction has been associated predominantly to β1-integrins interaction (Heckmann et al., 2006). In this context, adipocytic differentiation has been previously linked to a decreased expression and activity of β1-integrins, which is concomitant to the morphological changes that fibroblastic-shaped precursors undergo into rounded adipocytes (Kawaguchi et al., 2003; Rodríguez Fernández & Ben-Ze'ev, 1989). On the contrary, during early stages of osteogenic differentiation of hBMSCs, the surface levels of β1-integrins has been reported to be upregulated (Martino et al., 2009).

4.1.2.2. Role of matrix metalloproteinases and their inhibitors in collagen matrix remodeling

Another related factor that may contribute to the observed differences in the final size of the gels is the extent of matrix proteolytic cleavage by proteases such as MMPs (Daley et al., 2008). Indeed, collagenase activity has been found to enhance fibroblast-mediated contraction of collagen gels while chemical inhibition of MMP activity hampers the ability to contract the matrix (Daniels et al., 2003; Phillips & Bonassar, 2005; Scott et al., 1998), which correlates with diminished cell protrusion (Martin-Martin et al., 2011). Hence, a higher net activity of MMPs may contribute to a more extensive matrix remodeling by osteoblasts compared to adipocytes, due to increased MMP-mediated matrix degradation and contraction.

Consistent with the observed differences in matrix remodeling, adipogenic and osteogenic differentiation in 3D collagen gels resulted in distinct relative mRNA levels of MMPs (Figure 13). For instance, the relative mRNA levels of MMP2 and MT1-MMP did not change after adipogenic induction but they were upregulated after osteogenic differentiation. Although the mRNA levels of MMP13 were highly upregulated in both differentiation pathways, given that MMP13 is secreted as an inactive form that can be activated by MT1-MMP and MMP2 (Knäuper et al., 1996), a major activity under osteogenic conditions could be expected. On the other hand, the MMP inhibitor TIMP1 was slightly downregulated in both differentiation pathways while TIMP2 was upregulated only during osteogenesis.

Differences in the expression of matrix remodeling markers have been previously reported for differentiating hBMSC seeded on collagen films (Mauney & Volloch, 2010), although contrasting conclusions were drawn in that case. Mauney and colleagues associated adipogenesis with increased MMP and decreased TIMP expression, while osteogenesis was found to induce the inverse pattern. Concordant observations with our work were the upregulation of MMP13 and the downregulation of TIMP1 under adipogenic conditions together with the upregulation of TIMP2 under osteogenic stimulation. The mRNA levels of MMP13, though, were not found to be regulated after osteogenic differentiation. Nevertheless, the analysis by Mauney and colleagues was restricted to the collagenases MMP1, MMP8 and MMP13 and since their system involves a 2D culture of hBMSCs onto a collagen film and not a 3D setting, differences in the regulation of MMP and TIMP activities are to be expected.

The observed differential expression of MT1-MMP, upregulated after osteogenic but not adipogenic differentiation, may be of particular relevance in accounting for the difference in gels sizes. MT1-MMP expression has been found to be essential for conferring hMSCs with collagen degradation activity as well with invasive capacity when cultured on top of collagen gels (Lu et al., 2010). Remarkably, MT1-MMP expression has also been found to be necessary for osteogenic

differentiation inside collagen gels (Lu et al., 2010), suggesting that remodeling of the collagen matrix is a prerequisite for osteogenesis. Similarly, mice with a conditional deletion of MT1-MMP in mesenchymal progenitors display aberrant osteogenesis together with increased marrow adipogenesis (Tang et al., 2013). As expected, when isolated mutant progenitors are induced to differentiate embedded in collagen gels osteogenic differentiation is diminished whereas adipogenesis is enhanced, although differentiation is not affected in a 2D setting. Tang and colleagues further associated this mutant MT1-MMP phenotype with an incapacity to generate the cell-shape changes needed to activate β1-integrins in a 3D collagenous microenvironment, which seems to be the downstream mechanism responsible for the commitment bias.

Contrasting the more proteolytic expression profile observed for the osteogenic pathway in terms of MMP mRNA levels, TIMP2 was found to be upregulated following osteogenic commitment. Although the increased expression of a MMP inhibitor may suggest counteraction of the proteolytic activity, TIMP2 expression has been positively associated with the ability of hBMSCs to invade reconstituted basement membranes (Ries et al., 2007). As Ries and colleagues argued, this pro-migratory effect of TIMP2 is probably due to its role as an adaptor between MT1-MMP and pro-MMP2. Despite the inhibition of the bound MT1-MMP molecule, the formation of this complex allows the activation of MMP2 by a second MT1-MMP molecule (Butler et al., 1998; Itoh et al., 2001). TIMP1, on the contrary, was found by Ries and colleagues to play a repressive role in hBMSC migration (Ries et al., 2007).

4.2. FGF signaling in hBMSC differentiation

An important amount of evidence supports the fact that *in vitro* hBMSC adipogenic and osteogenic differentiation are inversely correlated, with a number of factors and conditions enhancing one of the differentiation pathways displaying an inhibitory role on the other. *In vivo*, an analogous inverse relationship is observed between bone mass and marrow fat, suggesting that the differentiation of the common multipotent stromal progenitor in the bone marrow is inversely regulated as well (Sadie-Van Gijsen et al., 2013).

The FGF signaling ligand FGF1 has been previously proposed by our group as a potential modulator of hBMSC differentiation balance upon the observation that FGF1 is inversely regulated at the mRNA level after switching osteogenic/adipogenic induction conditions (Schilling et al., 2008). Supporting the hypothesis of a differential role in both differentiation pathways, a down-regulation of FGF1 mRNA levels after adipogenic but not osteogenic differentiation in collagen gels was observed in this work (Figure 16). Therefore, in order to investigate the role of FGF1 signaling on adipogenic and osteogenic differentiation of hBMSCs, the

effect of the continuous stimulation with rhFGF1 throughout the differentiation induction in collagen gels was assessed. Additionally, rhFGF2 was included in this study in order to test if both growth factors would elicit the same response in hBMSC differentiation. Differences were initially hypothesized based on the fact that, unlike FGF1, FGF2 was not found to be reciprocally regulated after osteogenic/adipogenic condition switching by Schilling and colleagues but only downregulated after osteogenic-to-adipogenic switching (Schilling et al., 2008). Our results showed that both rhFGF1 and rhFGF2 hindered in a dose-dependent manner the *in vitro* 3D adipogenic differentiation of hBMSCs, indicating that the continuous signaling exerts an inhibitory role (Figures 17-22). As expected, rhFGF1 and rhFGF2 inhibitory effect was dependent on FGFR signaling, since chemical blockage using the specific small molecule inhibitors PD166866 (Panek et al., 1998) and SU5452 (Mohammadi et al., 1997) rescued the adipogenic differentiation capacity of hBMSCs under rhFGF treatments (Figure 19). However, neither rhFGF1 nor rhFGF2 enhanced osteogenic differentiation of hBMSCs in collagen gels but, on the contrary, inhibited matrix mineralization.

In this work, all experiments involving stimulations with rhFGF1 and rhFGF2 were performed in the presence of heparin, which was essential for the inhibitory effects observed for rhFGF1. For rhFGF2, on the other hand, the presence of heparin is not indispensable, although it has been shown to maximize FGF2 activity (Caldwell & Svendsen, 1998). Nevertheless, we also applied heparin together with rhFGF2 to allow for direct comparison with rhFGF1 treatment and a heparin alone condition was always used as a control. Since heparin, as well as cell surface heparan sulfate proteoglycans, functions as co-receptors for FGFR-mediated signaling of both FGFs, the reason behind the strict requirement of heparin only for FGF1 is most likely due to a stabilization effects. Evidence of this stabilizer role includes studies showing that heparin extends the half-life of FGF1 in culture medium at 37ºC (Damon et al., 1989; Mueller et al., 1989), in part by protecting it from proteolytic degradation (Damon et al., 1989; Rosengart et al., 1988). In contrast to data from 2D hBMSC differentiation on tissue culture plastic (TCP) from our group, differentiation in collagen gels was not significantly affected by treatment with heparin alone, although we found a small but significant upregulation of LPL in the case of adipogenic differentiation (Figure 18). As described previously by our group (Simann et al., 2015), heparin was found to enhance osteogenic differentiation while inhibiting the adipogenic pathway in the 2D culture system. A plausible explanation would be that exogenous heparin might significantly contribute as a cofactor to diverse receptor signaling in the 2D but not the 3D setting, in which also endogenous heparan sulfate proteoglycans may dominate.

4.2.1. Role of FGF1 and FGF2 in adipogenic differentiation

Several works have previously reported the effect of exogenous FGF1 and FGF2 in adipogenesis, mainly in conventional 2D culture systems, with conflicting results. For instance, in agreement with our results, an inhibitory activity of FGF1 and FGF2 has been predominantly reported on murine adipocytic cell lines (Hayashi et al., 1981; Krieger-Brauer & Kather, 1995; Navre & Ringold, 1989), although low concentrations (~2 pg/ml) of FGF1 have been shown to favor adipogenesis of 3T3-LI preadipocytes (Krieger-Brauer & Kather, 1995). However, in rat adipocyte precursors FGF1 and FGF2 have shown no inhibitory effect on adipogenesis (Serrero, 1987; Vassaux et al., 1994). In the case of human adipose progenitors, no significant effect in terms of lipid accumulation were found by Hauner and colleagues (Hauner et al., 1995). A possible explanation for these discrepant observations may be species-specific variability as well as differences in the degree of the adipogenic commitment of those progenitor cells, which, in case of being already irreversible, it would render the adipogenic precursors insensitive to the inhibitory role of FGF signaling.

Interestingly, Hutley and colleagues identified FGF1 as a pro-adipogenic factor for human pre-adipocytes secreted by microvascular endothelial cells (Hutley et al., 2004). *In vitro*, treatment of human pre-adipocytes with FGF1 during growth and differentiation phases enhanced adipogenesis. This positive effect on differentiation was accompanied by increased proliferation. Moreover, the authors found in a subsequent study that, upon FGF1 treatment, PPARγ expression was already upregulated at the end of the proliferation phase, before the start of the differentiation induction, suggesting a role for FGF1 in the commitment of precursor cells to the adipocyte lineage (Newell et al., 2006). However, when the exogenous FGF1 stimulus was applied only during the differentiation phase, adipogenesis was not affected or even slightly diminished (Hutley et al., 2004). It is worth noting that the concentration of FGF1 used in those studies was the lowest concentration tested in the present work, 1 ng/ml FGF1, which slightly affected adipogenesis of hBMSCs in collagen gels.

Regarding hBMSCs, dexamethasone-induced adipogenic differentiation has been shown to be accelerated, although not increased, by co-stimulation with FGF2, which also enhanced cell proliferation (Locklin et al., 1999). This stimulatory effect on adipogenesis contradicts the inhibitory effect that we observed. It is probable that in this case the discrepancy can be explained by differences in the culture conditions, for example, the use of dexamethasone as the sole differentiation trigger. Similarly, FGF2 treatment throughout the *in vitro* differentiation of human adipose-derived stem cells has been reported to have no effect on adipogenesis (Kakudo et al., 2007).

Interestingly, a dose-dependent positive effect of FGF1 and a concentration-dependent biphasic effect of FGF2 on adipogenic differentiation of human adipose-derived stromal cells (ASCs) has been recently reported (Kim et al., 2015). However, in that work the cells were pre-treated with FGF1 or FGF2 one day before the differentiation induction, which was then conducted in the absence of the factors. Nevertheless, the authors found that FGF2 pre-treatment at lower than 2 ng/ml increases adipogenesis while concentrations higher than 10 ng/ml are inhibitory. This response was attributed to the persistent phosphorylation of ERK induced by FGF2 only at high concentrations, which in turn deactivated PPARγ.

In the case of rat BMSCs and in direct opposition to the inhibitory effect we describe in this work for hBMSCs, Neubauer and colleagues reported that FGF2 treatment increases adipogenesis when applied during proliferation, differentiation or both culture phases and that this effect is probably mediated by the upregulation of PPARγ expression (Neubauer et al., 2004). Furthermore, the authors observed in a subsequent study that rat BMSC adipogenesis in a 3D poly(lactic-co-glycolic acid) scaffold was strongly enhanced by FGF2 (Neubauer et al., 2005). Similarly, FGF2 was previously shown to strongly induce proliferation of rat BMSCs and enhance adipogenic differentiation in monolayer cultures when kept during differentiation induction (Locklin et al., 1995). This enhancing effect of FGF2 on rat BMSC adipogenesis suggests that its role in adipogenic differentiation of marrow stromal precursors is species-specific and hence, rat BMSC adipogenesis may not represent a good model of hBMSC adipogenesis, at least with respect to the role of FGF signaling pathway.

4.2.2. Role of FGF1 and FGF2 in osteogenic differentiation

Compared with adipogenesis, the role of FGF signaling on osteogenesis has been more extensively studied, yet its role is not fully understood. Additionally, its effect on *in vitro* osteogenic differentiation seems to be highly dependent on the tissue of origin and species of the precursor cells, their differentiation stage as well as the culture and treatment conditions.

Here, we have shown that a continuous treatment with exogenous rhFGF1 or rhFGF2 *in vitro* negatively affected osteogenic differentiation of hBMSCs in collagen gels, by inhibiting matrix mineralization in a dose-dependent manner and increasing cell numbers (Figures 21-23). Several works have previously drawn similar results despite using different model systems and experimental settings.

For instance, in the work by Biver and colleagues, FGF2 treatment was implicated in the inhibition of osteogenic differentiation and enhancement of proliferation of hBMSC in conventional 2D culture. The extent of differentiation inhibition correlated with the duration of FGF2 stimulation, indicating the reversibility of the inhibitory effect, and was linked to the hampering of BMP

ligands and receptors upregulation, mediated by ERK and JNK transduction activation (Biver et al., 2012).

Intriguingly, a positive effect of exogenous FGF2 on hBMSC osteogenesis was concluded by Pri-Chen and colleagues. Under osteogenic conditions, FGF2 stimulated osteocalcin production and matrix mineralization. However, a key difference in this report is the use of the osteogenic induction cocktail also during a preceding passage, which most probably rendered the hBMSC population into differentiating osteoblasts before the FGF2 stimulation. Nevertheless, the authors included in their report a condition in which FGF2 was present during both passages, also resulting in increased osteocalcin secretion and mineral deposition when compared with cells that were only stimulated with FGF2 during the first or second induction passage (Pri-Chen et al., 1998).

In the same line as the present results, studies using murine BMSCs have reported that a constant stimulation with FGF2 throughout osteogenic differentiation strongly decreased alkaline phosphatase activity as well as matrix mineralization (Huang et al., 2009; Kalajzic et al., 2003). Interestingly, based on the levels of FGF2 mRNA during osteogenic induction in murine BMSCs (Huang et al., 2007), Huang and colleagues additionally tested the effect of a profiled FGF2 stimulation that followed the expression pattern of FGF2, showing the same inhibitory outcome as the constant treatment (Huang et al., 2009).

Supporting the observations on progenitors derived from murine bone marrow, FGF2 has also been shown to display an inhibitory effect on the osteogenic differentiation of murine ASCs (Quarto & Longaker, 2006). Osteogenic induction under FGF treatment resulted in dose-dependent and reversible enhancement of proliferation together with lower alkaline phosphatase activity, reduced osteocalcin expression and blocked mineralization. Strikingly, the same authors reported that osteogenic differentiation of human ASCs was not affected by FGF2 (Quarto et al., 2008). Investigating the molecular mechanisms behind the FGF2-mediated inhibition of osteogenesis in murine ASCs, the authors concluded that FGF2 interferes with the crucial upregulation of the BMP receptor BMPR-IB during osteogenic differentiation, which is induced in murine ASC by the osteogenic factor retinoic acid. Human ASCs on the other hand, do not require retinoid acid for differentiation, most likely because they constitutively express higher levels of BMPR-IB, which seems to render them immune to the negative effects of FGF2 (Quarto et al., 2008). These FGF2-BMP signaling axis seems, therefore, to play a crucial role in the FGF2-mediated inhibition of osteogenesis in murine ASCs as well as in hBMSCs, as mentioned previously.

Strikingly, experiments performed on rat BMSCs have shown that FGF2 rather stimulates osteogenic differentiation. FGF2 treatment during differentiation induction has been linked to

higher alkaline phosphatase activity, collagen synthesis and mineral deposition, which was also coupled with enhanced proliferation (Noff et al., 1989; Scutt & Bertram, 1999). Likewise, in contrast to our results, Oh and colleagues (Oh et al., 2012) described the enhancement of rat BMSC proliferation, osteogenic marker expression and mineralized matrix deposition in collagen gels loaded with FGF2. However, a direct comparison between both studies is hampered by the different experimental approaches employed; Oh and colleagues incorporated FGF2 into the collagen gels at the beginning of the 3D culture and no further doses of the growth factor were added during the differentiation period, hence, the effective concentration declined in time due to the released of the incorporated FGF2. Instead, we provided a constant stimulation by adding rhFGF1 or rhFGF2 into the culture medium at regular time points throughout the differentiation induction. Nonetheless, the results by Oh and colleagues are in line with the previous observations in 2D for rat BMSCs (Noff et al., 1989), showing that alkaline phosphatase levels were higher in FGF2-loaded gels as well as the mRNA levels of type I collagen, osteopontin, bone sialoprotein and osteocalcin, together with increased matrix mineralization. In conclusion, these discrepant observations concerning human and rat BMSC osteogenesis further support the idea that FGF signaling may regulate differently BMSC differentiation in these species, as hypothesized before for adipogenic differentiation.

In 2D culture of primary rat early osteoblasts, however, FGF1 has been reported to lower alkaline phosphatase activity, hinder the upregulation of osteocalcin secretion, decrease calcium levels and enhance proliferation when applied in an early phase of the differentiation induction (Tang et al., 1996), indicating that, beside species-specific differences, differentiation stage can be determinant for defining the role of FGF stimulation.

Remarkably, the differentiation stage of human osteoblastic cells *in vitro*, in particular human calvarial cells, has been shown also to be determinant on the effect of FGF2 on proliferation and osteogenesis (Debiais et al., 1998). Cells under a 4-weeks differentiation scheme showed augmented proliferation and diminished osteogenic features only when FGF2 was present from the beginning of the differentiation induction, whereas a later treatment after one week had no effect on proliferation, moderately decreased alkaline phosphatase activity and collagen synthesis but favored matrix mineralization and osteocalcin expression. The conclusion reached by Debiais and colleagues that there is a differentiation stage-specific effect of FGF2 may explain some of the divergent reports on this matter found in the literature.

Interestingly, Mansukhani and colleagues also found differences in the response of osteoblastic cells to FGF stimulation depending of the differentiation stage, in this case using murine calvarial cells (Mansukhani et al., 2000). However, in contrast to the enhanced mineralization described by Debiais and colleagues resulting from FGF2 stimulation of human mature osteoblastic cells (Debiais et al., 1998), Mansukhani and colleagues reported the inhibition of mineralization and

even induction of apoptosis by FGF1 treatment of differentiating murine osteoblasts. These differences, however, do not appear to be due to the use of FGF2 in one study and FGF1 in the other, since Mansukhani and colleagues were able to show that FGF2 overexpression as well as the expression of a constitutively-activated FGFR2 mutant form resulted in increased apoptosis in the murine calvaria *in vivo,* restating the effect triggered by FGF1 *in vitro*. The molecular mechanisms behind this FGF-mediated inhibition of differentiation in murine calvarial osteoblasts *in vitro* have been further shown to involve the inhibition of canonical Wnt signaling (Ambrosetti et al., 2008; Mansukhani et al., 2005).

4.2.3. Inhibition of differentiation versus enhanced proliferation in collagen gels

The existing evidence recognizes a positive effect of FGF stimulation on hBMSC proliferation in conventional monolayer cultures (see 4.3.1 for further discussion). However, a different scenario has been described for cells, particularly fibroblasts, grown in free-floating collagen gels.

In this work, we found that inhibition of hBMSC differentiation by FGF signaling was associated with a tendency to increase cell content in collagen gels (Figure 23), indicative of enhanced proliferation in detriment of differentiation. This observation contrasts the idea based on studies involving fibroblasts that cells inside floating collagen gels do not engage in proliferation and are irresponsive to FGF and other growth factors signaling stimulation (Nakagawa et al., 1989; Sarber et al., 1981).

4.2.4. Inhibition of FGFR signaling and hBMSC differentiation

Despite that observation that a constant stimulation of FGF signaling with exogenous FGF1 or FGF2 resulted in inhibitory effects in both differentiation pathways, basal FGF signaling in differentiating hBMSCs showed to play a differential role in adipogenic and osteogenic differentiation.

With respect to the contribution of the basal FGFR signaling to the *in vitro* adipogenic differentiation of hBMSCs in collagen gels, our results obtained by using the specific FGFR inhibitors PD166866 (Panek et al., 1998) and SU5452 (Mohammadi et al., 1997) indicate that, at least under the specific induction conditions used in this study, signaling through FGFRs is not required for adipogenesis to occur. Interestingly, a contrasting outcome has been previously reported for the final differentiation of human pre-adipocytes in monolayer culture, for which a fully functional FGFR signaling was shown to be indispensable (Patel et al., 2005). In that work, the inhibition of FGFR signaling by PD166866 or by the expression of a dominant negative form of FGFR1 resulted in an almost complete inhibition of lipid droplet accumulation. However, both

experimental conditions were also associated with a reduction in cell content, and therefore, the mitigated adipogenic differentiation may be the result of a lower cell density rather a direct effect of FGFR on adipogenic pathways.

In the case of osteogenic differentiation in collagen gels, however, inhibition of FGFR signaling by PD166866 substantially enhanced matrix mineralization (Figure 26) without significantly affecting the expression of differentiation markers, suggesting that, in our model, endogenous FGFR signaling is not indispensable for hBMSC osteogenic differentiation but participates in the control of mineralization.

Remarkably, using conditional knockout mice for FGFR1 in either osteoprogenitors or differentiated osteoblasts, Jacob and colleagues described a stage-dependent role of FGFR1 signaling in osteogenic differentiation (Jacob et al., 2006). On one hand, when cultured *in vitro*, murine osteoprogenitors lacking FGFR1 proliferated more and displayed delayed osteogenic differentiation. However, this was not the case in our work, as indicated by the expression of osteogenic differentiation markers, suggesting that osteogenic commitment of hBMSCs was not susceptible to FGFR signaling inhibition in our 3D collagen system. On the other hand, when Jacob and colleagues disrupted FGFR1 signaling in immature osteoblasts, *in vitro* differentiation induction resulted in increased levels of mineralization, as we observed for osteoblastic differentiated hBMSCs, supporting the role of FGFR in controlling mineralization.

Strikingly, the chemical inhibition of FGFR in hBMSCs during differentiation induction in TCP monolayer cultures in our group did not affect mineralized matrix deposition (Simann et al., 2017), suggesting that the control of osteoblastic mineralization behaves differently in the 3D collagenous microenvironment than in 2D TCP conditions.

Nevertheless, it needs to be taken into account that FGFR inhibition causes not only the disruption of autocrine/paracrine FGF1 and FGF2 signaling, but also of other FGF ligands expressed by hBMSCs and the osteoblastic lineage. For instance, endocrine FGFs, such as FGF21 and FGF23, have been shown capable of acting in a paracrine manner, influencing skeletal metabolism (Wei et al., 2012; Xiao et al., 2013). Exogenous FGF21 has been found to enhance adipogenic differentiation of murine BMSCs while decreasing osteogenic differentiation. Furthermore, FGF21-knockout BMSCs display enhanced osteogenesis and diminished adipogenesis (Wei et al., 2012). Given that we did not observe significant effects of FGFR inhibition on hBMSC differentiation, it is probable that FGF21 signaling does not play a relevant role in our system. FGF23 signaling through FGFR1, on the other hand, has been reported to play a critical role in mineralization. For instance, rat calvarial cells overexpressing FGF23 display hampered mineralization *in vitro* (Wang et al., 2008). Moreover, murine BMSCs overexpressing HMW FGF2 isoforms show increased FGF23 expression and FGF23-mediated inhibition of mineralization *in*

vitro (Xiao et al., 2013). Given that FGF23 is mostly expressed by osteocytes, its role might be particularly relevant in 3D conditions where osteoblast-to-osteocyte transition may be accelerated, although we did not detect upregulation in the expression of the osteocytic marker DMP1 under FGFR inhibition (Figure 26).

4.3. FGF signaling during hBMSC expansion and differentiation potential

With the fast emergence of a variety of potential biomedical uses for hBMSCs, mostly focused on tissue engineering and regeneration, tight control and maintenance of their potency during *in vitro* expansion and a profound understanding of differentiation mechanisms and the role of relevant molecular players are of critical value.

Differentiation potential of hBMSCs is known to decrease with mitotic expansion *in vitro*, while a higher proportion of cells enters senescence (Wagner et al., 2008). Therefore, growth factors allowing accelerated proliferation without negatively affecting the subsequent differentiation process are highly desired.

Several works have linked FGF1 and FGF2 stimulation with a priming into the chondrogenic fate of hBMSCs, indicating that FGF signaling indeed play a role in hBMSC potency (Hagmann et al., 2013; Handorf & Li, 2011; Solchaga et al., 2005). In this work, we aimed to determine if rhFGF1 treatment during hBMSC expansion affected in a differential way the adipogenic and osteogenic capacities of hBMSCs once embedded in collagen gels.

4.3.1. FGF-induced proliferation and hBMSC potency

In the performed experiments involving expansion of hBMSCs in the presence of rhFGF1 or rhFGF2 during one passage in monolayer culture a significant increase in cell number was observed (Figures 32 and 33), consistent with published reports of enhanced proliferation of hBMSCs induced by FGF signaling *in vitro*.

The growth rate of hBMSC populations has been previously found to be enhanced by the presence of FGF2 (Oliver et al., 1990), as confirmed by the present results and other reports (Martin et al., 1997; Solchaga et al., 2005; Tsutsumi et al., 2001). At a clonal level, although expansion of hBMSCs under FGF2 supplementation reduces the efficiency of colony formation, the size of the formed colonies largely increases (Martin et al., 1997). Moreover, expansion under FGF stimulation have been also shown to alter the gene expression profile of hBMSCs, mainly affecting genes related to this particular cellular process (Solchaga et al., 2005).

Mechanistically, signaling through FGFR1 has been identified as a major mitogenic regulator of hBMSCs *in vitro*, which, when impaired, results in the blockage of cell cycle progression. FGFR1 activation has been shown to exert its mitogenic effect via the PI3K/AKT, ERK1/2 and c-Myc pathways, resulting in the inhibition of cyclin-dependent kinase inhibitors (Dombrowski et al., 2013). Additionally, Ahn and colleagues have shown that the JNK transduction pathway, which is transiently activated by FGF2 stimulation, plays a fundamental role in the induction of proliferation in hBMSCs (Ahn et al., 2009). In murine BMSCs, consistent observations have been reported (Choi et al., 2008), implicating the activation of ERK1/2 and AKT as well as the upregulation of c-Jun to the pro-proliferative effect of FGF2 on Sca-1$^+$ BMSCs.

Accompanying its pro-proliferative role, FGF signaling has also been found to overcome replicative senescence after *in vitro* expansion (Coutu et al., 2011; Ito et al., 2007). For hBMSCs, TGF-β has been described as a promotor of senescence, inducing the upregulation of the cyclin-dependent kinase inhibitors p21 and p16. FGF2 has been found to inhibit the upregulation of TGF-β2 occurring after long-term expansion and hence, it is able to suppress the senescent phenotype (Ito et al., 2007).

The multipotency of BMSCs, on the other hand, is acknowledged to be attenuated with prolong *in vitro* culture (Banfi et al., 2000; Digirolamo et al., 1999; Muraglia et al., 2000; Tsutsumi et al., 2001). Several works have implicated a participation of FGF signaling in BMSC differentiation potency. For instance, Muraglia and colleagues, utilizing a clonal culture approach, have demonstrated that clonal expansion of hBMSCs in the presence of FGF2 raises the frequency of tripotent clones, i.e. clones with osteogenic, chondrogenic and adipogenic differentiation capacity, probably by maintaining their multipotency for longer time during *in vitro* expansion (Muraglia et al., 2000). The same group showed later that the enhanced proliferation of a heterogeneous hBMSC population under FGF2 stimulation is accompanied by a positive selection of a subpopulation of earlier progenitor cells with longer telomeres, which would result in a higher proportion of multipotent cells present in the expanded population (Bianchi et al., 2003). Further evidence of phenotype selection comes from a study reporting changes in the expression of surface markers in hBMSC populations induced by FGF2 (Hagmann et al., 2013).

4.3.2. FGF signaling and adipogenic potential

After enhanced expansion under rhFGF1 or rhFGF2 stimulation, subsequent adipogenic differentiation of hBMSCs in collagen gels was found to be unaffected (Figure 36-37). Previous evidence found in the literature is, however, controversial and highly dependent on the particular BMSC species. In agreement with the present results, other studies performed in conventional 2D cultures have shown that the presence of FGF2 during expansion of hBMSCs for several passages

has no impact on adipogenic differentiation in monolayers (Tsutsumi et al., 2001), although a positive effect has also been reported (Ahn et al., 2009).

Contrasting these observations, the adipogenic potential of murine BMSCs has been found to be negatively influenced by a preceding FGF2 stimulation, although withdrawal of FGF2 5 or 7 days prior of adipogenic induction restored the adipogenic capacity, demonstrating the reversibility of the suppressive effect of FGF2 (Baddoo et al., 2003). This result suggests that the negative effect of FGF signaling on adipogenesis may be longer-lasting in murine BMSCs, hence, even when the factor is no longer present these cells seem to stay locked in a non-differentiating state, needing more time than human cells to overcome this differentiation blockage.

Strikingly, another different scenario has been described for rat BMSCs. When cells were grown for one passage under FGF2 stimulation, a major extent of adipogenic differentiation has been documented (Neubauer et al., 2004), even though the FGF2 stimulus was maintained in the next passage during a short pre-expansion phase before differentiation induction.

4.3.3. FGF signaling and osteogenic potential

When hBMSCs were expanded for one passage as 2D monolayers in the presence of rhFGF1 or rhFGF2, alterations in osteogenic differentiation in collagen gels were observed. On one hand, the late osteogenic marker osteocalcin was induced in the FGF-treated populations after differentiation induction (Figure 39), suggesting enhanced osteogenesis. On the other hand, however, matrix mineralization was found to be prevented by the preceding FGF stimulation, indicating that maturation of differentiating osteoblasts was, at least, delayed by FGF pre-treatment (Figure 39).

As for adipogenic potential, published reports on the effect of FGF signaling on osteogenic potential are variable in their outcome. Several works point out to an enhancement of osteogenic potential triggered by FGF stimulation during proliferation, resulting in increased mineralization. For example, despite showing reduced levels of ALP activity after *in vitro* expansion, hBMSCs grown in the presence of FGF2 have shown, contrary to our results, higher levels of matrix mineralization after FGF2-free osteogenic induction as well as enhanced ectopic bone formation capacity when implanted *in vivo* (Martin et al., 1997). A similar observation was reported by Tsutsumi and colleagues, who after expanding hBMSCs under FGF2 stimulation for different passage numbers noticed increased calcium deposition after osteogenic differentiation when compared to cells expanded without the growth factor (Tsutsumi et al., 2001). Remarkably, these authors observed the enhancing effect of FGF2 on mineralization only after expansion of low-density but not of high-density cultures, given that only the former displayed reducing levels of calcium content with passage number while the latter maintained the deposited calcium levels

constant. Therefore, this observation further supports the idea that FGF2 is able to preserve or even enrich the osteogenic potential of hBMSCs throughout extensive *in vitro* expansion. The same attenuation of osteogenic potential loss with *in vitro* expansion mediated by FGF2 has been reported for murine ASCs, which after several rounds of expansion passages without FGF2 lost their ability to differentiate (Quarto & Longaker, 2006).

Conversely, osteogenic differentiation of murine BMSCs has been found to be inhibited by a 7-days pre-stimulation with FGF2, characterized by a suppression of mineralization and reduced expression of ALP, osteocalcin and bone sialoprotein. This observation was mechanistically associated to the upregulation and subcellular redistribution of the transcription factor *Twist2* and the receptor tyrosine kinase signaling inhibitor *Spry4*, as well as with the inhibition of ERK phosphorylation (Lai et al., 2011). However, the scheme of a proliferation phase followed by an immediate differentiation phase used in that work presents the inconvenience that, due to the enhanced proliferation induced by FGF, the observed effects may be not directly related to FGF signaling but to the differences in cell numbers and densities among experimental conditions. In a similar setting, dexamethasone-induced differentiation of rat BMSCs has been shown to be positively affected by the presence of FGF2 during a 6-day expansion phase (Hanada et al., 1997), supporting again the notion that important differences for the role of FGF signaling exist between species.

Importantly, all the mentioned studies regarding the effect of FGF signaling on MSC differentiation potential were conducted using FGF2 and therefore, none of them included heparin in their experimental conditions as in the present study. Nevertheless, the observed results are in concordance with the existing evidence with regard to the maintenance of the osteogenic differentiation potential of hBMSCs and the increased levels of the late osteogenic marker osteocalcin induced by rhFGF1 and rhFGF2 after expansion and even before embedding in collagen or inducing differentiation (Figure 40) could be interpreted as a priming into the osteogenic pathway or enrichment of osteo-committed cells. A major difference with published literature is the inhibition of mineralization observed in collagen gels after expansion under FGF stimulation. Interesting, this phenomenon could be related to the upregulation of osteocalcin expression, although *in vitro* and *in vivo* evidence regarding its role in matrix mineralization is controversial.

In vitro, osteocalcin has been shown to delay the formation and/or inhibit the growth of hydroxyapatite crystal in solution (Doi et al., 1992; Menanteau et al., 1982; Romberg et al., 1986) as well as when incorporated into agarose gels (Hunter et al., 1996). *In vivo*, however, osteocalcin knockout mice do not present bone abnormalities at birth but overtime they exhibit augmented mineralized bone mass due to increased bone formation. Surprisingly, bone mineralization did not seem to be affected in these mice. Since osteoblast numbers are not altered, increased rate of

matrix deposition could be the cause behind increased bone formation (Ducy et al., 1996). Later it was found that cortical bone from these knockout animals is less mature than bone from wildtypes at six-month of age, as they present a lower carbonate:phosphate ratio and smaller crystal sizes, revealing a minor role of osteocalcin in mineral maturation (Boskey et al., 1998). Osteocalcin overexpression in osteoblasts, on the other hand, does not result in altered bone mineralization (Murshed et al., 2004). Hence, according to the *in vivo* evidence, osteocalcin does not act as an inhibitor of mineralization, at least in murine models. A FGF2-mediated induction of osteocalcin has been previously reported in murine osteoblastic cell lines and was found to be dependent of Runx2 phosphorylation and activation via the MAPK pathway, however, effects on matrix mineralization were not addresses (Xiao et al., 2002).

In an attempt to find an upstream commitment factor that could be related to the increased expression of osteocalcin after FGF stimulation of hBMSCs, the mRNA levels of the non-canonical Wnt agonist WNT5A were determined (Figure 40). Both canonical (β-catenin-dependent) and non-canonical (β-catenin-independent) Wnt signaling have been implicated in the control of hBMSC stemness and commitment playing opposite roles (Baksh & Tuan, 2007; Etheridge et al., 2004). While canonical Wnt signaling favors proliferation of hBMSCs and suppresses osteogenic differentiation, the non-canonical pathway has been shown to promote osteogenesis (Baksh et al., 2007; Boland et al., 2004; Liu et al., 2009). In this work, WNT5A mRNA levels were found to be slightly upregulated in hBMSCs after expansion under FGF stimulation (Figure 40). Overexpression of WNT5A in hBMSCs has been shown to increase, under osteogenic conditions, the mRNA levels and the activity of alkaline phosphatase as well as the mRNA levels of osteocalcin, but not the levels of Runx2 mRNA, which matches our observation, although mineralization was found to be similar between control and WNT5A overexpressing cells (Boland et al., 2004). Moreover, WNT5A enhances the activity of an osteocalcin promoter reporter (Baksh et al., 2007), while WNT5A knockout murine calvarial cells are not able to induce osteocalcin in response to osteogenic induction *in vitro* (Maeda et al., 2012), further supporting the involvement of non-canonical Wnt signaling in the regulation of osteocalcin expression.

4.4. FGF signaling and hBMSC matrix remodeling ability

Besides the impairment of adipogenic and osteogenic differentiation caused by rhFGF1 and rhFGF2 stimulation in hBMSCs, a noticeable parallel effect was the attenuation of the size reduction of the collagen gels observed throughout the differentiation period (Figure 28). As discussed in 4.1.2, gel size reduction reflects the ability of hBMSCs to remodel the 3D collagen matrix and therefore, perturbations in collagen contraction or degradation capacity by FGF signaling may explain the observed differences.

Notably, rhFGF1 and rhFGF2 stimulation during an expansion passage in 2D conditions also resulted in diminished early contraction ability when subsequently embedded in collagen gels (Figure 34). This lack of contraction capacity may be, at least in part, a result of morphological and cytoskeletal changes triggered by FGF signaling in hBMSC. While heparin alone induced a cuboidal shape and the formation of thick actin stress fibers, FGF stimulation resulted in thin and elongated cells lacking actin fibers (Figure 35), which reduces the traction capacity of these cells.

Supporting observations have been previously reported, mainly for fibroblastic cells. For instance, human dermal fibroblasts embedded in collagen gels and cultured in the presence of FGF1 have been shown to display a dose-dependent inhibition of matrix contraction (Dubertret et al., 1991). Similarly, Imaizumi and colleagues have observed that both FGF1 and FGF2 hampered the ability of human dermal fibroblast to contract collagen gels in a reversible manner (Imaizumi et al., 1996). Furthermore, murine fibroblasts pretreated with FGF1 or secreting a FGF1 chimeric form have been shown to be unable to contract collagen gels when seeded on top (Ding et al., 2000). The lack of contractile activity was accompanied by the absence of an organized actin cytoskeleton, as observed by us (Figure 35), together with an enhanced migration capacity.

Surprisingly, opposite observations have been reported for FGF2 as well. Finesmith and colleagues, for example, have found that low concentrations of FGF2, ranging from 0.1 to 1 ng/ml, slightly enhanced contraction of collagen gels when rat wound fibroblasts were seeded on top of the matrices, while higher concentrations reestablished the basal contraction ability (Finesmith et al., 1990). Moreover, FGF2 has been reported to slightly increase contraction of collagen sponges by human dermal fibroblasts derived from normal tissue (Eisinger et al., 1988).

Besides a possible divergent effect of FGF1 and FGF2 on certain fibroblastic cells, the opposite effect on contraction abilities after exposure to FGF1 and FGF2 reported in the aforementioned studies could be the result of cell type-specific differences in the response or the use of different culture conditions. One particular difference between FGF1- and FGF2-based studies, as previously mentioned, is the use of heparin in the former. From the aforementioned works, only the one by Imaizumi and colleagues used heparin in combination with FGF2 as well as with FGF1 and it was also the only one reporting an inhibitory effect of FGF2 on collagen contraction (Imaizumi et al., 1996).

Interestingly, the presence of heparin alone during differentiation induction also influenced the final size of the gels to a certain extent in the same direction as both rhFGFs, i.e., it slightly attenuated the size reduction of the collagen matrix (Figure 28). The interaction of heparin with endogenously secreted FGF1 or FGF2 is one of the possible explanations for this effect. However, heparin does not only interact with FGF ligands but with a wide variety of growth factors and

other molecules (Ori et al., 2008) and therefore, it cannot be ruled out that one or more of these interactions triggered the inhibition of collagen matrix remodeling. Concordantly, an inhibitory effect of heparin on collagen contraction has been recognized for other cell types embedded in collagen gels such as human skin fibroblasts (Ehrlich et al., 1986) and intestinal smooth muscle cells (Graham et al., 1987). Although the specific mechanisms for this effect was not addressed nor an association with other molecules was implicated, Ehrlich and colleagues described a parallel architectural alteration of the actin cytoskeleton induced by heparin in both 2D monolayers and collagen gels, characterized by the appearance of marked stress fibers (Ehrlich et al., 1986), equivalent to the one observed by us after expansion of hBMSCs with heparin (Figure 35). Noteworthy, this effect opposes the one induced by FGFs on the actin cytoskeleton, suggesting that the mechanisms behind matrix contraction inhibition by heparin are independent from the induced modification of the cytoskeletal architecture.

One of the key processes taking part in collagen remodeling is the MMP-mediated matrix degradation (discussed in 4.1.2). In this work, FGF stimulation throughout adipogenic differentiation induction resulted in significant changes in the mRNA levels of MMP13 and TIMP1 compared with the heparin control (Figure 29). MMP13, whose mRNA levels highly incremented under standard adipogenic conditions (Figure 13), was further upregulated by rhFGF1 and rhFGF2 (Figure 29). Notably, despite been downregulated at the transcriptional level during adipogenesis, TIMP1 displayed upregulated expression under rhFGF1 and rhFGF2 treatment, both at the mRNA (Figure 29) and protein (Figure 30) levels.

Inhibition of hBMSC osteogenesis by FGF stimulation paralleled with lower mRNA levels of MMP2 and TIMP2 (Figure 31). Since both remodeling markers are upregulated after osteogenic differentiation (Figure 13), the lower levels observed under rhFGF treatments, which are although higher than the basal level before differentiation induction, could therefore be a result from the differentiation inhibition rather than a direct effect of FGF stimulation.

Worthy of notice, the mRNA levels of MT1-MMP and TIMP1, in the case of adipogenic and osteogenic conditions, respectively, significantly increased under FGF stimulation only when compared to the BSA control but not to the heparin control (Figures 29 and 31). Since any observed effect for the heparin alone condition might be either the result of the enhancement of the basal FGF signaling, i.e. mediated by endogenously secreted ligands or the ones found in the fetal calf serum, or it might correspond to unspecific effects, for instance, due to the interaction with other growth factors, caution should be taken when interpreting these results.

In addition to the aforementioned changes in MMP/TIMP expression, downregulated mRNA levels of collagen type I under osteogenic conditions were found after rhFGF1 and rhFGF2 treatments (Figure 31).

In conclusion, FGF-mediated differentiation inhibition triggered changes in the expression profile of matrix remodeling markers in 3D collagen gels, which might translate into an altered MMP/TIMP balance in detriment of MMP activity, especially in the case of adipogenic condition due to the high upregulation of TIMP1. However, enhanced activity levels of TIMP1 would not fully explain the lower remodeling activity associated to FGF stimulation. For instance, TIMP1 does not inhibit MT1-MMP, which, as discussed in 4.1.2.2, is expected to play a major role in collagen matrix remodeling by hBMSCs. Additionally, in the case of osteogenic condition, it is less clear that the changes induced by FGF treatments in the MMP/TIMP profile are inhibitory of matrix remodeling, since both MMP2 and TIMP2 mRNA levels were found to be lower. Therefore, additional mechanisms are certainly involved, being a diminished contractile activity triggered by FGF signaling a likely candidate. Finally, although alterations in the MMP/TIMP balance may be, as previously discussed, triggers of differentiation bias by themselves, the molecular mechanisms behind the altered MMP/TIMP profiles observed in this work are most probably a consequence of the differentiation inhibition, rather than a cause. Additionally, as shown by our group, FGF-mediated inhibition of differentiation occurs in 2D culture systems as well (Simann et al., 2017), and therefore, it is independent of a 3D collagenous microenvironment remodeling.

5. Conclusion

Concordant with bone mass and marrow adipose tissue inverse relationship, osteogenic and adipogenic differentiation of hBMSCs display reciprocity under a variety of conditions. Hence, the search for molecular mechanisms that may modulate their differentiation in one pathway or another is particularly relevant in the context of pathological conditions of bone remodeling such as osteoporosis.

Based on the hypothesis that FGF1 signaling might have played an anti-adipogenic/pro-osteogenic modulating role, we tested the impact of FGF1 stimulation on hBMSCs differentiation using a 3D culture model in order to better represent the physiological microenvironment. However, the presented results did not support this hypothesis, given that FGF1, as well as FGF2, stimulation proved to hinder both differentiation pathways although without blocking the differentiation potential but enhancing proliferation (Figure 41).

Interestingly, basal FGFR signaling displayed a strong inhibitory role in matrix mineralization in 3D but not in adipocyte formation, suggesting that FGFR signaling indeed plays a differential role in adipogenesis and osteogenesis at the maturation level (Figure 41).

Remarkably, the use of a 3D culture system based on a collagenous matrix allowed for the identification of matrix remodeling effects associated with FGF signaling which would not had been identified in a conventional 2D system, providing further evidence that 3D models can be much more informative.

In summary, this work indicates that FGF signaling sustains the expansion of both adipogenic and osteogenic stromal precursors, exerts inhibitory effects on adipogenesis and osteogenesis and induces phenotypic changes that result in altered matrix interactions within a 3D collagenous microenvironment.

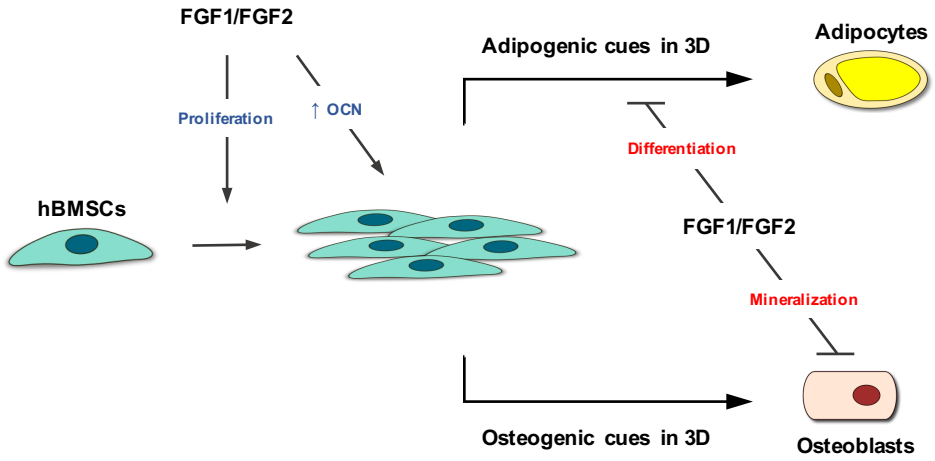

Figure 41. Effect of FGF signaling on hBMSC proliferation and differentiation.
FGF1/FGF2 signaling enhances proliferation of hBMSCs without affecting their differentiation potential. Sustained FGF signaling during hBMSCs differentiation induction in 3D culture negatively impacts adipogenesis and osteogenic differentiation, at least at the level of maturation/matrix mineralization.

6. References

Ahn, H. J., Lee, W. J., Kwack, K., & Kwon, Y. D. (2009). FGF2 stimulates the proliferation of human mesenchymal stem cells through the transient activation of JNK signaling. *FEBS Letters*, *583*(17), 2922–2926.

Aimes, R. T., & Quigley, J. P. (1995). Matrix metalloproteinase-2 is an interstitial collagenase. Inhibitor-free enzyme catalyzes the cleavage of collagen fibrils and soluble native type I collagen generating the specific 3/4- and 1/4-length fragments. *Journal of Biological Chemistry*, *270*(11), 5872–5876.

Ambrosetti, D., Holmes, G., Mansukhani, A., & Basilico, C. (2008). Fibroblast growth factor signaling uses multiple mechanisms to inhibit Wnt-induced transcription in osteoblasts. *Molecular and Cellular Biology*, *28*(15), 4759–4771.

Arnaud, E., Touriol, C., Boutonnet, C., Gensac, M. C., Vagner, S., Prats, H., & Prats, A. C. (1999). A new 34-kilodalton isoform of human fibroblast growth factor 2 is cap dependently synthesized by using a non-AUG start codon and behaves as a survival factor. *Molecular and Cellular Biology*, *19*(1), 505–514.

Astudillo, P., Ríos, S., Pastenes, L., Pino, A. M., & Rodríguez, J. P. (2008). Increased adipogenesis of osteoporotic human-mesenchymal stem cells (MSCs) characterizes by impaired leptin action. *Journal of Cellular Biochemistry*, *103*(4), 1054–1065.

Baddoo, M., Hill, K., Wilkinson, R., Gaupp, D., Hughes, C., Kopen, G. C., & Phinney, D. G. (2003). Characterization of mesenchymal stem cells isolated from murine bone marrow by negative selection. *Journal of Cellular Biochemistry*, *89*(6), 1235–1249.

Bae, J. H., Boggon, T. J., Tomé, F., Mandiyan, V., Lax, I., & Schlessinger, J. (2010). Asymmetric receptor contact is required for tyrosine autophosphorylation of fibroblast growth factor receptor in living cells. *Proceedings of the National Academy of Sciences of the United States of America*, *107*(7), 2866–2871.

Baksh, D., & Tuan, R. S. (2007). Canonical and non-canonical Wnts differentially affect the development potential of primary isolate of human bone marrow mesenchymal stem cells. *Journal of Cellular Physiology*, *212*(3), 817–826.

Baksh, D., Boland, G. M., & Tuan, R. S. (2007). Cross-talk between Wnt signaling pathways in human mesenchymal stem cells leads to functional antagonism during osteogenic differentiation. *Journal of Cellular Biochemistry*, *101*(5), 1109–1124.

Banfi, A., Muraglia, A., Dozin, B., Mastrogiacomo, M., Cancedda, R., & Quarto, R. (2000). Proliferation kinetics and differentiation potential of ex vivo expanded human bone marrow stromal cells: Implications for their use in cell therapy. *Experimental Hematology*, *28*(6), 707–715.

Baraniak, P. R., & McDevitt, T. C. (2012). Scaffold-free culture of mesenchymal stem cell spheroids in suspension preserves multilineage potential. *Cell and Tissue Research*, *347*(3), 701–711.

Beenken, A., & Mohammadi, M. (2009). The FGF family: biology, pathophysiology and therapy. *Nature Reviews. Drug Discovery*, *8*(3), 235–253.

Bell, E., Ivarsson, B., & Merrill, C. (1979). Production of a tissue-like structure by contraction of collagen lattices by human fibroblasts of different proliferative potential in vitro. *Proceedings of the National Academy of Sciences of the United States of America*, *76*(3), 1274–1278.

Bellus, G. A., Gaudenz, K., Zackai, E. H., Clarke, L. A., Szabo, J., Francomano, C. A., & Muenke, M. (1996). Identical mutations in three different fibroblast growth factor receptor genes in autosomal dominant craniosynostosis syndromes. *Nature Genetics*, *14*(2), 174–176.

Belov, A. A., & Mohammadi, M. (2013). Molecular mechanisms of fibroblast growth factor signaling in physiology and pathology. *Cold Spring Harbor Perspectives in Biology*, *5*(6).

Benvenuti, S., Cellai, I., Luciani, P., Deledda, C., Baglioni, S., Giuliani, C., et al. (2007). Rosiglitazone stimulates adipogenesis and decreases osteoblastogenesis in human mesenchymal stem cells. *Journal of Endocrinological Investigation*, *30*(9), RC26–30.

Bianchi, G., Banfi, A., Mastrogiacomo, M., Notaro, R., Luzzatto, L., Cancedda, R., & Quarto, R. (2003). Ex vivo enrichment of mesenchymal cell progenitors by fibroblast growth factor 2. *Experimental Cell Research*, *287*(1), 98–105.

Bianco, P. (2014). "Mesenchymal" stem cells. *Annual Review of Cell and Developmental Biology*, *30*, 677–704.

Bianco, P., & Robey, P. G. (2015). Skeletal stem cells. *Development*, *142*(6), 1023–1027.

Bianco, P., Kuznetsov, S. A., Riminucci, M., & Gehron Robey, P. (2006). Postnatal skeletal stem cells. *Methods in Enzymology*, *419*, 117–148.

Bilezikian, J. P., Raisz, L. G., & Rodan, G. A. (Eds.). (2002). Principles of Bone Biology. Academic Press.

Biver, E., Soubrier, A. S., Thouverey, C., Cortet, B., Broux, O., Caverzasio, J., & Hardouin, P. (2012). Fibroblast growth factor 2 inhibits up-regulation of bone morphogenic proteins and their receptors during osteoblastic differentiation of human mesenchymal stem cells. *Biochemical and Biophysical Research Communications*, *427*(4), 737–742.

Boland, G. M., Perkins, G., Hall, D. J., & Tuan, R. S. (2004). Wnt 3a promotes proliferation and suppresses osteogenic differentiation of adult human mesenchymal stem cells. *Journal of Cellular Biochemistry*, *93*(6), 1210–1230.

Bonaventure, J., Rousseau, F., Legeai Mallet, L., Le Merrer, M., Munnich, A., & Maroteaux, P. (1996). Common mutations in the fibroblast growth factor receptor 3 (FGFR 3) gene account for achondroplasia, hypochondroplasia, and thanatophoric dwarfism. *American Journal of Medical Genetics*, *63*(1), 148–154.

Boskey, A. L., Gadaleta, S., Gundberg, C., Doty, S. B., Ducy, P., & Karsenty, G. (1998). Fourier transform infrared microspectroscopic analysis of bones of osteocalcin-deficient mice provides insight into the function of osteocalcin. *Bone*, *23*(3), 187–196.

Bouleau, S., Grimal, H., Rincheval, V., Godefroy, N., Mignotte, B., Vayssière, J. L., & Renaud, F. (2005). FGF1 inhibits p53-dependent apoptosis and cell cycle arrest via an intracrine pathway. *Oncogene*, *24*(53), 7839–7849.

Bugler, B., Amalric, F., & Prats, H. (1991). Alternative initiation of translation determines cytoplasmic or nuclear localization of basic fibroblast growth factor. *Molecular and Cellular Biology*, *11*(1), 573–577.

Burdick, J. A., & Vunjak-Novakovic, G. (2009). Engineered microenvironments for controlled stem cell differentiation. *Tissue Engineering. Part A*, *15*(2), 205–219.

Butler, G. S., Butler, M. J., Atkinson, S. J., Will, H., Tamura, T., Schade van Westrum, S., et al. (1998). The TIMP2 membrane type 1 metalloproteinase "receptor" regulates the concentration and efficient activation of progelatinase A. A kinetic study. *Journal of Biological Chemistry*, *273*(2), 871–880.

Calabrese, R., & Kaplan, D. L. (2012). Silk ionomers for encapsulation and differentiation of human MSCs. *Biomaterials*, *33*(30), 7375–7385.

Caldwell, M. A., & Svendsen, C. N. (1998). Heparin, but not other proteoglycans potentiates the mitogenic effects of FGF-2 on mesencephalic precursor cells. *Experimental Neurology*, *152*(1), 1–10.

Cawthorn, W. P., Bree, A. J., Yao, Y., Du, B., Hemati, N., Martinez-Santibañez, G., & MacDougald, O. A. (2012). Wnt6, Wnt10a and Wnt10b inhibit adipogenesis and stimulate osteoblastogenesis through a β-catenin-dependent mechanism. *Bone*, *50*(2), 477–489.

Cawthorn, W. P., Scheller, E. L., Learman, B. S., Parlee, S. D., Simon, B. R., Mori, H., et al. (2014). Bone marrow adipose tissue is an endocrine organ that contributes to increased circulating adiponectin during caloric restriction. *Cell Metabolism*, *20*(2), 368–375.

Chan, B. P., Hui, T. Y., Wong, M. Y., Yip, K. H. K., & Chan, G. C. F. (2010). Mesenchymal stem cell-encapsulated collagen microspheres for bone tissue engineering. *Tissue Engineering. Part C, Methods*, *16*(2), 225–235.

Chan, B. P., Hui, T. Y., Yeung, C. W., Li, J., Mo, I., & Chan, G. C. F. (2007). Self-assembled collagen-human mesenchymal stem cell microspheres for regenerative medicine. *Biomaterials*, *28*(31), 4652–4666.

Chen, H., Xu, C. F., Ma, J., Eliseenkova, A. V., Li, W., Pollock, P. M., et al. (2008). A crystallographic snapshot of tyrosine trans-phosphorylation in action. *Proceedings of the National Academy of Sciences of the United States of America*, *105*(50), 19660–19665.

Chen, X. D. (2010). Extracellular matrix provides an optimal niche for the maintenance and propagation of mesenchymal stem cells. *Birth Defects Research Part C: Embryo Today: Reviews*, *90*(1), 45–54.

Chevallay, B., & Herbage, D. (2000). Collagen-based biomaterials as 3D scaffold for cell cultures: applications for tissue engineering and gene therapy. *Medical & Biological Engineering & Computing*, *38*(2), 211–218.

Chlebova, K., Bryja, V., Dvorak, P., Kozubik, A., Wilcox, W. R., & Krejci, P. (2009). High molecular weight FGF2: the biology of a nuclear growth factor. *Cellular and Molecular Life Sciences*, *66*(2), 225–235.

Choi, S. C., Kim, S. J., Choi, J. H., Park, C. Y., Shim, W. J., & Lim, D. S. (2008). Fibroblast growth factor-2 and -4 promote the proliferation of bone marrow mesenchymal stem cells by the activation of the PI3K-Akt and ERK1/2 signaling pathways. *Stem Cells and Development*, *17*(4), 725–736.

Clarke, B. (2008). Normal bone anatomy and physiology. *Clinical Journal of the American Society of Nephrology*, *3 Suppl 3*, S131–9.

Coffin, J. D., Florkiewicz, R. Z., Neumann, J., Mort-Hopkins, T., Dorn, G. W., Lightfoot, P., et al. (1995). Abnormal bone growth and selective translational regulation in basic fibroblast growth factor (FGF-2) transgenic mice. *Molecular Biology of the Cell*, *6*(12), 1861–1873.

Coutu, D. L., François, M., & Galipeau, J. (2011). Inhibition of cellular senescence by developmentally regulated FGF receptors in mesenchymal stem cells. *Blood*, *117*(25), 6801–6812.

Cukierman, E., Pankov, R., Stevens, D. R., & Yamada, K. M. (2001). Taking cell-matrix adhesions to the third dimension. *Science*, *294*(5547), 1708–1712.

Dahlmann-Noor, A. H., Martin-Martin, B., Eastwood, M., Khaw, P. T., & Bailly, M. (2007). Dynamic protrusive cell behaviour generates force and drives early matrix contraction by fibroblasts. *Experimental Cell Research*, *313*(20), 4158–4169.

Daley, W. P., Peters, S. B., & Larsen, M. (2008). Extracellular matrix dynamics in development and regenerative medicine. *Journal of Cell Science*, *121*(Pt 3), 255–264.

Dallas, S. L., & Bonewald, L. F. (2010). Dynamics of the transition from osteoblast to osteocyte. *Annals of the New York Academy of Sciences*, *1192*, 437–443.

Damon, D. H., Lobb, R. R., D'Amore, P. A., & Wagner, J. A. (1989). Heparin potentiates the action of acidic fibroblast growth factor by prolonging its biological half-life. *Journal of Cellular Physiology*, *138*(2), 221–226.

Daniels, J. T., Cambrey, A. D., Occleston, N. L., Garrett, Q., Tarnuzzer, R. W., Schultz, G. S., & Khaw, P. T. (2003). Matrix metalloproteinase inhibition modulates fibroblast-mediated matrix contraction and collagen production in vitro. *Investigative Ophthalmology & Visual Science*, *44*(3), 1104–1110.

Debiais, F., Hott, M., Graulet, A. M., & Marie, P. J. (1998). The effects of fibroblast growth factor-2 on human neonatal calvaria osteoblastic cells are differentiation stage specific. *Journal of Bone and Mineral Research*, *13*(4), 645–654.

Di Iorgi, N., Mo, A. O., Grimm, K., Wren, T. A. L., Dorey, F., & Gilsanz, V. (2010). Bone acquisition in healthy young females is reciprocally related to marrow adiposity. *Journal of Clinical Endocrinology and Metabolism*, *95*(6), 2977–2982.

Di Iorgi, N., Rosol, M., Mittelman, S. D., & Gilsanz, V. (2008). Reciprocal relation between marrow adiposity and the amount of bone in the axial and appendicular skeleton of young adults. *Journal of Clinical Endocrinology and Metabolism*, *93*(6), 2281–2286.

Digirolamo, C. M., Stokes, D., Colter, D., Phinney, D. G., Class, R., & Prockop, D. J. (1999). Propagation and senescence of human marrow stromal cells in culture: a simple colony-forming assay identifies samples with the greatest potential to propagate and differentiate. *British Journal of Haematology*, *107*(2), 275–281.

Ding, Q., Gladson, C. L., Guidry, C. R., Santoro, S. A., Dickeson, S. K., Shin, J. T., & Thompson, J. A. (2000). Extracellular FGF-1 inhibits cytoskeletal organization and promotes fibroblast motility. *Growth Factors*, *18*(2), 93–107.

Doi, Y., Horiguchi, T., Kim, S. H., Moriwaki, Y., Wakamatsu, N., Adachi, M., et al. (1992). Effects of non-collagenous proteins on the formation of apatite in calcium beta-glycerophosphate solutions. *Archives of Oral Biology*, *37*(1), 15–21.

Dombrowski, C., Helledie, T., Ling, L., Grünert, M., Canning, C. A., Jones, C. M., et al. (2013). FGFR1 signaling stimulates proliferation of human mesenchymal stem cells by inhibiting the cyclin-dependent kinase inhibitors p21(Waf1) and p27(Kip1). *Stem Cells*, *31*(12), 2724–2736.

Dono, R., Texido, G., Dussel, R., Ehmke, H., & Zeller, R. (1998). Impaired cerebral cortex development and blood pressure regulation in FGF-2-deficient mice. *EMBO Journal*, *17*(15), 4213–4225.

Dubertret, L., Brunner-Ferber, F., Misiti, J., Thomas, K. A., & Dubertret, M. L. (1991). Activities of human acidic fibroblast growth factor in an in vitro dermal equivalent model. *Journal of Investigative Dermatology*, *97*(5), 793–798.

Ducy, P., Desbois, C., Boyce, B., Pinero, G., Story, B., Dunstan, C., et al. (1996). Increased bone formation in osteocalcin-deficient mice. *Nature*, *382*(6590), 448–452.

Ducy, P., Starbuck, M., Priemel, M., Shen, J., Pinero, G., Geoffroy, V., et al. (1999). A Cbfa1-dependent genetic pathway controls bone formation beyond embryonic development. *Genes & Development*, *13*(8), 1025–1036.

Dunstan, C. R., Boyce, R., Boyce, B. F., Garrett, I. R., Izbicka, E., Burgess, W. H., & Mundy, G. R. (1999). Systemic administration of acidic fibroblast growth factor (FGF-1) prevents bone loss and increases new bone formation in ovariectomized rats. *Journal of Bone and Mineral Research*, *14*(6), 953–959.

Duque, G., & Rivas, D. (2007). Alendronate has an anabolic effect on bone through the differentiation of mesenchymal stem cells. *Journal of Bone and Mineral Research*, *22*(10), 1603–1611.

Duque, G., & Troen, B. R. (2008). Understanding the mechanisms of senile osteoporosis: new facts for a major geriatric syndrome. *Journal of the American Geriatrics Society*, *56*(5), 935–941.

Ehrlich, H. P., Griswold, T. R., & Rajaratnam, J. B. (1986). Studies on vascular smooth muscle cells and dermal fibroblasts in collagen matrices. Effects of heparin. *Experimental Cell Research*, *164*(1), 154–162.

Eisinger, M., Sadan, S., Silver, I. A., & Flick, R. B. (1988). Growth regulation of skin cells by epidermal cell-derived factors: implications for wound healing. *Proceedings of the National Academy of Sciences of the United States of America*, *85*(6), 1937–1941.

Elabd, C., Basillais, A., Beaupied, H., Breuil, V., Wagner, N., Scheideler, M., et al. (2008). Oxytocin controls differentiation of human mesenchymal stem cells and reverses osteoporosis. *Stem Cells*, *26*(9), 2399–2407.

Elbaz, A., Wu, X., Rivas, D., Gimble, J. M., & Duque, G. (2010). Inhibition of fatty acid biosynthesis prevents adipocyte lipotoxicity on human osteoblasts in vitro. *Journal of Cellular and Molecular Medicine*, *14*(4), 982–991.

Engler, A. J., Sen, S., Sweeney, H. L., & Discher, D. E. (2006). Matrix elasticity directs stem cell lineage specification. *Cell*, *126*(4), 677–689.

Etheridge, S. L., Spencer, G. J., Heath, D. J., & Genever, P. G. (2004). Expression profiling and functional analysis of wnt signaling mechanisms in mesenchymal stem cells. *Stem Cells*, *22*(5), 849–860.

Exposito, J. Y., Valcourt, U., Cluzel, C., & Lethias, C. (2010). The fibrillar collagen family. *International Journal of Molecular Sciences*, *11*(2), 407–426.

Eyre, D. R., & Wu, J. J. (2005). Collagen Cross-Links. In *Collagen: Primer in Structure, Processing and Assembly* (pp. 207–229). Berlin, Heidelberg: Springer Berlin Heidelberg.

Feng, X., & McDonald, J. M. (2011). Disorders of bone remodeling. *Annual Review of Pathology*, *6*, 121–145.

Finesmith, T. H., Broadley, K. N., & Davidson, J. M. (1990). Fibroblasts from wounds of different stages of repair vary in their ability to contract a collagen gel in response to growth factors. *Journal of Cellular Physiology*, *144*(1), 99–107.

Florencio-Silva, R., Sasso, G. R. D. S., Sasso-Cerri, E., Simões, M. J., & Cerri, P. S. (2015). Biology of Bone Tissue: Structure, Function, and Factors That Influence Bone Cells. *BioMed Research International*, *2015*, 421746.

Florkiewicz, R. Z., & Sommer, A. (1989). Human basic fibroblast growth factor gene encodes four polypeptides: three initiate translation from non-AUG codons. *Proceedings of the National Academy of Sciences of the United States of America*, *86*(11), 3978–3981.

Frantz, C., Stewart, K. M., & Weaver, V. M. (2010). The extracellular matrix at a glance. *Journal of Cell Science*, *123*(24), 4195–4200.

Friedenstein, A. J., Chailakhyan, R. K., Latsinik, N. V., Panasyuk, A. F., & Keiliss-Borok, I. V. (1974). Stromal cells responsible for transferring the microenvironment of the hemopoietic tissues. Cloning in vitro and retransplantation in vivo. *Transplantation*, *17*(4), 331–340.

Frith, J. E., Mills, R. J., Hudson, J. E., & Cooper-White, J. J. (2012). Tailored integrin-extracellular matrix interactions to direct human mesenchymal stem cell differentiation. *Stem Cells and Development*, *21*(13), 2442–2456.

Furdui, C. M., Lew, E. D., Schlessinger, J., & Anderson, K. S. (2006). Autophosphorylation of FGFR1 kinase is mediated by a sequential and precisely ordered reaction. *Molecular Cell*, *21*(5), 711–717.

Galderisi, U., & Giordano, A. (2014). The gap between the physiological and therapeutic roles of mesenchymal stem cells. *Medicinal Research Reviews*, *34*(5), 1100–1126.

Goetz, R., & Mohammadi, M. (2013). Exploring mechanisms of FGF signalling through the lens of structural biology. *Nature Reviews. Molecular Cell Biology*, *14*(3), 166–180.

Goto, H., Osaki, M., Fukushima, T., Sakamoto, K., Hozumi, A., Baba, H., & Shindo, H. (2011). Human bone marrow adipocytes support dexamethasone-induced osteoclast differentiation and function through RANKL expression. *Biomedical Research*, *32*(1), 37–44.

Gotoh, N. (2008). Regulation of growth factor signaling by FRS2 family docking/scaffold adaptor proteins. *Cancer Science*, *99*(7), 1319–1325.

Graham, M. F., Drucker, D. E., Perr, H. A., Diegelmann, R. F., & Ehrlich, H. P. (1987). Heparin modulates human intestinal smooth muscle cell proliferation, protein synthesis, and lattice contraction. *Gastroenterology*, *93*(4), 801–809.

Greenspan, D. S. (2005). Biosynthetic Processing of Collagen Molecules. In *Collagen* (pp. 149–183). Springer Berlin Heidelberg.

Grinnell, F. (2000). Fibroblast-collagen-matrix contraction: growth-factor signalling and mechanical loading. *Trends in Cell Biology*, *10*(9), 362–365.

Gronthos, S., Simmons, P. J., Graves, S. E., & Robey, P. G. (2001). Integrin-mediated interactions between human bone marrow stromal precursor cells and the extracellular matrix. *Bone*, *28*(2), 174–181.

Gunaratnam, K., Vidal, C., Gimble, J. M., & Duque, G. (2014). Mechanisms of palmitate-induced lipotoxicity in human osteoblasts. *Endocrinology*, *155*(1), 108–116.

Hagmann, S., Moradi, B., Frank, S., Dreher, T., Kämmerer, P. W., Richter, W., & Gotterbarm, T. (2013). FGF-2 addition during expansion of human bone marrow-derived stromal cells alters MSC surface marker distribution and chondrogenic differentiation potential. *Cell Proliferation*, *46*(4), 396–407.

Hakkinen, K. M., Harunaga, J. S., Doyle, A. D., & Yamada, K. M. (2011). Direct comparisons of the morphology, migration, cell adhesions, and actin cytoskeleton of fibroblasts in four different three-dimensional extracellular matrices. *Tissue Engineering. Part A*, *17*(5-6), 713–724.

Hamilton, R., & Campbell, F. R. (1991). Immunochemical localization of extracellular materials in bone marrow of rats. *The Anatomical Record*, *231*(2), 218–224.

Hamm, J. K., Park, B. H., & Farmer, S. R. (2001). A role for C/EBPbeta in regulating peroxisome proliferator-activated receptor gamma activity during adipogenesis in 3T3-L1 preadipocytes. *Journal of Biological Chemistry*, *276*(21), 18464–18471.

Hanada, K., Dennis, J. E., & Caplan, A. I. (1997). Stimulatory effects of basic fibroblast growth factor and bone morphogenetic protein-2 on osteogenic differentiation of rat bone marrow-derived mesenchymal stem cells. *Journal of Bone and Mineral Research*, *12*(10), 1606–1614.

Handorf, A. M., & Li, W. J. (2011). Fibroblast growth factor-2 primes human mesenchymal stem cells for enhanced chondrogenesis. *PLoS ONE*, *6*(7), e22887.

Hardouin, P., Rharass, T., & Lucas, S. (2016). Bone Marrow Adipose Tissue: To Be or Not To Be a Typical Adipose Tissue? *Frontiers in Endocrinology*, *7*, 85.

Hauner, H., Röhrig, K., & Petruschke, T. (1995). Effects of epidermal growth factor (EGF), platelet-derived growth factor (PDGF) and fibroblast growth factor (FGF) on human adipocyte development and function. *European Journal of Clinical Investigation*, *25*(2), 90–96.

Hayashi, I., Nixon, T., Morikawa, M., & Green, H. (1981). Adipogenic and anti-adipogenic factors in the pituitary and other organs. *Proceedings of the National Academy of Sciences of the United States of America*, *78*(6), 3969–3972.

Haynesworth, S. E., Goshima, J., Goldberg, V. M., & Caplan, A. I. (1992). Characterization of cells with osteogenic potential from human marrow. *Bone*, *13*(1), 81–88.

Heckmann, L., Fiedler, J., Mattes, T., & Brenner, R. E. (2006). Mesenchymal progenitor cells communicate via alpha and beta integrins with a three-dimensional collagen type I matrix. *Cells, Tissues, Organs*, *182*(3-4), 143–154.

Heim, M., Frank, O., Kampmann, G., Sochocky, N., Pennimpede, T., Fuchs, P., et al. (2004). The phytoestrogen genistein enhances osteogenesis and represses adipogenic differentiation of human primary bone marrow stromal cells. *Endocrinology*, *145*(2), 848–859.

Heino, J. (2007). The collagen family members as cell adhesion proteins. *BioEssays: News and Reviews in Molecular, Cellular and Developmental Biology*, *29*(10), 1001–1010.

Higuchi, A., Ling, Q. D., Hsu, S. T., & Umezawa, A. (2012). Biomimetic cell culture proteins as extracellular matrices for stem cell differentiation. *Chemical Reviews*, *112*(8), 4507–4540.

Holt, V., Caplan, A. I., & Haynesworth, S. E. (2014). Identification of a subpopulation of marrow MSC-derived medullary adipocytes that express osteoclast-regulating molecules: marrow adipocytes express osteoclast mediators. *PLoS ONE*, *9*(10), e108920.

Homer-Bouthiette, C., Doetschman, T., Xiao, L., & Hurley, M. M. (2014). Knockout of nuclear high molecular weight FGF2 isoforms in mice modulates bone and phosphate homeostasis. *Journal of Biological Chemistry*, *289*(52), 36303–36314.

Hong, J. H., Hwang, E. S., McManus, M. T., Amsterdam, A., Tian, Y., Kalmukova, R., et al. (2005). TAZ, a transcriptional modulator of mesenchymal stem cell differentiation. *Science*, *309*(5737), 1074–1078.

Huang, Z., Nelson, E. R., Smith, R. L., & Goodman, S. B. (2007). The sequential expression profiles of growth factors from osteoprogenitors [correction of osteroprogenitors] to osteoblasts in vitro. *Tissue Engineering*, *13*(9), 2311–2320.

Huang, Z., Ren, P.-G., Ma, T., Smith, R. L., & Goodman, S. B. (2009). Modulating osteogenesis of mesenchymal stem cells by modifying growth factor availability. *Cytokine*, *51*(3), 305–310.

Huebsch, N., Arany, P. R., Mao, A. S., Shvartsman, D., Ali, O. A., Bencherif, S. A., et al. (2010). Harnessing traction-mediated manipulation of the cell/matrix interface to control stem-cell fate. *Nature Materials*, *9*(6), 518–526.

Hung, I. H., Yu, K., Lavine, K. J., & Ornitz, D. M. (2007). FGF9 regulates early hypertrophic chondrocyte differentiation and skeletal vascularization in the developing stylopod. *Developmental Biology*, *307*(2), 300–313.

Hunter, G. K., Hauschka, P. V., Poole, A. R., Rosenberg, L. C., & Goldberg, H. A. (1996). Nucleation and inhibition of hydroxyapatite formation by mineralized tissue proteins. *The Biochemical Journal*, *317 (1)*, 59–64.

Hutley, L., Shurety, W., Newell, F., McGeary, R., Pelton, N., Grant, J., et al. (2004). Fibroblast Growth Factor 1: A Key Regulator of Human Adipogenesis. *Diabetes*, *53*(12), 3097–3106.

Hynes, R. O. (2002). Integrins: bidirectional, allosteric signaling machines. *Cell*, *110*(6), 673–687.

Imaizumi, T., Jean-Louis, F., Dubertret, M. L., Bailly, C., Cicurel, L., Petchot-Bacqué, J. P., & Dubertret, L. (1996). Effect of human basic fibroblast growth factor on fibroblast proliferation, cell volume, collagen lattice contraction: in comparison with acidic type. *Journal of Dermatological Science*, *11*(2), 134–141.

Imamura, T., Engleka, K., Zhan, X., Tokita, Y., Forough, R., Roeder, D., et al. (1990). Recovery of mitogenic activity of a growth factor mutant with a nuclear translocation sequence. *Science*, *249*(4976), 1567–1570.

Ito, T., Sawada, R., Fujiwara, Y., Seyama, Y., & Tsuchiya, T. (2007). FGF-2 suppresses cellular senescence of human mesenchymal stem cells by down-regulation of TGF-beta2. *Biochemical and Biophysical Research Communications*, *359*(1), 108–114.

Itoh, N., & Ornitz, D. M. (2004). Evolution of the Fgf and Fgfr gene families. *Trends in Genetics*, *20*(11), 563–569.

Itoh, N., & Ornitz, D. M. (2011). Fibroblast growth factors: from molecular evolution to roles in development, metabolism and disease. *Journal of Biochemistry*, *149*(2), 121–130.

Itoh, Y., Takamura, A., Ito, N., Maru, Y., Sato, H., Suenaga, N., et al. (2001). Homophilic complex formation of MT1-MMP facilitates proMMP-2 activation on the cell surface and promotes tumor cell invasion. *EMBO Journal*, *20*(17), 4782–4793.

Jabs, E. W., Li, X., Scott, A. F., Meyers, G., Chen, W., Eccles, M., et al. (1994). Jackson-Weiss and Crouzon syndromes are allelic with mutations in fibroblast growth factor receptor 2. *Nature Genetics*, *8*(3), 275–279.

Jacob, A. L., Smith, C., Partanen, J., & Ornitz, D. M. (2006). Fibroblast growth factor receptor 1 signaling in the osteo-chondrogenic cell lineage regulates sequential steps of osteoblast maturation. *Developmental Biology*, *296*(2), 315–328.

Jaiswal, N., Haynesworth, S. E., Caplan, A. I., & Bruder, S. P. (1997). Osteogenic differentiation of purified, culture-expanded human mesenchymal stem cells in vitro. *Journal of Cellular Biochemistry*, *64*(2), 295–312.

James, A. W. (2013). Review of Signaling Pathways Governing MSC Osteogenic and Adipogenic Differentiation. *Scientifica*, *2013*, 684736.

Jokinen, J., Dadu, E., Nykvist, P., Käpylä, J., White, D. J., Ivaska, J., et al. (2004). Integrin-mediated cell adhesion to type I collagen fibrils. *Journal of Biological Chemistry*, *279*(30), 31956–31963.

Jonker, J. W., Suh, J. M., Atkins, A. R., Ahmadian, M., Li, P., Whyte, J., et al. (2012). A PPARγ-FGF1 axis is required for adaptive adipose remodelling and metabolic homeostasis. *Nature*, *485*(7398), 391–394.

Justesen, J., Stenderup, K., Ebbesen, E. N., Mosekilde, L., Steiniche, T., & Kassem, M. (2001). Adipocyte tissue volume in bone marrow is increased with aging and in patients with osteoporosis. *Biogerontology*, *2*(3), 165–171.

Kabiri, M., Kul, B., Lott, W. B., Futrega, K., Ghanavi, P., Upton, Z., & Doran, M. R. (2012). 3D mesenchymal stem/stromal cell osteogenesis and autocrine signalling. *Biochemical and Biophysical Research Communications*, *419*(2), 142–147.

Kadler, K. E., Baldock, C., Bella, J., & Boot-Handford, R. P. (2007). Collagens at a glance. *Journal of Cell Science*, *120*(Pt 12), 1955–1958.

Kadler, K. E., Hill, A., & Canty-Laird, E. G. (2008). Collagen fibrillogenesis: fibronectin, integrins, and minor collagens as organizers and nucleators. *Current Opinion in Cell Biology*, *20*(5), 495–501.

Kakudo, N., Shimotsuma, A., & Kusumoto, K. (2007). Fibroblast growth factor-2 stimulates adipogenic differentiation of human adipose-derived stem cells. *Biochemical and Biophysical Research Communications*, *359*(2), 239–244.

Kalajzic, I., Kalajzic, Z., Hurley, M. M., Lichtler, A. C., & Rowe, D. W. (2003). Stage specific inhibition of osteoblast lineage differentiation by FGF2 and noggin. *Journal of Cellular Biochemistry*, *88*(6), 1168–1176.

Kanatani, N., Fujita, T., Fukuyama, R., Liu, W., Yoshida, C. A., Moriishi, T., et al. (2006). Cbfβ regulates Runx2 function isoform-dependently in postnatal bone development. *Developmental Biology*, *296*(1), 48–61.

Kanzaki, M., & Pessin, J. E. (2001). Insulin-stimulated GLUT4 translocation in adipocytes is dependent upon cortical actin remodeling. *Journal of Biological Chemistry*, *276*(45), 42436–42444.

Kassem, M., & Marie, P. J. (2011). Senescence-associated intrinsic mechanisms of osteoblast dysfunctions. *Aging Cell*, *10*(2), 191–197.

Kawaguchi, N., Sundberg, C., Kveiborg, M., Moghadaszadeh, B., Asmar, M., Dietrich, N., et al. (2003). ADAM12 induces actin cytoskeleton and extracellular matrix reorganization during early adipocyte differentiation by regulating beta1 integrin function. *Journal of Cell Science*, *116*(19), 3893–3904.

Kilian, K. A., Bugarija, B., Lahn, B. T., & Mrksich, M. (2010). Geometric cues for directing the differentiation of mesenchymal stem cells. *Proceedings of the National Academy of Sciences of the United States of America*, *107*(11), 4872–4877.

Kim, S., Ahn, C., Bong, N., Choe, S., & Lee, D. K. (2015). Biphasic effects of FGF2 on adipogenesis. *PLoS ONE*, *10*(3), e0120073.

Knäuper, V., Will, H., López-Otin, C., Smith, B., Atkinson, S. J., Stanton, H., et al. (1996). Cellular mechanisms for human procollagenase-3 (MMP-13) activation. Evidence that MT1-MMP (MMP-14) and gelatinase a (MMP-2) are able to generate active enzyme. *Journal of Biological Chemistry*, *271*(29), 17124–17131.

Kolodney, M. S., & Wysolmerski, R. B. (1992). Isometric contraction by fibroblasts and endothelial cells in tissue culture: a quantitative study. *Journal of Cell Biology*, *117*(1), 73–82.

Komori, T., Yagi, H., Nomura, S., Yamaguchi, A., Sasaki, K., Deguchi, K., et al. (1997). Targeted disruption of Cbfa1 results in a complete lack of bone formation owing to maturational arrest of osteoblasts. *Cell*, *89*(5), 755–764.

Koopman, R., Schaart, G., & Hesselink, M. K. (2001). Optimisation of oil red O staining permits combination with immunofluorescence and automated quantification of lipids. *Histochemistry and Cell Biology*, *116*(1), 63–68.

Krieger-Brauer, H. I., & Kather, H. (1995). Antagonistic effects of different members of the fibroblast and platelet-derived growth factor families on adipose conversion and NADPH-dependent H_2O_2 generation in 3T3 L1-cells. *Biochemical Journal*, *307 (2)*, 549–556.

Kundu, M., Javed, A., Jeon, J. P., Horner, A., Shum, L., Eckhaus, M., et al. (2002). Cbfbeta interacts with Runx2 and has a critical role in bone development. *Nature Genetics*, *32*(4), 639–644.

Kuznetsov, S. A., Krebsbach, P. H., Satomura, K., Kerr, J., Riminucci, M., Benayahu, D., & Robey, P. G. (1997). Single-colony derived strains of human marrow stromal fibroblasts form bone after transplantation in vivo. *Journal of Bone and Mineral Research*, *12*(9), 1335–1347.

Lai, W. T., Krishnappa, V., & Phinney, D. G. (2011). Fibroblast growth factor 2 (Fgf2) inhibits differentiation of mesenchymal stem cells by inducing Twist2 and Spry4, blocking extracellular regulated kinase activation, and altering Fgf receptor expression levels. *Stem Cells*, *29*(7), 1102–1111.

Langenbach, F., & Handschel, J. (2013). Effects of dexamethasone, ascorbic acid and β-glycerophosphate on the osteogenic differentiation of stem cells in vitro. *Stem Cell Research & Therapy*, *4*(5), 117.

Lee, E. Y., Parry, G., & Bissell, M. J. (1984). Modulation of secreted proteins of mouse mammary epithelial cells by the collagenous substrata. *Journal of Cell Biology*, *98*(1), 146–155.

Lefterova, M. I., Zhang, Y., Steger, D. J., Schupp, M., Schug, J., Cristancho, A., et al. (2008). PPARgamma and C/EBP factors orchestrate adipocyte biology via adjacent binding on a genome-wide scale. *Genes & Development*, *22*(21), 2941–2952.

Leitinger, B. (2011). Transmembrane collagen receptors. *Annual Review of Cell and Developmental Biology*, *27*, 265–290.

Li, X., Cui, Q., Kao, C., Wang, G.-J., & Balian, G. (2003). Lovastatin inhibits adipogenic and stimulates osteogenic differentiation by suppressing PPARgamma2 and increasing Cbfa1/Runx2 expression in bone marrow mesenchymal cell cultures. *Bone*, *33*(4), 652–659.

Liu, G., Vijayakumar, S., Grumolato, L., Arroyave, R., Qiao, H., Akiri, G., & Aaronson, S. A. (2009). Canonical Wnts function as potent regulators of osteogenesis by human mesenchymal stem cells. *Journal of Cell Biology*, *185*(1), 67–75.

Liu, L. F., Shen, W. J., Zhang, Z. H., Wang, L. J., & Kraemer, F. B. (2010). Adipocytes decrease Runx2 expression in osteoblastic cells: roles of PPARγ and adiponectin. *Journal of Cellular Physiology*, *225*(3), 837–845.

Liu, Z., Xu, J., Colvin, J. S., & Ornitz, D. M. (2002). Coordination of chondrogenesis and osteogenesis by fibroblast growth factor 18. *Genes & Development*, *16*(7), 859–869.

Locklin, R. M., Oreffo, R. O., & Triffitt, J. T. (1999). Effects of TGFbeta and bFGF on the differentiation of human bone marrow stromal fibroblasts. *Cell Biology International*, *23*(3), 185–194.

Locklin, R. M., Williamson, M. C., Beresford, J. N., Triffitt, J. T., & Owen, M. E. (1995). In vitro effects of growth factors and dexamethasone on rat marrow stromal cells. *Clinical Orthopaedics and Related Research*, (313), 27–35.

Lowe, C. E., O'Rahilly, S., & Rochford, J. J. (2011). Adipogenesis at a glance. *Journal of Cell Science*, *124*(Pt 16), 2681–2686.

Lu, C., Li, X. Y., Hu, Y., Rowe, R. G., & Weiss, S. J. (2010). MT1-MMP controls human mesenchymal stem cell trafficking and differentiation. *Blood*, *115*(2), 221–229.

Lund, A. W., Stegemann, J. P., & Plopper, G. E. (2009a). Mesenchymal Stem Cells Sense Three Dimensional Type I Collagen through Discoidin Domain Receptor 1. *The Open Stem Cell Journal*, *1*, 40–53.

Lund, A. W., Yener, B., Stegemann, J. P., & Plopper, G. E. (2009b). The natural and engineered 3D microenvironment as a regulatory cue during stem cell fate determination. *Tissue Engineering Part B: Reviews*, *15*(3), 371–380.

Maeda, K., Kobayashi, Y., Udagawa, N., Uehara, S., Ishihara, A., Mizoguchi, T., et al. (2012). Wnt5a-Ror2 signaling between osteoblast-lineage cells and osteoclast precursors enhances osteoclastogenesis. *Nature Medicine*, *18*(3), 405–412.

Mansukhani, A., Ambrosetti, D., Holmes, G., Cornivelli, L., & Basilico, C. (2005). Sox2 induction by FGF and FGFR2 activating mutations inhibits Wnt signaling and osteoblast differentiation. *Journal of Cell Biology*, *168*(7), 1065–1076.

Mansukhani, A., Bellosta, P., Sahni, M., & Basilico, C. (2000). Signaling by fibroblast growth factors (FGF) and fibroblast growth factor receptor 2 (FGFR2)-activating mutations blocks mineralization and induces apoptosis in osteoblasts. *Journal of Cell Biology*, *149*(6), 1297–1308.

Martin, I., Muraglia, A., Campanile, G., Cancedda, R., & Quarto, R. (1997). Fibroblast growth factor-2 supports ex vivo expansion and maintenance of osteogenic precursors from human bone marrow. *Endocrinology*, *138*(10), 4456–4462.

Martin-Martin, B., Tovell, V., Dahlmann-Noor, A. H., Khaw, P. T., & Bailly, M. (2011). The effect of MMP inhibitor GM6001 on early fibroblast-mediated collagen matrix contraction is correlated to a decrease in cell protrusive activity. *European Journal of Cell Biology*, *90*(1), 26–36.

Martino, M. M., Mochizuki, M., Rothenfluh, D. A., Rempel, S. A., Hubbell, J. A., & Barker, T. H. (2009). Controlling integrin specificity and stem cell differentiation in 2D and 3D environments through regulation of fibronectin domain stability. *Biomaterials*, *30*(6), 1089–1097.

Mauney, J., & Volloch, V. (2010). Adult human bone marrow stromal cells regulate expression of their MMPs and TIMPs in differentiation type-specific manner. *Matrix Biology*, *29*(1), 3–8.

Maurin, A. C., Chavassieux, P. M., Vericel, E., & Meunier, P. J. (2002). Role of polyunsaturated fatty acids in the inhibitory effect of human adipocytes on osteoblastic proliferation. *Bone*, *31*(1), 260–266.

McBeath, R., Pirone, D. M., Nelson, C. M., Bhadriraju, K., & Chen, C. S. (2004). Cell shape, cytoskeletal tension, and RhoA regulate stem cell lineage commitment. *Developmental Cell*, *6*(4), 483–495.

Menanteau, J., Neuman, W. F., & Neuman, M. W. (1982). A study of bone proteins which can prevent hydroxyapatite formation. *Metabolic Bone Disease & Related Research*, *4*(2), 157–162.

Meshel, A. S., Wei, Q., Adelstein, R. S., & Sheetz, M. P. (2005). Basic mechanism of three-dimensional collagen fibre transport by fibroblasts. *Nature Cell Biology*, *7*(2), 157–164.

Meunier, P., Aaron, J., Edouard, C., & Vignon, G. (1971). Osteoporosis and the replacement of cell populations of the marrow by adipose tissue. A quantitative study of 84 iliac bone biopsies. *Clinical Orthopaedics and Related Research*, *80*, 147–154.

Mezey, E. (2011). The therapeutic potential of bone marrow-derived stromal cells. *Journal of Cellular Biochemistry*, *112*(10), 2683–2687.

Miller, D. L., Ortega, S., Bashayan, O., Basch, R., & Basilico, C. (2000). Compensation by fibroblast growth factor 1 (FGF1) does not account for the mild phenotypic defects observed in FGF2 null mice. *Molecular and Cellular Biology*, *20*(6), 2260–2268.

Mohammadi, M., McMahon, G., Sun, L., Tang, C., Hirth, P., Yeh, B. K., et al. (1997). Structures of the tyrosine kinase domain of fibroblast growth factor receptor in complex with inhibitors. *Science*, *276*(5314), 955–960.

Montero, A., Okada, Y., Tomita, M., Ito, M., Tsurukami, H., Nakamura, T., et al. (2000). Disruption of the fibroblast growth factor-2 gene results in decreased bone mass and bone formation. *Journal of Clinical Investigation*, *105*(8), 1085–1093.

Mueller, S. N., Thomas, K. A., Di Salvo, J., & Levine, E. M. (1989). Stabilization by heparin of acidic fibroblast growth factor mitogenicity for human endothelial cells in vitro. *Journal of Cellular Physiology*, *140*(3), 439–448.

Muenke, M., Gripp, K. W., McDonald-McGinn, D. M., Gaudenz, K., Whitaker, L. A., Bartlett, S. P., et al. (1997). A unique point mutation in the fibroblast growth factor receptor 3 gene (FGFR3) defines a new craniosynostosis syndrome. *American Journal of Human Genetics*, *60*(3), 555–564.

Muraglia, A., Cancedda, R., & Quarto, R. (2000). Clonal mesenchymal progenitors from human bone marrow differentiate in vitro according to a hierarchical model. *Journal of Cell Science*, *113* (7), 1161–1166.

Murphy, G. (2011). Tissue inhibitors of metalloproteinases. *Genome Biology*, *12*(11), 233.

Murshed, M., Schinke, T., McKee, M. D., & Karsenty, G. (2004). Extracellular matrix mineralization is regulated locally; different roles of two gla-containing proteins. *Journal of Cell Biology*, *165*(5), 625–630.

Nagase, H., Visse, R., & Murphy, G. (2006). Structure and function of matrix metalloproteinases and TIMPs. *Cardiovascular Research*, *69*(3), 562–573.

Nakagawa, S., Pawelek, P., & Grinnell, F. (1989). Extracellular matrix organization modulates fibroblast growth and growth factor responsiveness. *Experimental Cell Research*, *182*(2), 572–582.

Nakashima, K., Zhou, X., Kunkel, G., Zhang, Z., Deng, J. M., Behringer, R. R., & de Crombrugghe, B. (2002). The novel zinc finger-containing transcription factor osterix is required for osteoblast differentiation and bone formation. *Cell*, *108*(1), 17–29.

Navre, M., & Ringold, G. M. (1989). Differential effects of fibroblast growth factor and tumor promoters on the initiation and maintenance of adipocyte differentiation. *Journal of Cell Biology*, *109*(4 Pt 1), 1857–1863.

Neubauer, M., Fischbach, C., Bauer-Kreisel, P., Lieb, E., Hacker, M., Tessmar, J., et al. (2004). Basic fibroblast growth factor enhances PPARgamma ligand-induced adipogenesis of mesenchymal stem cells. *FEBS Letters*, *577*(1-2), 277–283.

Neubauer, M., Hacker, M., Bauer-Kreisel, P., Weiser, B., Fischbach, C., Schulz, M. B., et al. (2005). Adipose tissue engineering based on mesenchymal stem cells and basic fibroblast growth factor in vitro. *Tissue Engineering*, *11*(11-12), 1840–1851.

Neuss, S., Stainforth, R., Salber, J., Schenck, P., Bovi, M., Knuchel, R., & Perez-Bouza, A. (2008). Long-term survival and bipotent terminal differentiation of human mesenchymal stem cells (hMSC) in combination with a commercially available three-dimensional collagen scaffold. *Cell Transplantation*, *17*(8), 977–986.

Newell, F. S., Su, H., Tornqvist, H., Whitehead, J. P., Prins, J. B., & Hutley, L. J. (2006). Characterization of the transcriptional and functional effects of fibroblast growth factor-1 on human preadipocyte differentiation. *FASEB Journal*, *20*(14), 2615–2617.

Nickel, W. (2011). The unconventional secretory machinery of fibroblast growth factor 2. *Traffic*, *12*(7), 799–805.

Nishio, Y., Dong, Y., Paris, M., O'Keefe, R. J., Schwarz, E. M., & Drissi, H. (2006). Runx2-mediated regulation of the zinc finger Osterix/Sp7 gene. *Gene*, *372*, 62–70.

Noack, C., Hempel, U., Preissler, C., & Dieter, P. (2016). Prostaglandin E_2 impairs osteogenic and facilitates adipogenic differentiation of human bone marrow stromal cells. *Prostaglandins, Leukotrienes and Essential Fatty Acids*, *94*, 91–98.

Noff, D., Pitaru, S., & Savion, N. (1989). Basic fibroblast growth factor enhances the capacity of bone marrow cells to form bone-like nodules in vitro. *FEBS Letters*, *250*(2), 619–621.

Noth, U., Rackwitz, L., Heymer, A., Weber, M., Baumann, B., Steinert, A., et al. (2007). Chondrogenic differentiation of human mesenchymal stem cells in collagen type I hydrogels. *Journal of Biomedical Materials Research Part A*, *83*(3), 626–635.

Oh, S. A., Lee, H. Y., Lee, J. H., Kim, T. H., Jang, J. H., Kim, H. W., & Wall, I. (2012). Collagen three-dimensional hydrogel matrix carrying basic fibroblast growth factor for the cultivation of mesenchymal stem cells and osteogenic differentiation. *Tissue Engineering. Part A*, *18*(9-10), 1087–1100.

Ohbayashi, N., Shibayama, M., Kurotaki, Y., Imanishi, M., Fujimori, T., Itoh, N., & Takada, S. (2002). FGF18 is required for normal cell proliferation and differentiation during osteogenesis and chondrogenesis. *Genes & Development*, *16*(7), 870–879.

Ohuchi, E., Imai, K., Fujii, Y., Sato, H., Seiki, M., & Okada, Y. (1997). Membrane type 1 matrix metalloproteinase digests interstitial collagens and other extracellular matrix macromolecules. *Journal of Biological Chemistry,* 272(4), 2446-2451.

Oliver, L. J., Rifkin, D. B., Gabrilove, J., Hannocks, M. J., & Wilson, E. L. (1990). Long-term culture of human bone marrow stromal cells in the presence of basic fibroblast growth factor. *Growth Factors*, *3*(3), 231–236.

Olsen, S. K., Garbi, M., Zampieri, N., Eliseenkova, A. V., Ornitz, D. M., Goldfarb, M., & Mohammadi, M. (2003). Fibroblast growth factor (FGF) homologous factors share structural but not functional homology with FGFs. *Journal of Biological Chemistry*, *278*(36), 34226–34236.

Ori, A., Wilkinson, M. C., & Fernig, D. G. (2008). The heparanome and regulation of cell function: structures, functions and challenges. *Frontiers in Bioscience*, *13*, 4309–4338.

Ornitz, D. M., & Itoh, N. (2015). The Fibroblast Growth Factor signaling pathway. *Wiley Interdisciplinary Reviews. Developmental Biology*, *4*(3), 215–266.

Ornitz, D. M., Xu, J., Colvin, J. S., McEwen, D. G., MacArthur, C. A., Coulier, F., et al. (1996). Receptor specificity of the fibroblast growth factor family. *Journal of Biological Chemistry*, *271*(25), 15292–15297.

Ortega, S., Ittmann, M., Tsang, S. H., Ehrlich, M., & Basilico, C. (1998). Neuronal defects and delayed wound healing in mice lacking fibroblast growth factor 2. *Proceedings of the National Academy of Sciences of the United States of America*, *95*(10), 5672–5677.

Pampaloni, F., Reynaud, E. G., & Stelzer, E. H. K. (2007). The third dimension bridges the gap between cell culture and live tissue. *Nature Reviews. Molecular Cell Biology*, *8*(10), 839–845.

Panek, R. L., Lu, G. H., Dahring, T. K., Batley, B. L., Connolly, C., Hamby, J. M., & Brown, K. J. (1998). In vitro biological characterization and antiangiogenic effects of PD 166866, a selective inhibitor of the FGF-1 receptor tyrosine kinase. *Journal of Pharmacology and Experimental Therapeutics*, *286*(1), 569–577.

Park, J. S., Chu, J. S., Tsou, A. D., Diop, R., Tang, Z., Wang, A., & Li, S. (2011). The effect of matrix stiffness on the differentiation of mesenchymal stem cells in response to TGF-β. *Biomaterials*, *32*(16), 3921–3930.

Patel, N. G., Kumar, S., & Eggo, M. C. (2005). Essential role of fibroblast growth factor signaling in preadipoctye differentiation. *Journal of Clinical Endocrinology and Metabolism*, *90*(2), 1226–1232.

Pfaffl, M. W. (2001). A new mathematical model for relative quantification in real-time RT-PCR. *Nucleic Acids Research*, *29*(9), e45.

Phillips, J. A., & Bonassar, L. J. (2005). Matrix metalloproteinase activity synergizes with alpha2beta1 integrins to enhance collagen remodeling. *Experimental Cell Research*, *310*(1), 79–87.

Pittenger, M. F. M., Mackay, A. M. A., Beck, S. C. S., Jaiswal, R. K. R., Douglas, R. R., Mosca, J. D. J., et al. (1999). Multilineage potential of adult human mesenchymal stem cells. *Science*, *284*(5411), 143–147.

Poloni, A., Maurizi, G., Serrani, F., Mancini, S., Zingaretti, M. C., Frontini, A., et al. (2013). Molecular and functional characterization of human bone marrow adipocytes. *Experimental Hematology*, *41*(6), 558–566.e2.

Prats, H., Kaghad, M., Prats, A. C., Klagsbrun, M., Lélias, J. M., Liauzun, P., et al. (1989). High molecular mass forms of basic fibroblast growth factor are initiated by alternative CUG codons. *Proceedings of the National Academy of Sciences of the United States of America*, *86*(6), 1836–1840.

Pri-Chen, S., Pitaru, S., Lokiec, F., & Savion, N. (1998). Basic fibroblast growth factor enhances the growth and expression of the osteogenic phenotype of dexamethasone-treated human bone marrow-derived bone-like cells in culture. *Bone*, *23*(2), 111–117.

Quarto, N., & Longaker, M. T. (2006). FGF-2 Inhibits Osteogenesis in Mouse Adipose Tissue-Derived Stromal Cells and Sustains their Proliferative and Osteogenic Potential State. *Tissue Engineering*, *12*(6), 1405–1418.

Quarto, N., Wan, D. C., & Longaker, M. T. (2008). Molecular mechanisms of FGF-2 inhibitory activity in the osteogenic context of mouse adipose-derived stem cells (mASCs). *Bone*, *42*(6), 1040–1052.

Ra, H. J., & Parks, W. C. (2007). Control of matrix metalloproteinase catalytic activity. *Matrix Biology*, *26*(8), 587–596.

Ramakers, C., Ruijter, J. M., Deprez, R. H. L., & Moorman, A. F. M. (2003). Assumption-free analysis of quantitative real-time polymerase chain reaction (PCR) data. *Neuroscience Letters*, *339*(1), 62–66.

Rapraeger, A. C., Krufka, A., & Olwin, B. B. (1991). Requirement of heparan sulfate for bFGF-mediated fibroblast growth and myoblast differentiation. *Science*, *252*(5013), 1705–1708.

Reardon, W., Winter, R. M., Rutland, P., Pulleyn, L. J., Jones, B. M., & Malcolm, S. (1994). Mutations in the fibroblast growth factor receptor 2 gene cause Crouzon syndrome. *Nature Genetics*, *8*(1), 98–103.

Ricard-Blum, S. (2011). The collagen family. *Cold Spring Harbor Perspectives in Biology*, *3*(1), a004978.

Ries, C., Egea, V., Karow, M., Kolb, H., Jochum, M., & Neth, P. (2007). MMP-2, MT1-MMP, and TIMP-2 are essential for the invasive capacity of human mesenchymal stem cells: differential regulation by inflammatory cytokines. *Blood*, *109*(9), 4055–4063.

Rodríguez Fernández, J. L., & Ben-Ze'ev, A. (1989). Regulation of fibronectin, integrin and cytoskeleton expression in differentiating adipocytes: inhibition by extracellular matrix and polylysine. *Differentiation*, *42*(2), 65–74.

Rodríguez, J. P., Garat, S., Gajardo, H., Pino, A. M., & Seitz, G. (1999). Abnormal osteogenesis in osteoporotic patients is reflected by altered mesenchymal stem cells dynamics. *Journal of Cellular Biochemistry*, *75*(3), 414–423.

Rodríguez, J. P., Montecinos, L., Ríos, S., Reyes, P., & Martínez, J. (2000). Mesenchymal stem cells from osteoporotic patients produce a type I collagen-deficient extracellular matrix favoring adipogenic differentiation. *Journal of Cellular Biochemistry*, *79*(4), 557–565.

Romberg, R. W., Werness, P. G., Riggs, B. L., & Mann, K. G. (1986). Inhibition of hydroxyapatite crystal growth by bone-specific and other calcium-binding proteins. *Biochemistry*, *25*(5), 1176–1180.

Rosen, C. J. (Ed.). (2013). Primer on the Metabolic Bone Diseases and Disorders of Mineral Metabolism. American Society for Bone and Mineral Research. John Wiley & Sons.

Rosen, C. J., Ackert-Bicknell, C., Rodriguez, J. P., & Pino, A. M. (2009). Marrow fat and the bone microenvironment: developmental, functional, and pathological implications. *Critical Reviews in Eukaryotic Gene Expression*, *19*(2), 109–124.

Rosengart, T. K., Johnson, W. V., Friesel, R., Clark, R., & Maciag, T. (1988). Heparin protects heparin-binding growth factor-I from proteolytic inactivation in vitro. *Biochemical and Biophysical Research Communications*, *152*(1), 432–440.

Roskelley, C. D., Desprez, P. Y., & Bissell, M. J. (1994). Extracellular matrix-dependent tissue-specific gene expression in mammary epithelial cells requires both physical and biochemical signal transduction. *Proceedings of the National Academy of Sciences of the United States of America*, *91*(26), 12378–12382.

Sacchetti, B., Funari, A., Michienzi, S., Di Cesare, S., Piersanti, S., Saggio, I., et al. (2007). Self-renewing osteoprogenitors in bone marrow sinusoids can organize a hematopoietic microenvironment. *Cell*, *131*(2), 324–336.

Sadie-Van Gijsen, H., Crowther, N. J., Hough, F. S., & Ferris, W. F. (2013). The interrelationship between bone and fat: from cellular see-saw to endocrine reciprocity. *Cellular and Molecular Life Sciences*, *70*(13), 2331–2349.

Santiago, J. A., Pogemiller, R., & Ogle, B. M. (2009). Heterogeneous differentiation of human mesenchymal stem cells in response to extended culture in extracellular matrices. *Tissue Engineering. Part A*, *15*(12), 3911–3922.

Sarber, R., Hull, B., Merrill, C., Soranno, T., & Bell, E. (1981). Regulation of proliferation of fibroblasts of low and high population doubling levels grown in collagen lattices. *Mechanisms of Ageing and Development*, *17*(2), 107–117.

Scheller, E. L., & Rosen, C. J. (2014). What's the matter with MAT? Marrow adipose tissue, metabolism, and skeletal health. *Annals of the New York Academy of Sciences*, *1311*, 14–30.

Schilling, T., Küffner, R., Klein-Hitpass, L., Zimmer, R., Jakob, F., & Schutze, N. (2008). Microarray analyses of transdifferentiated mesenchymal stem cells. *Journal of Cellular Biochemistry*, *103*(2), 413–433.

Schilling, T., Noth, U., Klein-Hitpass, L., Jakob, F., & Schutze, N. (2007). Plasticity in adipogenesis and osteogenesis of human mesenchymal stem cells. *Molecular and Cellular Endocrinology*, *271*(1-2), 1–17.

Schindelin, J., Arganda-Carreras, I., Frise, E., Kaynig, V., Longair, M., Pietzsch, T., et al. (2012). Fiji: an open-source platform for biological-image analysis. *Nature Methods*, *9*(7), 676–682.

Schiro, J. A., Chan, B. M., Roswit, W. T., Kassner, P. D., Pentland, A. P., Hemler, M. E., et al. (1991). Integrin alpha 2 beta 1 (VLA-2) mediates reorganization and contraction of collagen matrices by human cells. *Cell*, *67*(2), 403–410.

Schlessinger, J., Plotnikov, A. N., Ibrahimi, O. A., Eliseenkova, A. V., Yeh, B. K., Yayon, A., et al. (2000). Crystal structure of a ternary FGF-FGFR-heparin complex reveals a dual role for heparin in FGFR binding and dimerization. *Molecular Cell*, *6*(3), 743–750.

Schneider, R. K., Puellen, A., Kramann, R., Raupach, K., Bornemann, J., Knuechel, R., et al. (2010). The osteogenic differentiation of adult bone marrow and perinatal umbilical mesenchymal stem cells and matrix remodelling in three-dimensional collagen scaffolds. *Biomaterials*, *31*(3), 467–480.

Scott, K. A., Wood, E. J., & Karran, E. H. (1998). A matrix metalloproteinase inhibitor which prevents fibroblast-mediated collagen lattice contraction. *FEBS Letters*, *441*(1), 137–140.

Scutt, A., & Bertram, P. (1999). Basic fibroblast growth factor in the presence of dexamethasone stimulates colony formation, expansion, and osteoblastic differentiation by rat bone marrow stromal cells. *Calcified Tissue International*, *64*(1), 69–77.

Serrero, G. (1987). EGF inhibits the differentiation of adipocyte precursors in primary cultures. *Biochemical and Biophysical Research Communications*, *146*(1), 194–202.

Shih, Y. R. V., Tseng, K. F., Lai, H. Y., Lin, C. H., & Lee, O. K. (2011). Matrix stiffness regulation of integrin-mediated mechanotransduction during osteogenic differentiation of human mesenchymal stem cells. *Journal of Bone and Mineral Research*, *26*(4), 730–738.

Shrivastava, A., Radziejewski, C., Campbell, E., Kovac, L., McGlynn, M., Ryan, T. E., et al. (1997). An orphan receptor tyrosine kinase family whose members serve as nonintegrin collagen receptors. *Molecular Cell*, *1*(1), 25–34.

Simann, M., Le Blanc, S., Schneider, V., Zehe, V., Lüdemann, M., Schutze, N., et al. (2017). Canonical FGFs Prevent Osteogenic Lineage Commitment and Differentiation of Human Bone Marrow Stromal Cells Via ERK1/2 Signaling. *Journal of Cellular Biochemistry*, *118*(2), 263–275.

Simann, M., Schneider, V., Le Blanc, S., Dotterweich, J., Zehe, V., Krug, M., et al. (2015). Heparin affects human bone marrow stromal cell fate: Promoting osteogenic and reducing adipogenic differentiation and conversion. *Bone*, *78*, 102–113.

Sims, N. A., & Gooi, J. H. (2008). Bone remodeling: Multiple cellular interactions required for coupling of bone formation and resorption. *Seminars in Cell & Developmental Biology*, *19*(5), 444–451.

Sobue, T., Naganawa, T., Xiao, L., Okada, Y., Tanaka, Y., Ito, M., et al. (2005). Over-expression of fibroblast growth factor-2 causes defective bone mineralization and osteopenia in transgenic mice. *Journal of Cellular Biochemistry*, *95*(1), 83–94.

Solchaga, L. A., Penick, K., Porter, J. D., Goldberg, V. M., Caplan, A. I., & Welter, J. F. (2005). FGF-2 enhances the mitotic and chondrogenic potentials of human adult bone marrow-derived mesenchymal stem cells. *Journal of Cellular Physiology*, *203*(2), 398–409.

Spinella-Jaegle, S., Rawadi, G., Kawai, S., Gallea, S., Faucheu, C., Mollat, P., et al. (2001). Sonic hedgehog increases the commitment of pluripotent mesenchymal cells into the osteoblastic lineage and abolishes adipocytic differentiation. *Journal of Cell Science*, *114*(11), 2085–2094.

Stamenkovic, I. (2003). Extracellular matrix remodelling: the role of matrix metalloproteinases. *Journal of Pathology*, *200*(4), 448–464.

Stopak, D., & Harris, A. K. (1982). Connective tissue morphogenesis by fibroblast traction. I. Tissue culture observations. *Developmental Biology*, *90*(2), 383–398.

Taipaleenmäki, H., Abdallah, B. M., Aldahmash, A., Säämänen, A. M., & Kassem, M. (2011). Wnt signalling mediates the cross-talk between bone marrow derived pre-adipocytic and pre-osteoblastic cell populations. *Experimental Cell Research*, *317*(6), 745–756.

Tang, K. T., Capparelli, C., Stein, J. L., Stein, G. S., Lian, J. B., Huber, A. C., et al. (1996). Acidic fibroblast growth factor inhibits osteoblast differentiation in vitro: altered expression of collagenase, cell growth-related, and mineralization-associated genes. *Journal of Cellular Biochemistry*, *61*(1), 152–166.

Tang, Q. Q., & Lane, M. D. (2012). Adipogenesis: from stem cell to adipocyte. *Annual Review of Biochemistry*, *81*, 715–736.

Tang, Y., Rowe, R. G., Botvinick, E. L., Kurup, A., Putnam, A. J., Seiki, M., et al. (2013). MT1-MMP-dependent control of skeletal stem cell commitment via a β1-integrin/YAP/TAZ signaling axis. *Developmental Cell*, *25*(4), 402–416.

Teven, C. M., Farina, E. M., Rivas, J., & Reid, R. R. (2014). Fibroblast growth factor (FGF) signaling in development and skeletal diseases. *Genes & Diseases*, *1*(2), 199–213.

Théry, M., Racine, V., Piel, M., Pépin, A., Dimitrov, A., Chen, Y., et al. (2006). Anisotropy of cell adhesive microenvironment governs cell internal organization and orientation of polarity. *Proceedings of the National Academy of Sciences of the United States of America*, *103*(52), 19771–19776.

Thomas, T., Gori, F., Khosla, S., Jensen, M. D., Burguera, B., & Riggs, B. L. (1999). Leptin acts on human marrow stromal cells to enhance differentiation to osteoblasts and to inhibit differentiation to adipocytes. *Endocrinology*, *140*(4), 1630–1638.

Titushkin, I., & Cho, M. (2007). Modulation of cellular mechanics during osteogenic differentiation of human mesenchymal stem cells. *Biophysical Journal*, *93*(10), 3693–3702.

Trappmann, B., Gautrot, J. E., Connelly, J. T., Strange, D. G. T., Li, Y., Oyen, M. L., et al. (2012). Extracellular-matrix tethering regulates stem-cell fate. *Nature Materials*, *11*(7), 642–649.

Tsutsumi, S., Shimazu, A., Miyazaki, K., Pan, H., Koike, C., Yoshida, E., et al. (2001). Retention of Multilineage Differentiation Potential of Mesenchymal Cells during Proliferation in Response to FGF. *Biochemical and Biophysical Research Communications*, *288*(2), 413–419.

Ugarte, F., Ryser, M., Thieme, S., Fierro, F. A., Navratiel, K., Bornhäuser, M., & Brenner, S. (2009). Notch signaling enhances osteogenic differentiation while inhibiting adipogenesis in primary human bone marrow stromal cells. *Experimental Hematology*, *37*(7), 867–875.e1.

van Susante, J. L., Buma, P., van Osch, G. J., Versleyen, D., van der Kraan, P. M., van der Berg, W. B., & Homminga, G. N. (1995). Culture of chondrocytes in alginate and collagen carrier gels. *Acta Orthopaedica Scandinavica*, *66*(6), 549–556.

Vandesompele, J., De Preter, K., Pattyn, F., Poppe, B., Van Roy, N., De Paepe, A., & Speleman, F. (2002). Accurate normalization of real-time quantitative RT-PCR data by geometric averaging of multiple internal control genes. *Genome Biology*, *3*(7), RESEARCH0034.

Vassaux, G., Négrel, R., Ailhaud, G., & Gaillard, D. (1994). Proliferation and differentiation of rat adipose precursor cells in chemically defined medium: differential action of anti-adipogenic agents. *Journal of Cellular Physiology*, *161*(2), 249–256.

Verma, S., Rajaratnam, J. H., Denton, J., Hoyland, J. A., & Byers, R. J. (2002). Adipocytic proportion of bone marrow is inversely related to bone formation in osteoporosis. *Journal of Clinical Pathology*, *55*(9), 693–698.

Visse, R., & Nagase, H. (2003). Matrix metalloproteinases and tissue inhibitors of metalloproteinases: structure, function, and biochemistry. *Circulation Research*, *92*(8), 827–839.

Vogel, W., Brakebusch, C., Fässler, R., Alves, F., Ruggiero, F., & Pawson, T. (2000). Discoidin domain receptor 1 is activated independently of beta(1) integrin. *Journal of Biological Chemistry*, *275*(8), 5779–5784.

Vogel, W., Gish, G. D., Alves, F., & Pawson, T. (1997). The discoidin domain receptor tyrosine kinases are activated by collagen. *Molecular Cell*, *1*(1), 13–23.

Wagner, W., Horn, P., Castoldi, M., Diehlmann, A., Bork, S., Saffrich, R., et al. (2008). Replicative senescence of mesenchymal stem cells: a continuous and organized process. *PLoS ONE*, *3*(5), e2213.

Wang, H., Yoshiko, Y., Yamamoto, R., Minamizaki, T., Kozai, K., Tanne, K., et al. (2008). Overexpression of fibroblast growth factor 23 suppresses osteoblast differentiation and matrix mineralization in vitro. *Journal of Bone and Mineral Research*, *23*(6), 939–948.

Wang, W., Itaka, K., Ohba, S., Nishiyama, N., Chung, U.-I., Yamasaki, Y., & Kataoka, K. (2009). 3D spheroid culture system on micropatterned substrates for improved differentiation efficiency of multipotent mesenchymal stem cells. *Biomaterials*, *30*(14), 2705–2715.

Wei, W., Dutchak, P. A., Wang, X., Ding, X., Wang, X., Bookout, A. L., et al. (2012). Fibroblast growth factor 21 promotes bone loss by potentiating the effects of peroxisome proliferator-activated receptor γ. *Proceedings of the National Academy of Sciences of the United States of America*, *109*(8), 3143–3148.

Wilkie, A. O., Slaney, S. F., Oldridge, M., Poole, M. D., Ashworth, G. J., Hockley, A. D., et al. (1995). Apert syndrome results from localized mutations of FGFR2 and is allelic with Crouzon syndrome. *Nature Genetics*, *9*(2), 165–172.

Winer, J. P., Janmey, P. A., McCormick, M. E., & Funaki, M. (2009). Bone marrow-derived human mesenchymal stem cells become quiescent on soft substrates but remain responsive to chemical or mechanical stimuli. *Tissue Engineering. Part A*, *15*(1), 147–154.

Wren, T. A. L., Chung, S. A., Dorey, F. J., Bluml, S., Adams, G. B., & Gilsanz, V. (2011). Bone Marrow Fat Is Inversely Related to Cortical Bone in Young and Old Subjects. *Journal of Clinical Endocrinology and Metabolism*, *96*(3), 782–786.

Wu, Z., Rosen, E. D., Brun, R., Hauser, S., Adelmant, G., Troy, A. E., et al. (1999). Cross-regulation of C/EBP alpha and PPAR gamma controls the transcriptional pathway of adipogenesis and insulin sensitivity. *Molecular Cell*, *3*(2), 151–158.

Xiao, G., Jiang, D., Gopalakrishnan, R., & Franceschi, R. T. (2002). Fibroblast growth factor 2 induction of the osteocalcin gene requires MAPK activity and phosphorylation of the osteoblast transcription factor, Cbfa1/Runx2. *Journal of Biological Chemistry*, *277*(39), 36181–36187.

Xiao, L., Esliger, A., & Hurley, M. M. (2013). Nuclear fibroblast growth factor 2 (FGF2) isoforms inhibit bone marrow stromal cell mineralization through FGF23/FGFR/MAPK in vitro. *Journal of Bone and Mineral Research*, *28*(1), 35–45.

Xiao, L., Liu, P., Li, X., Doetschman, T., Coffin, J. D., Drissi, H., & Hurley, M. M. (2009). Exported 18-kDa isoform of fibroblast growth factor-2 is a critical determinant of bone mass in mice. *Journal of Biological Chemistry*, *284*(5), 3170–3182.

Xiao, L., Naganawa, T., Lorenzo, J., Carpenter, T. O., Coffin, J. D., & Hurley, M. M. (2010a). Nuclear isoforms of fibroblast growth factor 2 are novel inducers of hypophosphatemia via modulation of FGF23 and KLOTHO. *Journal of Biological Chemistry*, *285*(4), 2834–2846.

Xiao, L., Sobue, T., Esliger, A., Kronenberg, M. S., Coffin, J. D., Doetschman, T., & Hurley, M. M. (2010b). Disruption of the Fgf2 gene activates the adipogenic and suppresses the osteogenic program in mesenchymal marrow stromal stem cells. *Bone*, *47*(2), 360–370.

Xue, R., Li, J. Y. S., Yeh, Y., Yang, L., & Chien, S. (2013). Effects of matrix elasticity and cell density on human mesenchymal stem cells differentiation. *Journal of Orthopaedic Research*, *31*(9), 1360–1365.

Yan, C., & Boyd, D. D. (2007). Regulation of matrix metalloproteinase gene expression. *Journal of Cellular Physiology*, *211*(1), 19–26.

Yayon, A., Klagsbrun, M., Esko, J. D., Leder, P., & Ornitz, D. M. (1991). Cell surface, heparin-like molecules are required for binding of basic fibroblast growth factor to its high affinity receptor. *Cell*, *64*(4), 841–848.

Yeh, W. C., Cao, Z., Classon, M., & McKnight, S. L. (1995). Cascade regulation of terminal adipocyte differentiation by three members of the C/EBP family of leucine zipper proteins. *Genes & Development*, *9*(2), 168–181.

Yoneno, K., Ohno, S., Tanimoto, K., Honda, K., Tanaka, N., Doi, T., et al. (2005). Multidifferentiation potential of mesenchymal stem cells in three-dimensional collagen gel cultures. *Journal of Biomedical Materials Research Part A*, *75*(3), 733–741.

Young, M. F. (2003). Bone matrix proteins: their function, regulation, and relationship to osteoporosis. *Osteoporosis International*, *14 Suppl 3*, S35–42.

Zakrzewska, M., Marcinkowska, E., & Wiedlocha, A. (2008). FGF-1: from biology through engineering to potential medical applications. *Critical Reviews in Clinical Laboratory Sciences*, *45*(1), 91–135.

Zhang, L., Su, P., Xu, C., Chen, C., Liang, A., Du, K., et al. (2010). Melatonin inhibits adipogenesis and enhances osteogenesis of human mesenchymal stem cells by suppressing PPARγ expression and enhancing Runx2 expression. *Journal of Pineal Research*, *49*(4), 364–372.

Zhang, X., Ibrahimi, O. A., Olsen, S. K., Umemori, H., Mohammadi, M., & Ornitz, D. M. (2006). Receptor specificity of the fibroblast growth factor family. The complete mammalian FGF family. *The Journal of Biological Chemistry*, *281*(23), 15694–15700.

Zhou, M., Sutliff, R. L., Paul, R. J., Lorenz, J. N., Hoying, J. B., Haudenschild, C. C., et al. (1998). Fibroblast growth factor 2 control of vascular tone. *Nature Medicine*, *4*(2), 201–207.

List of Figures

List of Tables

List of Abbreviations

°C	Degree Celsius
2D	Two-dimensional
3D	Three-dimensional
ALP	Alkaline phosphatase
ANOVA	Analysis of variance
aP2	Adipocyte protein 2
Arg	Arginine
ARS	Alizarin Red S
ASC	Adipose-derived stromal cell
Asp	Aspartic acid
BMP	Bone morphogenetic protein
BMPR	BMP receptor
BMSC	Bone marrow stromal cell
bp	Base pair
BSA	Bovine serum albumin
CBFβ1	Core binding factor β1
cDNA	Complementary DNA
C/EBP	CCAAT-enhancer-binding protein
COL1A1	Collagen 1 A1
COL2A1	Collagen 2 A1
dH_2O	Distilled water
ddH_2O	Double-distilled water
DMEM	Dulbecco's modified Eagle's medium
DMP1	Dentin matrix acidic phosphoprotein 1
DMSO	Dimethylsulfoxide
DNA	Deoxyribonucleic acid
dNTPs	Deoxynucleotide triphosphates
DDR	Discoidin domain receptor
ECM	Extracellular matrix
EDTA	Ethylendiamintetraacetic acid
ERK	Extracellular signal-regulated kinase
FABP4	Fatty acid binding protein 4
FCS	Fetal calf serum
FGF	Fibroblast growth factor

FGFR	FGF receptor
FRS2α	FGFR substrate 2α
g	Grams
Gly	Glycine
GPDH	Glycerol-3-phosphate dehydrogenase
h	Hours
H&E	Hematoxylin and eosin
hBMSCs	Human bone marrow stromal cells
Hep	Heparin
HMW	High molecular weight
HPLC	High performance liquid chromatography
HS	Heparan sulfate
IBMX	3-isobutyl-1-methylxanthine
IGF	Insulin-like growth factor
JNK	c-Jun N-terminal kinase
kDa	Kilodaltons
l	Liters
LMW	Low molecular weight
LPL	Lipoprotein lipase
m	meter
M	Molar
MAPK	Mitogen-activated protein kinase
min	Minutes
M-MLV	Moloney murine leukemia virus
MMP	Matrix metalloproteinase
mRNA	Messenger RNA
MT-MMP	Membrane type MMP
OCN	Osteocalcin
OPN	Osteopontin
ORO	Oil Red O
PBS	Phosphate buffered saline
PBS^{+}	PBS with Ca^{2+}/Mg^{2+}
PCR	Polymerase chain reaction
PI	Propidium iodide
PI3K	Phosphoinositide 3-kinase
PPARγ2	Peroxisome proliferator-activated receptor γ 2
qPCR	Quantitative PCR
RNA	Ribonucleic acid

RGD	Adhesion sequence Arg-Gly-Asp
rhFGF1	Recombinant human FGF1
rhFGF2	Recombinant human FGF2
RPS27A	Ribosomal protein S27a
RPLP0	Ribosomal protein, large, P0
RT	Reverse transcriptase
Runx2	Runt-related transcription factor 2
s	Seconds
SOST	Sclerostin
TAZ	Transcriptional co-activator with PDZ-binding motif
TCP	Tissue culture plastic
TGF-β	Transforming growth factor β
TIMP	Tissue inhibitor of metalloproteinases
x g	Relative centrifugal force
v/v	Volume/volume

List of Publications

Le Blanc, S., Simann, M., Jakob, F., Schutze, N., & Schilling, T. (2015). Fibroblast growth factors 1 and 2 inhibit adipogenesis of human bone marrow stromal cells in 3D collagen gels. *Experimental Cell Research*, *338*(2), 136–148.

Simann, M., Schneider, V., **Le Blanc, S.**, Dotterweich, J., Zehe, V., Krug, M., Jakob, F., Schilling, T., and Schutze, N. (2015). Heparin affects human bone marrow stromal cell fate: Promoting osteogenic and reducing adipogenic differentiation and conversion. *Bone*, *78*, 102–113.

Simann, M., **Le Blanc, S.**, Schneider, V., Zehe, V., Lüdemann, M., Schutze, N., et al. (2017). Canonical FGFs Prevent Osteogenic Lineage Commitment and Differentiation of Human Bone Marrow Stromal Cells Via ERK1/2 Signaling. *Journal of Cellular Biochemistry*, *118*(2), 263–275.